UILU-ENG 86-3608

Report No. 131

FATIGUE CRACK INITIATION AND EARLY GROWTH IN TENSILE-SHEAR SPOT WELDMENTS

by

James C. McMahon and Frederick V. Lawrence, Jr.
Department of Metallurgy and Mining Engineering

A Report of the

MATERIALS ENGINEERING - MECHANICAL BEHAVIOR

College of Engineering, University of Illinois at Urbana-Champaign

August 1986

ACKNOWLEDGEMENTS

The author acknowledges K. Ewing and her associates at the General Motors Technical Center for supplying the material and assistance in the welding of specimens; R. Landgraf and S. Downing for supplying the Ford Variable History; and Hibbitt, Karlsson and Sorensen, Inc. for providing the finite element package **ABAQUS.** The author also acknowledges the encouragement and ideas given to him by many of his colleagues.

S. Whitlow and K. Gignac are thanked for their invaluable assistance in the laboratory. C. Petrie, J. Hubbard and C. Kimbrough deserve special credit for the careful preparation of this document, and R. Winburn is gratefully acknowledged for the drafting of the graphs and figures.

The author is grateful to the members of his Final Examination Committee for their direction which began early in the initial stages of this study, especially to H. Corten for his assistance in the development and evaluation of specimen designs and to his advisor, F. V. Lawrence, for providing five years of valuable guidance and for his careful review of the text.

A. Johnson of the American Iron and Steel Institute; S. Errera, Chairman of the Committee of Sheet Steel Producers; and member companies of the committee are acknowledged for the support given to the University of Illinois during the initial phases of this study. Additional funds to help support this study were provided by the Fracture Control Program of the College of Engineering at the University of Illinois.

TABLE OF CONTENTS

Section		Page
1.	INTRODUCTION	1
2.	EXPERIMENTAL PROGRAM	6
3.	RESULTS OF THE OBSERVATION OF FATIGUE CRACKS	13
4.	MODELS FOR PREDICTING THE FATIGUE LIFE OF TENSILE-SHEAR SPOT WELDMENTS	18
5.	DISCUSSION	24
6.	SUMMARY AND SUGGESTIONS FOR FURTHER RESEARCH	30
TABLES		33
FIGURES		54
APPENDIX A:	EXAMPLE FIGURES OF ORIGINAL DATA	84
APPENDIX B:	REVIEW OF MODELS FOR PREDICTING THE FATIGUE LIFE OF SPOT WELDMENTS	90
APPENDIX C:	COMPUTER PROGRAM AND SAMPLE EXECUTION	109
REFERENCES		117
VITA		119

1. INTRODUCTION

The fatigue behavior of electrical resistance spot welds has recently received much attention principally because the automobile industry has used thinner gauges of steel to replace thicker sections in an effort to reduce vehicle weight. The change to unit-body construction practices resulted in considerable weight savings but caused spot welds to become the main structural welds and required them to endure the cyclic loading conditions experienced by automobiles.

Spot welds are employed as structural joints in several ways; and spot-weld specimens used for fatigue tests commonly have three different configurations or designs as shown in Fig. 1: the tensile-shear (TS), the coach-peel (CP), and the cross-tension (CT). The TS configuration is the strongest and most effective use of the spot weld; and therefore, it is the subject of this work.

1.1 Scope of the Present Study

The fatigue life of TS spot weldments has been studied in this work through the direct observation of fatigue crack initiation and growth. The observations regarding fatigue crack development were used to refine an analytical model proposed by Wang (1) which predicts spot weld fatigue life and to explain the fatigue life improvement imparted using post-weld treatments.

The questions addressed by this study are: Can fatigue crack development and fatigue crack initiation sites be monitored in the inaccessible notch-root area of a tensile-shear spot weldment? What is the relative importance of fatigue crack initiation and propagation in a tensile-shear spot-welded joint? How does the importance of initiation change for long and short lives, loading conditions and loading histories? Can the total fatigue

life (at long lives) be estimated by an initiation-propagation model, and is it possible to predict the total life using estimates of the initiation life?

1.2 Review Spot Weld Fatigue Life

Wang (1) summarized the variables which influence the fatigue resistance of spot welds, the most important of which are: material properties (tensile and yield strengths), geometry (specimen configuration, nugget size and shape), and processing variables (weld time and current, electrode force, temper cycle).

Wang (1) divided the fatigue of TS specimens into three stages: Stage I --crack initiation, Stage II--through-thickness propagation, Stage III--across-width propagation. Wang designated the lives corresponding to these three stages as N_I (for the life of Stage I), N_{pt} (Stage II), and N_{pw} (Stage III). The initiation life, N_I, is defined as the number of cycles required to create a crack at a notch or to establish a crack of a given length. The two stages of propagation (Stages II and III) are illustrated in Fig. 2. The through-thickness propagation life, N_{pt}, was the number of cycles to propagate the initiated crack to the outside surface of the specimen. The across-width propagation, N_{pw}, was the cycles required for the crack to propagate across the width of the specimen (through the base metal) as shown in the top diagram of Fig. 2. Point "a" in Fig. 3 denotes the transition between Stage II and Stage III, which is the boundary between propagation around the nugget and propagation across the sheet.

1.3 Stages of Fatigue Failure in Spot-Welded Joints

Comparison of the fatigue resistance of different joints and spot weld configurations is difficult without a uniform definition of failure. For example, the difference in fatigue strengths of two TS spot-welded

specimens, identical except for width, may be attributed to the extra propagation across the wider joint. Such a comparison would have more meaning if each of the stages of fatigue life could be recorded and directly compared.

In studies at the University of Illinois (2,3), failure was usually defined as the separation of the two sheets of the joint (Stages I+II+III). Davidson (4) at U.S. Steel terminated fatigue tests after the nugget failed by shear or after "thumbnail-size" cracks developed at the edge of the nugget on the outer surface of the specimen. The latter condition corresponds to all of the initiation (Stage I) and through-thickness propagation (Stage II) plus a small amount of the across-width propagation (Stage III). Orts (5) and Wilson and Fine (6) defined failure as a predetermined ram stroke of 0.25 in. (6 mm), which for most specimens corresponded to complete specimen separation (Stages I+II+III). Smith (7) defined failure as specimen separation but recorded a life called N_T' which was the observed fatigue life at which the crack reached the outside surface of the sheet (Stages I+II).

The current study referred to fatigue life at specimen separation as N_T and used Smith's definition of life to indicate the sum of the initiation and through-thickness propagation lives (N_T'), however the notation $N_{0.055}$ is used instead of N_T' to indicate the life when a crack reached a depth of the sheet thickness (1.4 mm, 0.055 in.). Similarly, $N_{0.01}$ indicates the number of cycles completed when the crack reached a depth of 0.25 mm (0.01 in.).

1.4 Relative Importance of Initiation and Propagation in Spot Weldments

Davidson (4) and also more recently Cooper and Smith (8) maintain that the fatigue life of tensile-shear spot weldments is primarily a crack-propagation phenomenon because the severe, crack-like notch of the spot-welded tensile-shear joint greatly reduces any initiation life and that most of the life is spent propagating the crack to failure. The notch of a tensile-shear

specimen (shown in Fig. 1) results from the gap between the two sheets of the joint. This gap is not actually a crack but a sharp notch which is aligned parallel to the direction of loading.

It is controversial whether some life is required to initiate a crack at an angle from the root of this notch. Lawrence et al. (2) recently proposed that since fatigue failure of weldments is a series of initiation and propagation events, their fatigue lives could be predicted using multi-stage models. Their model suggests that initiation consumes the majority of the life of the specimen at long lives.

1.5 Monitoring of Fatigue Cracks in Spot-Welded Joints

Little direct evidence of the initiation of cracks has been presented in the literature because the early stages of fatigue crack growth in TS spot welds are not directly observable during fatigue testing. The disagreement on the relative importance of fatigue crack initiation and propagation discussed above has prompted interest in the monitoring of fatigue cracks and their development in spot-welded joints. Although the development of a fatigue crack in a tensile-shear spot weldment is not visible for much of its life, there are methods of directly and indirectly monitoring the crack's growth including radiography--Wojnowski (9), sectioning--Smith (7), and electrical potential difference--Cooper and Smith (8) (see Table 1 for a summary of these methods). The companion-specimen method of Smith (7) was chosen for the current study because it allows direct measurement of the intiation and early growth of fatigue cracks in TS spot weldments. A second technique was developed during the current study in which fatigue cracks in TS spot weldments were directly observed in presectioned specimens during fatigue cycling.

Section 2, outlines a new method of monitoring fatigue cracks in spot welds; Section 3 summarizes measurements which give evidence of the relative importance of crack initiation and propagation in the fatigue life of spot weldments; and Section 4, reviews Wang's Initiation-Propagation model which predicts the fatigue life of spot weldments other models.

2. EXPERIMENTAL PROGRAM

Two of the destructive examination methods described in Section 1.5 were used to directly monitor the fatigue cracks in TS spot weldments. The first was the method developed by Smith (7) in which the fatigue cracks in specimens of a companion test series were measured to approximate the fatigue crack development of a single "composite" specimen. This companion-specimen method had the disadvantage of requiring several specimens for each loading condition. Furthermore, this method was unsuitable for obtaining accurate crack growth data because of the scatter which occurs in the long-life regime.

To overcome the drawbacks of the companion specimens, a second technique was developed in which testpieces were sectioned through the weld nugget, and the development of fatigue cracks on the section was monitored during fatigue testing. The results from these tests using the "presectioned" design shown in Fig. 5 were comparable to those of the companion specimens.

2.1 Material and Welding Conditions

A hot-rolled galvanized high-strength low-alloy (HSLA) sheet steel which had a yield strength of 60 ksi (414 MPa) was used in this study. The sheet thickness was 0.055 in. (1.4 mm) including the galvanized coating (G-90). This steel contained 0.06% carbon with Nb and Ce additions and is similar to SAE 960X. The mechanical properties are given in Table 2, and the nominal chemical composition is given in Table 3. Micrographs of the weld metal, heat-affected zone and base metal are shown in Fig. 6.

Tensile-shear spot weld specimens were welded at the General Motors Corporation Technical Center in Warren, Michigan. Spot welds were made with a Sciaky single-phase, microprocessor-controlled AC electrical resistance

spot welding unit. The nominal welding current (RMS value of the secondary current) was 12.1 kA and was monitored with a toroidal pick-up located around the lower electrode (see Table 4 for welding schedule). The welding time was 20 cycles, and the electrode force measured with a hydraulic force gauge was 3.6 kN (800 lbf). Pointed-nose cap type electrodes with flat ends were used for welding (RWMA Class II material). The electrode caps were conditioned by preparing 100 spot welds on excess sheet stock before welding the test specimens. Frequent monitoring of the welding parameters continued and peel tests were performed until consistent welding conditions and the desired nugget diameter were obtained (peel test is shown in Fig. 7).

The nominal welding schedule, marked as point 4 in Fig. 7, was taken from a welding lobe diagram which had been previously established (2). After every eight to ten welds, a peel test was conducted to measure nugget diameter. The welding current, monitored by the toroidal pick-up, was adjusted to maintain a constant nugget diameter throughout the welding of all specimens. Specimens showing expulsion or poor alignment were discarded.

Radiographic Inspection

Although precautions were taken to prepare uniform spot-welded specimens, some specimens had shapes or sizes which were not nominal. Variations from the normal weld specifications which were missed by visual inspection were detected by radiography. Photographs of the details of both surfaces of a spot-welded specimen are shown in Fig. 8-A and B. A typical radiograph of a spot weld is shown in Fig. 8-C. A high-density film was used, and the best contrast was found by using the parameters listed in Table 5. Specimens whose radiographs revealed excessive expulsion, undersized nuggets, or non-uniform nugget shape (see Fig. 9) were not tested.

2.2 Monitoring Fatigue Cracks Using Companion Specimens

Two designs of companion specimens were used in this study. The first design is shown in the top diagram of Fig. 4 and was used for the R=0 base-line fatigue tests and the R=0 companion-specimen tests performed by Smith (7) whose results have been included in this study. The second design is shown in the lower diagram of Fig. 4 and was used for the base-line and companion-specimen tests for R=-1 and variable loading histories as well as for the tests of spot-welded joints treated by the coining technique. Coining is a fatigue improvement method in which compressive residual stresses are induced in the notch-root area by the application of a compressive force on the face of the spot weld as shown in Fig. 10 (10).

All fatigue testing was conducted at the Materials Engineering Research Laboratory at the University of Illinois. The spot-welded specimens were tested in a 3-kip capacity MTS servo-hydraulic testing machine with a 436 control unit and a 406 controller. Testing was conducted under load control at frequencies of 10 to 20 cycles per second (sinusoidal wave form).

Base-line fatigue life data were obtained from R=-1 and R=0 constant amplitude tests. Separate tests were conducted to determine the effect of coining and variable load histories. The Edited Ford Variable Load History (11) was used and is shown in Fig. 11; this variable load history contains 5320 events and has an average mean stress close to zero. The results of the base-line tests are listed in Tables 6, 7, 29-B and 30-B and shown in Figs. 12-15.

After the baseline data were obtained, load levels were selected to yield short, intermediate and long lives in the TS spot weldments. For R=0, the load levels were: 0-3.6 kN (800 lbf)--projected life of 50,000 cycles, 0-2.2 kN (500 lbf)--400,000 cycles, 0-1.8 kN (400 lbf)--4,000,000 cycles, and 0-1.6 kN (350 lbf)--10,000,000 cycles. For R=-1, the load levels were: 3.1

kN (700 lbf)--20,000 cycles, 2.0 kN (450 lbf)--150,000 cycles, and 1.1 kN (250 lbf)--1,200,000 cycles.

Each specimen of a companion test series was fatigued at a selected load level for a predetermined number of cycles which corresponded to a percentage of its projected fatigue life. The typical increment in life between specimens of a series was 10%. Nine series of companion specimens were tested (Series A through I). In addition to the four series (A-D) of tests completed under R=0 by Smith (7), three series (E-G) were tested under R=-1, one series (H) tested coined specimens, and one series (I) was completed under a variable load history (Table 8).

Examination of Companion Specimens

After the prescribed number of cycles, the nugget of a specimen was sectioned parallel to the loading axis. The sectioning and polishing technique is shown schematically in Fig. 16. The first cut through the nugget was made with a low-speed saw using a diamond wafering blade. The first section was usually positioned 1.3 mm (0.05 in.) from the weld centerline. It was found that the fatigue cracks invariably initiated within this limit (see Section 5.1). The sectioned nugget was mounted in epoxy and was ground and polished using standard metallographic techniques. A hydrofluoric acid-based chemical polish (85% H_2O_2(30% conc.), 15% H_2O, 5% HF(48% conc.)) was employed to enhance the detail of any fatigue cracks and to eliminate smearing from mechanical polishing. Nital was not used as an etchant because the etched microstructure would obscure small fatigue cracks.

Photographs of the notch-root areas were taken for each section. The depths of any observed fatigue cracks were measured from the photographs and recorded. The length of a crack was measured from the crack's root to its tip. The specimen was then repolished, removing 0.05 to 0.13 mm (0.002 to

0.005 in.) of the weld nugget, and the measurement procedure was repeated. The series of measurements (example in Fig. 16) provided information on the shape of the fatigue specimen of a companion test series. The crack depth history for a TS spot weldment subjected to the conditions of the test series was estimated from the composite of data from all the specimens of the series.

2.3 Monitoring Fatigue Cracks Using Presectioned Specimens

Initial studies in the development of the "presectioned specimen" method of fatigue crack monitoring used specimens of the R=-1 design (Fig. 4) which had been cut lengthwise through the centerline of their nuggets (see top diagram of Fig. 5). This cut specimen's asymmetry caused a combined bending and torsional loading as a consequence of the single half-nugget being located on the edge rather than the centerline (load line) of the specimen.

A symmetrical specimen (see lower diagram of Fig. 5) was developed to overcome the problem of torsional loading discussed above. This symmetrical specimen was produced by spot welding two 64 mm (2.5 in.) wide sheets together in a lap joint with two spots, 38 mm (1.5 in.) apart. The outside edges of the specimen were machined along the centerline of the nuggets, leaving two half-welds exposed.

The free edge of the presectioned specimen influenced the stress-intensity factor. The quarter-elliptical crack shape of the presectioned specimens resulted in a higher stress-intensity factor than that of the companion specimens; and consequently, the loads of the presectioned specimens were adjusted to make the two cases equivalent. An analysis of these stress-intensity factors is given in Appendix B.

Presectioned Specimen Preparation

Each of these welds' exposed surfaces were ground and polished using standard metallographic techniques. The surfaces of each of the exposed half-nuggets were ground and polished. To facilitate polishing, specimens were machined so that the nugget areas would be raised about 1 mm from the grip ends of the specimens. The last stage of the polishing (0.05 micron alumina) was completed immediately before fatigue testing. Reference marks, scratched near the areas of interest on the polished surfaces with a razor blade, were used to locate specific positions on the surface when using the microscope.

The symmetrical specimen design provided a total of four notch-root locations for observation on each specimen: two locations (primary and secondary) on each of the two half-nuggets' surfaces. The specimen's configuration of two half-nuggets was assumed to be equivalent to a single nugget and to have balanced loading because of the symmetric design. However, it is possible that the load was not shared equally between the four sites.

Testing and Crack Depth Observations of Presectioned Specimens

Before fatigue testing and at each selected interval of life, the surfaces of the specimen were replicated with acetylcellulose film. To make a replica, the surface was cleaned with ethyl alcohol or methyl acetate and dusted with compressed gas. A small amount of high-purity methyl acetate was applied to the surface using a syringe with a fine needle. Before the solvent volatilized, a precut strip slightly larger than the nugget area was laid on the polished surface using tweezers. After drying for one minute, the replica was removed and placed between two glass microscope slides. The quality of the replica was checked under an optical microscope, and a second replica was made if necessary. The replicating procedure is shown

schematically in Fig. 17. The replicas provided information on the progress of a fatigue crack during its growth.

Crack depths were measured indirectly from the replica under an optical microscope using a calibrated eyepiece. Photographs of the surfaces of the presectioned specimens were not taken because the replicas provided a permanent record of the observed cracks. The sections observed by this technique were identical to the cross sections exposed by sectioning companion specimens. Fatigue cracks in the presectioned specimens were measured from their roots to their tips as shown in Fig. 17.

The tests of the presectioned specimens are summarized in Table 9. Three presectioned specimens were tested under R=0 conditions, nine under R=-1, and one under $R=-\infty$ (zero-to-compression). One coined specimen was presectioned and tested, and three specimens were tested under the variable load history.

3. RESULTS OF THE OBSERVATION OF FATIGUE CRACKS

3.1 Results from the Companion Specimens

Each nugget had two potential crack initiation sites. Cracks generally initiated at both sites, but usually one crack grew faster than the other and became dominant. The dominant crack was designated the primary crack and the other the secondary crack. Life was defined as the number of cycles required for the primary crack to grow to a depth equal to the sheet thickness, 1.4 mm (0.055 in.). This definition of life, $N_{0.055}$, was used to be consistent with the presectioned-specimen method in which testing was ended when the primary crack reach this depth or shortly thereafter.

Example results of the companion-specimen tests are shown in Figs. 41 to 44. Both primary (filled data points) and secondary (open data points) cracks are shown. The dashed line near the top of these figures represents the sheet thickness, 1.4 mm (0.055 in.). The line through the data represents a best-fit exponential power law for crack depth as a function of life. This was the exponential form of fitted line used by Smith (7), and it is generally a good fit for data over 0.13 mm (0.005 in.). This exponential form did not work well for the test series which exhibited large amounts of scatter. The scatter is inherent in the use of the companion specimens, particularly for specimens tested in the long-life regime under constant amplitude or variable load histories (Figs. 43 and 44). In the case of the coined companion specimens, variations in the coining treatment may have contributed to the scatter.

3.2 Results from the Presectioned Specimens

Life was defined as the number of cycles required for the first crack to reach a depth equal to the sheet thickness. When possible, the measurements

were continued until the other cracks of the specimen had also reached this depth. In some presectioned specimens, the cracks on one side were significantly longer than those of the other side. When these longer cracks reached a depth equal to the sheet thickness, "load shedding" to the opposite side occurred, bringing additional stress on the half-nugget having the smaller cracks which then grew more rapidly than the cracks of the first side. When the cracks of both half-nuggets were of comparable size, the growth rates remained similar as demonstrated by specimen 219; both of this specimen's primary cracks had lengths which remained nearly identical throughout the life of the specimen (see Fig. 45).

Measurements of the crack depths recorded from the replicas of the presectioned specimens are plotted on graphs such as shown in Figs. 45 to 47. The progress of all active cracks (four or less) is shown for each specimen in the upper graph. The data of the two primary cracks of each specimen were normalized and plotted on graphs having linear scales (lower graphs of Figs. 45 to 47). The abscissa is the number of cycles to grow a crack of given size divided by the life of the specimen, N(a)/N(t) (t=thickness). The ordinate is the crack depth divided by the sheet thickness, a/t. Values greater than 1.0 are possible for secondary cracks which were monitored after the first crack had reached a depth equal to the sheet thickness. All specimens display the upward curvature expected from a crack growth specimen cycled under constant loading and exhibit behavior similar to that of the "composite" curves developed for the companion specimen series.

3.3 Summary of Results from Companion and Presectioned Specimens

The results of both the companion specimens and presectioned specimens are summarized in Figs. 18-24 and were found to be similar in terms of the total life and in fractions of life to develop different size cracks. The

only difference between the two methods was observed for the data recorded at the 0.13 mm (0.005 in.) level from the R=0 tests (see Fig. 20). The fractions of life to grow cracks to small depths were greater for the presectioned specimens than for the fractions recorded for Smith's (7) companion specimens. The agreement between the two techniques was better for R=-1 data (see Fig. 21). Section 5.1 will discuss the possible error in measurement which can arise from the use of companion or presectioned specimens.

Figure 18 summarizes the fatigue crack development for the R=0 and R=-1 tests of both the companion specimens and presectioned specimens. The different symbols represent the growth of cracks in the specimens subjected to the loads listed along the vertical axis. The number of cycles required to establish cracks 0.25 mm (0.01 in.) and 1.4 mm (0.055 in.) deep are represented by the dashed and solid lines, respectively. It is apparent from Fig. 18 that the stress ratio (R) affects fatigue life, particularly at the lower load levels where the R=-1 specimens had lives that were nearly an order of magnitude greater than those of the R=0 specimens. Similar data for the specimens subjected to the variable load history are presented in Fig. 19.

The data are replotted in a normalized form in Figs. 20-24. For each point, the abscissa is the life of the specimen (in the case of the companion-specimen data, the average life), and the ordinate is the fraction of life required to grow the crack to the given depth. The data from each specimen (or series) are plotted vertically at the total life of the specimen ($N_{0.055}$). The specimen numbers (or companion-series letters) are listed below their respective groups of data. Figures 20 and 21 are summarized in Fig. 22, in which the data has been grouped into three ranges of lives, and the average fractions of lives required to grow the different size cracks are plotted for each range--less than 10^5, 10^5 to 10^6, and greater than 10^6 cycles. For the R=0 data, there appears to be little change in the fraction of lives required

to grow these cracks over the range in lives observed. For the R=-1 data, these fractions appear to be increasing with increasing lives. For both R ratios, at least 50% of the life of the specimens was required to develop a crack 0.25 mm (0.01 in.) deep at long lives (> 10^6 cycles).

The specimen which was tested under zero-to-compression loading (R=-∞) exhibited an unusual failure site (see Fig. 25). Tensile-shear spot weldments usually crack on one of the gripped sheets. Figure 25 shows where Specimen 217 cracked on the unloaded sheet. When this specimen was loaded in compression, the joint rotated as pictured, and the edge of the unloaded sheet hit the gripped sheet. This action placed a bending moment on the "unloaded" sheet, and the location of maximum tensile stress occurred near the notch on the opposite side of the normal crack site. This specimen had a life of 477,000 cycles which was significantly longer than those of the specimens tested under R=-1 (150,000 cycles) and R=0 (25,000) loading.

Results of the Coined Specimens

A series of spot-welded specimens were coined using a load of 45 kN (10 kips) as shown in Fig. 10. The coined specimen data is shown in Fig. 14 and 23. No trend with life was established for the coined specimens because only one load was used for the tests. Coined specimens (Series H) were cycled under completely reversed conditions, R=-1, with a load range of 6.2 kN (1400 lbf) and had lives of 500,000 cycles. As-welded specimens tested under the same loading conditions had an average life of only 20,000 cycles. The fractions of life required to grow different size cracks in the coined specimens are comparable to the fractions observed for the as-welded specimens even though the coined specimens had lives of twenty-five times that of the as-welded specimens. The fact that the improvement in life is shared nearly equally between Stages I and II indicates that the coining treatment affects both crack initiation and propagation.

Results of Tests Under the Ford Variable Load History

A companion series of specimens (I) was subjected to the Edited Ford History (Fig. 11) using a maximum load of 3.6 kN (800 lbf). Because scatter was observed in the data from Series I that was similar to that of the long-life companion specimens, monitoring of fatigue cracks under the variable load history was repeated using presectioned specimens. The variable load history data is summarized in Fig. 24 (fraction of life versus life).

The Edited Ford Variable Load History has no net mean stress. As expected, the trend of increasing fractions of life with increasing life is similar to that of the R=-1 constant amplitude data. However, the fractions of life required to develop small cracks are smaller for the variable load history than for the constant amplitude loading. This result may have been due to peak loads in the variable load history which reduced the amount of life that the fatigue cracks spent in the initiation and early growth period.

4. MODELS FOR PREDICTING THE FATIGUE LIFE OF TENSILE-SHEAR SPOT WELDMENTS

4.1 The Initiation-Propagation Fatigue Life Model

Wang (1) developed a three-stage initiation-propagation (TSIP) model for calculating the individual lives for each of the three stages of fatigue life of tensile-shear spot weldments. Wang's TSIP model was used to predict the total lives of the specimens tested in the current study, and the results of these predictions are shown in Table 10 and Figs. 26-28. The initiation life predictions using Wang's model were nonconservative, and the propagation life predictions were generally conservative. The total life predictions were nonconservative, especially for specimens having finite lives greater than 500,000 cycles.

The experiments of the current study partitioned the fatigue lives of spot weldments and provided data which was previously unavailable to Wang when his model was developed. The data from these experiments have been used to modify Wang's TSIP model. Appendix B discusses details of the Initiation-Propagation Model and additional information may be found in References (1,2,12).

Summaries of the procedures (given in Appendix B) used for estimating fatigue crack initiation and propagation lives of spot weldments are given below. The listing of the computer program used for making the fatigue life predictions is given in Appendix C.

Summary of Fatigue Crack Initiation Life Estimation

The steps used in calculating the initiation life, N_I, of a spot-welded joint are:

1. K_{fmax} is calculated.

2. The local maximum stress, σ_{max}, is found from the first reversal of the set-up cycle.

3. The local stress range is found from the second reversal of the set-up cycle. The maximum stress and stress range yield the mean stress.

4. The stress range and mean stress are used to solve for N_I. The above steps also outline the computer program (see Appendix C) written for estimating the fatigue crack initiation lives (and total lives) of spot weldments. The estimates of fatigue life made by this program for the specimens of the current study and specimens tested by other researchers will be presented later in this section. As detailed in Appendix B, N_I is a function of specimen geoemtry, material properties, residual stress, remote loading, and stress ratio.

Summary of Fatigue Crack Propagation Life Estimation

The steps used in predicting the fatigue crack propagation life, N_p, of a tensile-shear spot weldment are summarized below:

1. Determine the correction factors for K. Some are available in analytic form, while other require polynomial fits of experimental da/dN data.

2. Choose appropriate a_i and a_f for the integral of Eq. 30 (Appendix B).

3. Numerically integrate Eq. 30 from a_i to a_f. At each interval of crack depth, K is calculated. The increment of life is found from the growth rate da/dN, which is given by the Paris power law--Eq. 29 (Appendix B).

4. The propagation life is found by summing the increments of life found from the previous step.

The above steps outline the procedure given in Appendix B which

considered N_p to be a function of specimen geometry, material properties, remote loading, and stress ratio.

4.2 Predictions of Fatigue Life Using the IP Model

Predictions of Fatigue Crack Initiation Life

The fatigue crack initiation life estimates made using the program listed in Appendix C are given in Table 11 and shown in Fig. 29. The observed data are compared with the predicted lives for two conditions: when the crack was 0.25 mm (0.01 in.) deep and when the crack was as deep as the calculated value of the threshold crack size (a_{th}). With the exception of some results for lives greater than 500,000 cycles, the predictions are within a factor of two of the observed number of cycles when the cracks had reached depths equal to a_{th}. These predictions were in better agreement than those made using Wang's original model because of the modification made to Eq. 11 in which the term for the residual stress is divided by K_σ rather than K_f as outlined in Appendix B.

Predictions of Fatigue Crack Propagation Life

The fatigue crack propagation life estimates are listed in Table 12 and shown in Fig. 30. Again, two sets of data are shown representing both observations and predictions using a_{th} and 0.25 mm (0.01 in.) as the initial crack size at the beginning of propagation. Predictions of propagation life, using a_{th}, were within a factor of two of the observed data. Predictions for specimens having low and intermediate lives, were conservative using 0.01 in. (0.25 mm) as the lower limit of integration in Eq. 30. The difference between these predictions and those shown in Fig. 27 from Wang's unmodified model are attributed to the corrections made for the effect of mean stress.

Predictions of Total Fatigue Life

The fatigue crack initiation and propagation lives calculated from the previous two sections were added together to predict the total fatigue life. Again, the two sets of predictions are listed in Table 13 and shown in Fig. 31: those which used 0.25 mm (0.01 in.) and those which used a_{th} for the size of an initiated crack. The overall agreement between predictions and observed lives was generally within a factor of two.

Total life predictions, which were made for the material of the current study (Galv. HSLA) using only Stages I and II, were compared to the observed total lives through specimen separation (Tables 15-16). These tests were used to establish the S-N curves of Figs. 12-13. As can be seen in Fig. 32, there was good agreement between the predictions and observations, even though the predictions neglected Stage III.

4.3 Other Models for Predicting Spot Weld Fatigue Life

Models which estimate the fatigue life based solely on the calculated propagation life are also considered in Appendix B. The major drawback of these models is that one can not integrate the Paris power law from a crack depth of zero. Arbitrarily choosing a small, nonzero initial crack depth yields finite stress-intensity factors but generally results in nonconservative life predictions. Model 4 of Appendix B is an all-propagation model which avoids these problems by integrating the Paris power law from a crack depth of zero and using a finite initial value of stress-intensity factor (given by Pook (13) for the notch root of a spot weld).

Model 6 of Appendix B predicts the total life based solely on the estimated initiation life. Except in the long-life regime, the predictions for Model 6 were conservative (Fig. 55). Table 14 summarizes the different models used to predict the lives of the specimens tested in the current

study. As rated by the coefficient of variation (a parameter based on the differences between the predicted and observed fatigue lives), the best predictor of fatigue lives was Model 4 which used a constant, initial value of stress-intensity factor. The next best of the seven methods was the Initiation-Propagation Model (listed as Model 7 in Table 14).

4.4 Predictions of the Results from Other Studies

The IP model was used to predict the fatigue data reported in the studies of other researchers. These studies generally used specimens made of different strength steels and having different thicknesses and widths than those of the specimens of the current study. The results of these predictions are tabulated in Tables 17-19 and shown in Figs. 33-35. Only Stage I and Stage II lives were calculated because not all of the researchers used a common definition of failure, and some did not specify at which point in the across-width propagation that the fatigue tests were stopped. The calculated threshold crack size (see Appendix B) was used for the depth of an initiated crack because its use gave better estimates of fatigue life of the specimens of the current study than the use of the fixed, arbitrary initiated crack size of 0.25 mm (0.01 in.).

The HSLA steel used by Orts (5) was similar to that used by the current study, but it had a slightly higher yield strength. His tests provided an opportunity to test the IP model's ability to predict the effects of different geometries. Shown in Table 17 and Fig. 33 are the calculations made for a standard specimen, which was 50 mm (2 in.) wide, and for specimens half as wide and twice as wide as the standard specimen. The predictions were in agreement with the observed data by a factor of two. Also shown are predictions for coined spot welds whose improvement in fatigue life was predicted but underestimated.

Shinozaki et al. (14) studied the fatigue of spot-welded joints made from precipitation-hardening and dual-phase steels. Each steel was welded with a nominal schedule and an altered welding schedule--designed to induce compressive residual stresses. The agreement was good for both steels and the model correctly predicted the extent of improvement exhibited by the treated welds (see Table 18 and Fig. 34).

Kitagawa et al. (15) studies spot weldments made from low-carbon and rephosphorized steels. The steels had thicknesses almost half as thin as the steel of the current study and the predictions for this steel are given in Table 19 and are shown in Fig. 35. The predictions for the low-carbon steel agreed well with the reported data, while the predictions were nonconservative for the rephosphorized steel weldments.

Also shown in Fig. 35 are the predictions for the data reported by Cooper and Smith (8) who gave information on the initiation and propagation portions of life of their specimens (Table 19). For their data, predictions for both initiation and propagation life are shown. The results of this study will be discussed further in Section 5.

5. DISCUSSION

5.1 Effectiveness of the Companion- and Presectioned-Specimen Techniques

The presectioned-specimen technique was a successful alternative to the companion-specimen method. The use of companion specimens provided direct measurements of fatigue cracks, but specimen-to-specimen scatter made interpretation the crack growth data from the companion test series difficult. The presectioned specimens did not have the problem with the scatter because only one specimen was required for each loading condition rather than the several specimens used in each companion test series. A disadvantage of the presectioned specimens is the uncertainty of the load distribution between the two half-nuggets of the specimens. If the specimen is carefully machined, an even load distribution can be achieved at the beginning of fatigue testing but, as discussed in Section 3.2, the even distribution of load cannot be guaranteed after fatigue cracks have initiated.

Accuracy of the Measurements Made from Companion and Presectioned Specimens

Both the companion-specimen method and the presectioned-specimen method measured crack depths on a section perpendicular to the plane of the crack and near the plane of the crack's maximum depth. In the case of the companion-specimen method for which specimens were destructively examined, sufficiently small depths were polished off to minimize any larger error in finding the maximum crack depth. If a nugget had been polished through in only a few intervals, a small crack could have been missed entirely. Typical depths between polished sections in a specimen ranged from .125 to .25 mm (.005 to .010 in.). In the case of the presectioned specimen, a measurement error may have been introduced if the plane of the maximum crack depth was different

from the plane of the polished surface. This distance was generally found to be less than 0.25 mm (0.01 in.) (see Table 20).

An analysis of the maximum possible measurement error inherent in the two methods used in the current study is presented below:

Assume that the crack profile can be estimated as an ellipse (see Fig. 48):

$$\left(\frac{x}{c}\right)^2 + \left(\frac{y}{a}\right)^2 = 1 \qquad (1)$$

where c is the major axis of the ellipse and a is the maximum crack depth.

It is possible that the location of the measured crack depth, a_m, is a distance D from the maximum crack depth, a (see Fig. 36). The maximum depth of the crack could be larger than the measured crack depth:

$$a = \sqrt{a_m^2 + (D/R)^2} \qquad (2)$$

where R is the ratio c/a. The error in measurement is reduced when the distance D decreases or when the ratio c/a increases. The maximum size of a crack that could be missed entirely is represented by a' in Fig. 36. At a distance D from a', one would measure a crack depth of zero.

The maximum possible crack depth is a function of the measured crack depth and was derived from Eq. 2 for the worst-case condition of the current study:

$$a = \sqrt{a_m^2 + .0289} \qquad \text{(units in mm)} \qquad (3)$$

As shown in Fig. 36, the possible error decreases with increasing crack depth. At a crack depth of 0.25 mm (0.01 in.), this error could be as high

as 20%, and at worst, the maximum undetected crack depth could be no larger than 0.17 mm (0.0067 in.). However, the distance D was usually half of that assumed for the worst-case analysis, and the maximum crack depth that could have been missed was probably 0.08 mm (0.003 in). As shown by Fig. 37, the accuracy of the measurements from both the companion and presectioned specimens improves with increasing crack depths.

An Alternative Method of Monitoring Fatigue Cracks

The two methods used by the current study have the disadvantage of being destructive techniques. A successful nondestructive technique has been developed by Cooper and Smith (8). Nondestructive detection and indirect measurements of fatigue cracks in TS spot weldments were made by the electrical potential difference (PD) technique. However, potential difference values were calibrated to crack depths observed on facture surfaces of broken specimens and calibration was difficult for small depths (less than 0.22 mm) because of the reported difficulty in interpreting the fracture surfaces of small cracks.

The presectioned-specimen method of monitoring fatigue cracks in spot weldments gave reliable results (shown in Section 3 to be comparable to those of the companion-specimen method). The accuracy of the results using this method was generally 0.08 mm or less--0.08 mm at zero crack depth and less for larger cracks. The method is relatively easy to use and more rapid than other techniques.

5.2 Importance of Fatigue Crack Initiation in Tensile-Shear Spot Weldments

One "companion" specimen was sectioned 39 times by Smith (7). This specimen was cycled under a load of 2.2 kN (500 lbf R=0, for 3000,000 cycles, corresponding to 42% of the average fatigue life (710,000 cycles) of the test series. In some sections of this specimen, more than one crack was present, and as shown by Fig. 38, these overlapping cracks appear to have been in the earliest stages of crack growth--they had not yet formed a single crack front. From the crack shapes estimated by Smith (drawn through the data on Fig. 38), it appears that these cracks grew from multiple initiation sites.

The occurrence of multiple fatigue crack initiation sites was expected based on a finite element analysis performed by Ho (16) who found that the principal stress was 85%-90% of the maximum value (found at the nugget centerline) as far as 60 degrees from the centerline of the nugget (see Fig. 40). From Fig. 38, it can be seen that cracks may have initiated as far as 25 degrees from the weld centerline. In the specimens examined for the current study, cracks were found to initiate within 4 degrees (0.25 mm) of the centerline in more than 60% of the specimens (see Table 21 and Fig. 40). Also shown in Fig. 40 is the calculated stress concentration factor as a function of angle from the centerline of the spot weld. For small angles, this stress concentration factor is nearly as high as the maximum value found at the centerline. It is conceivable that slight perturbations in the nugget geometry or in the state of residual stress could cause the maximum stress, and therefore crack initiation, to occur a small distance away from the centerline as was observed in many specimens.

Section 1 raised the question of how important the initiation stage of fatigue crack development is in relation to the total life of spot weldments,

particularly for the sharply notched TS specimen. Cooper and Smith (8) suggested that crack initiation occupies a negligible proportion of fatigue life. As discussed in Appendix B, there are different definitions of the length of an initiated crack. If one defines the initiation life to be the number of cycles required to establish a crack 0.25 mm (0.01 in.) deep, the importance of initiation life cannot be decisively concluded from the results of Cooper and Smith (8) because of the difficulty of calibrating and monitoring small cracks using the PD technique.

The results of this study presented in Section 3 have shown that fatigue crack initiation is important and that the initiation of cracks 0.25 mm (0.01 in.) deep can consume up to 55% of the fatigue life of TS spot weldments. The portions of life to establish cracks of other depths are shown Figs. 20 to 24. For R=-1 testing conditions particularly, the importance of initiation life increased with increasing total life as shown in Fig. 21. Sufficiently long life tests required to confirm this trend for R=0 data were not carried out during this study, this trend was also observed for the variable load data (see Fig.25).

The importance of fatigue crack initiation life in tensile-shear spot weldments has been shown to be significant by the direct observation of companion and presectioned specimens. The observations of Smith (7) that the fatigue crack initiation sites can be off the weld nugget centerline were confirmed in this study; however, these sites were usually found to be within two to four degrees of the centerline.

5.3 Estimating the Total Fatigue Life with the Initiation-Propagation Model

As discussed in Section 4, modifications to Wang's Initiation-Propagation Model (1) improved the ability of the IP model to predict the fatigue lives of the TS specimens tested during the current study (Figs. 32 to 33. The modifications are detailed in Appendix B were made.

The ability of the IP model to predict the influence of material strength could not be confirmed directly from tests of the current study because only one material was used. However, the IP model correctly predicted the total lives of spot weldments made of the different strength steels reported by Shinozaki et al. (14) and by Kitagawa et al. (15) (see Figs. 35 and 36). Furthermore, the IP model successfully predicted the fatigue lives of specimens having geometries different than those of the specimens tested in the current study (see Figs. 33 and 35 for predictions made for the results reported by Orts (5) and Kitagawa (15)).

Fatigue life prediction models which were based solely on either the calculated initiation or propagation fatigue lives were considered in Section 4 and Appendix B. Most of these models yielded conservative estimates of life. However, at long lives, where initiation becomes increasingly important, the total lives could be estimated using only estimates of the fatigue crack initiation life (see Model 6 of Appendix B).

Model 4 of Appendix B, which is based entirely on propagation but uses Pook's (13) estimate for the initial value of the stress-intensity factor, gave the best total life predictions. Of the all-propagation models, Model 4 may be the best alternative to the IP model if it could be modified to account for the influence of residual stresses. This modification might be accomplished by altering the stress ratio to reflect the mean stresses at the notch-root which result from residual stresses.

6. SUMMARY AND SUGGESTIONS FOR FURTHER RESEARCH

6.1 Summary

1. The prosectioned-specimen method proved to be a reliable and convenient technique of measuring crack growth in an otherwise inaccessible area.

2. Initiation of cracks 0.25 mm (0.01 in.) deep consumed up to 55 percent of the fatigue life of tensile-shear spot weldments. The earliest cracks observed occurred between 10 and 20 percent of life; approximately 20 to 30 percent of life was required to produce cracks 0.13 mm (0.005 in.) long, a/t = 0.10. The portion of life devoted to initiation under variable load histories was lower than that under constant amplitude loading.

3. Tensile-shear spot weld specimens exhibited longer lives when the stress ratio was lowered from R=0 to R=-1. This shift occurred in both the initiation and propagation stages of fatigue life and resulted from the difference in mean stress at the notch-root area for the two different stress ratios.

4. The ten- to twenty-fold improvement in fatigue life resulting from the coining treatment was shared equally among the initiation and propagation stages of fatigue life.

5. The fatigue lives of TS spot weldments can be predicted by the Initiation-Propagation (IP) Model (see Appendix B). The IP model correctly predicted the lives of specimens made of other steels and having geometries different than those of the specimens of the current study.

6.2 Suggestions for Further Research

The advantages of monitoring fatigue crack growth in spot-welded specimens and of dividing the experimental data into the portions of life devoted to each stage of life are clear from the current study, and it is proposed that future researchers of spot weldment fatigue partition their data in a similar way. Specific topics for future work are suggested below:

1. The use of presectioned specimens for monitoring fatigue crack growth in spot-welded specimens could be conducted simultaneously using the potential difference method of Cooper and Smith (8). The presectioned specimens may prove to be a good means of calibrating the potential difference method.

2. The results of the variable loading did not conclusively determine the effect of histories on the initiation and early growth of tensile-shear spot weld specimens. A series of experiments should be conducted which tests presectioned specimens under simple block histories.

3. Fatigue crack growth experiments could be performed with the other standard spot weld specimens--the coach-peel (CP) and the cross-tension (CT).

4. The TS specimen undergoes a rotation because of its eccentric loading. Using presectioned specimens, the influence of this rotation on the various stages of life should be investigated, especially at the high load levels. The rotation could be measured and correlated with fatigue resistance following the work of by Davidson and Imoff (17).

5. Tests designed to observe nonpropagating cracks could be performed using presectioned specimens which would be fatigued under low loads and observed for several million cycles. After testing, each specimen should be sectioned and polished carefully in order to find profiles of the observed cracks which might be deeper than those at the plane of the original section.

6. Using a procedure described by Sehitoglu (18), presectioned specimens could be replicated several times during a single cycle of fatigue to monitor opening and closing levels of fatigue cracks in spot weldments. Specimens could be tested under different conditions to determine how the opening and closing levels change with load and stress ratio.

TABLE 1

Possible Methods of Monitoring Fatigue Crack Initiation and Growth in Tensile-Shear Spot Weldments

Monitoring Method	Stages Considered		Comments
As-Welded Specimen:			
Direct Observation	II-III	yes	Can be documented with replicas.
Overload Striations	I-II	yes	Provides crack profile at different lives. Can alter life.
Destructive Examination:			
Destructive Inspection	I-II	no	Limited resolution.
Companion Specimen	I-II	yes	Requires > 1 sample per condition.
Presectioned Specimen	I-II	yes	Only 1 specimen per condition.
Nondestructive Examination:			
Potential Drop	I-II	no	Calibration required. Only 1 specimen per condition.
Ultrasound	II	yes	Poor resolution.
Radiography	II	no	Limited resolution.

TABLE 2

Mechanical Properties of Galvanized HSLA Sheet Steel, 16-78B

Yield Strength, ksi (MPa)	61.5 (424)
Ultimate Tensile Strength, ksi (MPa)	69 (476)
Reduction in Area	69%
True Fracture Ductility, ε_f	1.17
Fatigue Strength Coefficient, σ_f', ksi (MPa)	80.2 (553)
Fatigue Strength Exponent, b	-0.054

TABLE 3

Nominal Chemical Composition of
Galvanized HSLA (16-78B)
Percent Weight

C	Mn	P	S	Si	Nb	Al	Ce
0.06	0.43	0.110	0.02	0.03	0.029	0.03	<0.008

TABLE 4

Typical[1] Welding Schedule for Galvanized HSLA (16-78B)

Electrode Force lbf (kN)	Hold Time Cycles[2]	Weld Time Cycles	Weld Current kA	Nugget Dia. in. (mm)
800 (3.6)	30	20	12.1	.24 (6.1)

1 Current was monitored and adjusted to maintain constant nugget diameter.

2 60 Cycles = 1 sec.

TABLE 5

Radiography Parameters

Parameter	
Material	Galvanized HSLA Sheet Steel
Thickness	.055 in. (1.4 mm) per sheet
No. of Sheets	Two sheets at spot weld
Total Thickness	.110 in. (2.8 mm) at weld
Film	Kodak R
Source to Specimen Distance	30 in. (760 mm)
Specimen to Film Distance	.04 in. (1 mm)
Current	4 A
Potential	120 kV
Time of Exposure	21 minutes

TABLE 6

Total Life Data for Untreated, Spot-welded
Tensile-Shear Specimens, Galvanized HSLA (16-78B)
R=0 Loading

Specimen No.	Load Range[1] lbf	kN	Total Life N_T (Cycles)
1	800	3.6	95,000
2	800	3.6	117,000
3	800	3.6	115,000
4	500	2.2	705,000
5	500	2.2	721,000
6	500	2.2	741,000
7	400	1.8	994,000
8	400	1.8	2,389,000
9	400	1.8	3,100,000
10	400	1.8	3,110,000
11	400	1.8	3,400,000
12	350	1.6	4,299,000
13	350	1.6	6,381,000
14	350	1.6	9,218,000
15	350	1.6	9,527,000
16	350	1.6	19,311,000

[1] Zero-to-tension loading (R=0).

TABLE 7

Total Life Data for Untreated, Spot-welded
Tensile-Shear Specimens, Galvanized HSLA (16-78B)
R=-1 Loading

Specimen No.	Load Range[1] lbf	kN	Total Life N_T (Cycles)
1	1570	7.1	18,000
4	1400	6.3	30,500
3	1400	6.3	37,850
2	1400	6.3	25,100
5	1124	5.0	68,230
8	900	4.0	160,600
7	900	4.0	274,500
6	900	4.0	232,600
13	600	2.7	579,700
12	600	2.7	1,217,000
11	600	2.7	710,000
10	600	2.7	1,420,000
9	600	2.7	1,668,200
15	550	2.5	1,760,700
14	550	2.5	824,000
16	500	2.2	>4,200,000
17	500	2.2	>3,000,000

[1] Completely reversed loading (R=-1).

TABLE 8

Summary of Tests Using the Companion-Specimen Method

Series	R Ratio	Condition	Load Range lbf	Load Range kN	Number of Tests	Life[1] Cycles
A	0	As welded	800	3.6	10	54,000
B	0	As welded	500	2.2	9	431,000
C	0	As welded	400	1.8	7	1,200,000
D	0	As welded	350	1.6	4	3,650,000
E	-1	As welded	1400	6.2	12	20,000
F	-1	As welded	900	4.0	11	151,000
G	-1	As welded	500	2.2	10	1,200,000
H	-1	Coined	1400	6.2	5	500,000
I	Variable Loading[2]		800 Maximum load	3.6	5	143 Blocks

[1] Life to crack depth of .055 in.

[2] Edited Ford Variable History, 5320 reversals/block

TABLE 9

Summary of Tests Using the Presectioned-Specimen Method

Spec. No.	R Ratio	Condition	Load Range lbf	Load Range kN	Life[1] Cycles
216	0	As welded	1000	4.5	25,000
219	0	As welded	600	2.2	320,000
224	0	As welded	400	1.8	1,600,000
209	-1	As welded	1000	4.5	150,000
201	-1	As welded	900	6.2	180,000
218	-1	As welded	700	3.3	600,000
203	-1	As welded	600	2.7	1,200,000
222	-1	As welded	500	2.2	1,857,000
225	-1	As welded	500	2.2	3,500,000
221	-1	As welded	500	2.2	8,000,000+
220	-1	As welded	500	2.2	10,000,000+
210	-1	As welded	450	2.0	7,000,000+
217	$-\infty$	As welded	1000	4.5	477,000
215	-1	Coined	1400	6.2	370,000
204	Variable	Load History[2]	800	3.6 Maximum	180 Blocks
208	Variable	Load History	800	3.6 Maximum	181 Blocks
207	Variable	Load History	600	2.7 Maximum	840 Blocks

[1] Life to crack depth of .055 in.

[2] Edited Ford Variable History, 5320 reversals/block

TABLE 10

Observed and Predicted Total Lives
Using Model Proposed by Wang

Specimen or Series	R	Load Range lbf	Initiation Obsv/Pred	Propagation Obsv/Pred	Total Obsv/Pred
				(Cycles, thousands)	
A	0	800	28/470	26/36	54/506
B	0	500	154/>10^4	278/375	432/>10^4
C	0	400	606/>10^4	600/1140	1190/>10^4
D	0	350	2220/>10^4	1430/3000	3650/>10^4
E	-1	1400	10/17	10/2	20/19
F	-1	900	75/153	76/20	151/173
G	-1	500	1670/>10^4	840/375	2510/>10^4
216	0	1000	12/68	13/12	25/80
219	0	600	195/>10^4	125/151	320/>10^4
224	0	400	530/>10^4	410/1140	940/>10^4
209	-1	1000	50/70	100/12	150/82
201	-1	900	90/153	90/20	180/173
218	-1	700	320/2100	330/120	650/2220
203	-1	600	300/>10^4	900/151	1200/>10^4
225	-1	500	2400/>10^4	1100/375	3500/>10^4

TABLE 11

Observed and Predicted Fatigue Crack Initiation Lives
Using the IP Model of the Current Study

Specimen or Series	R	Load Range lbf	a_{th} in.	Observed N_{ath}	Observed $N_{.01}$	Predicted N_I
				(Cycles, thousands)		
A	0	800	0.0020	10	28	53
B	0	500	0.0050	100	154	265
C	0	400	0.0075	500	606	2000
D	0	350	0.0100	2200	2200	7500
E	-1	1400	0.0015	2	10	4
F	-1	900	0.0030	40	75	31
G	-1	500	0.0100	1670	1670	475
216	0	1000	0.0012	5	12	12
219	0	600	0.0033	135	195	180
224	0	400	0.0076	500	530	2070
209	-1	1000	0.0035	35	50	15
201	-1	900	0.0030	60	90	31
218	-1	700	0.0040	230	320	159
203	-1	600	0.0010	300	300	288
225	-1	500	0.0010	2400	2400	474

TABLE 12

Observed and Predicted Fatigue Crack Propagation Lives
Using the IP Model of the Current Study

Specimen or Series	R	Load Range lbf	a_{th} in.	$N_{.055}-N_{ath}$ Obser	Pred	$N_{.055}-N_{.01}$ Obser	Pred
				(Cycles, thousands)			
A	0	800	0.0020	44	55	26	15
B	0	500	0.0050	332	251	278	154
C	0	400	0.0075	700	564	600	471
D	0	350	0.0100	1430	800	1430	800
E	-1	1400	0.0015	18	33	10	5
F	-1	900	0.0030	110	114	76	49
G	-1	500	0.0100	840	921	840	918
216	0	1000	0.0012	20	31	13	5
219	0	600	0.0033	185	134	125	62
224	0	400	0.0076	440	564	410	471
209	-1	1000	0.0035	115	82	100	30
201	-1	900	0.0030	120	114	90	49
218	-1	700	0.0040	420	270	330	171
203	-1	600	0.0010	900	470	900	470
225	-1	500	0.0010	1100	921	1100	921

TABLE 13

Observed and Predicted Total Lives
Using the IP of the Current Study

Specimen or Series	R	Load Range lbf	Load Range kN	Total Life, N_I+N_P Observed	Predicted Using N_{ath}	Predicted Using $N_{.01}$
				(Cycles, thousands)		
A	0	800	3.6	54	108	68
B	0	500	2.2	432	516	419
C	0	400	1.8	1190	2564	2471
D	0	350	1.6	3650	7500	8300
E	-1	1400	6.3	20	37	9
F	-1	900	4.0	151	145	80
G	-1	500	2.2	2510	1396	1396
216	0	1000	4.5	25	43	17
219	0	600	2.7	320	314	242
224	0	400	1.8	940	2634	2541
209	-1	1000	4.5	150	97	45
201	-1	900	4.0	180	145	80
218	-1	700	3.2	650	429	330
203	-1	600	2.7	1200	758	658
225	-1	500	2.2	3500	1396	1396

TABLE 14

Comparison of Different Prediction Models

Model	Coefficient of Variation	Remarks
1. LEFM, Propagation from 0.002 in. (0.05 mm)	0.154	Nonconservative
2. LEFM, Propagation from 0.01 in. (0.25 mm)	0.276	Conservative
3. LEFM, Propagation from a_{th}[1]	0.122	Conservative at long lives
4. LEFM from zero using Pook's initial value of K.	0.063	Best at short lives
5. LEFM with short crack growth up to a_{pz}[2]	0.143	Nonconservative at long lives
6. Initiation only	0.272	Conservative
7. Initiation-Propagation	0.111	Within a factor of two

[1] a_{th} The threshold crack size.

[2] a_{pz} The crack dpeth equal to the notch plastic zone size.

TABLE 15

Observed[1] and Predicted Total Lives
Tensile-Shear Specimens, Galvanized HSLA (16-78B)
R=-1 Loading

Specimen Total Life, N_I+N_P	Load Range				
	lbf	kN	Observed	Predicted Using N_{ath}	Predicted Using $N_{.01}$
				(Cycles, thousands)	
1	1,570	7.1	18	27	8
4	1,400	6.3	31	37	9
3	1,400	6.3	38	37	9
2	1,400	6.3	25	37	9
5	1,124	5.0	68	65	25
8	900	4.0	161	147	80
7	900	4.0	275	147	80
6	900	4.0	233	147	80
13	600	2.7	580	765	657
12	600	2.7	1,217	765	657
11	600	2.7	710	765	657
10	600	2.7	1,420	765	657
9	600	2.7	1,668	765	657
15	550	2.5	1,761	995	845
14	550	2.5	824	995	845
16	500	2.2	>4,200	1,400	1,400
17	500	2.2	>3,000	1,400	1,400

[1]Includes across-width propagation life.

TABLE 16

Observed[1] and Predicted Total Lives
Tensile-Shear Specimens, Galvanized HSLA (16-78B)
R=0 Loading

Specimen	Load Range		Total Life, N_I+N_P		
	lbf	kN	Observed	Predicted	
				Using N_{ath}	Using $N_{.01}$
			(Cycles, thousands)		
1	800	3.6	95	109	68
2	800	3.6	117	109	68
3	800	3.6	115	109	68
4	500	2.2	705	519	419
5	500	2.2	721	519	419
6	500	2.2	741	519	419
7	400	1.8	994	2,640	2,541
8	400	1.8	2,389	2,640	2,541
9	400	1.8	3,100	2,640	2,541
10	400	1.8	3,110	2,640	2,541
11	400	1.8	3,400	2,640	2,541
12	350	1.6	4,229	8,460	8,460
13	350	1.6	6,381	8,460	8,460
14	350	1.6	9,218	8,460	8,460
15	350	1.6	9,527	8,460	8,460
16	350	1.6	19,311	8,460	8,460

[1] Includes across-width propagation life.

TABLE 17

Predictions of Results from Other Research

Reference and Specimen	R Ratio	Load Range lbf	Load Range kN	Total Life, N_I+N_P Reported	Total Life, N_I+N_P Predicted
				(Cycles, thousands)	
Orts (5)					
Standard W=2.0 in.	0.2	460	2.0	5000	2300
		640	2.8	1000	502
		740	3.3	500	311
		890	3.9	200	145
		1030	4.6	100	85
		1170	5.2	50	53
		1620	7.2	10	24
Narrow W=1.0 in.	0.2	400	1.8	1200	2290
		420	1.9	1000	1460
		500	2.2	500	339
		640	2.7	200	195
		780	3.5	100	87
		920	4.1	50	55
Wide W=2.75 in.	0.2	580	2.5	2000	1690
		625	2.8	1370	1250
		666	3.0	1000	980
		770	3.4	500	650
		920	4.1	200	300
		1000	4.4	100	217
		210	5.4	50	109
		1670	7.4	10	42
Standard Coined	0.2	790	3.5	5000	2000
		890	4.0	2000	500
		960	4.3	1000	210
		1050	4.7	500	106
		1300	5.8	100	49
		1400	6.2	50	39
		1700	715	10	23

TABLE 18

Predictions

Reference and Specimen	R Ratio	Load Range lbf	Load Range kN	Total Life, N_I+N_P Reported	Total Life, N_I+N_P Predicted
				(Cycles, thousands)	
Shinozaki (14)	0	450	2.0	10,000	100,000
PPT. Hardening		560	2.5	5,000	30,000
		690	3.1	2,000	2,500
		860	3.7	1,000	770
		1,125	5.0	500	300
		1,400	6.2	200	150
		1,800	8.0	100	62
PPT. Hardening	0	910	5.0	10,000	12,000
With Temper		1,000	4.5	2,000	4,100
		1,125	5.0	1,000	1,600
		1,350	6.0	500	430
		1,800	8.0	200	77
Dual-Phase	0	620	2.7	5,000	100,000
		810	3.6	2,000	16,000
		1,010	4.5	1,000	2,500
		1,260	5.6	500	1,100
		1,590	7.1	200	324
		1,940	8.6	100	106
Dual-Phase	0	1,070	4.7	10,000	15,000
With Expulsion		1,170	5.2	5,000	8,000
		1,410	6.3	2,000	1,600
		1,460	6.5	1,000	1,270
		1,800	8.0	500	231

TABLE 19

Predictions

Reference and Specimen	R Ratio	Load Range lbf	Load Range kN	Total Life, N_I+Np Reported	Total Life, N_I+Np Predicted
				(Cycles, thousands)	
Kitagawa (15)	0	200	0.89	2,000	40,000
TS=315 MPa		210	0.93	1,000	10,000
		265	1.2	500	2,000
		315	1.4	200	475
		360	1.6	100	230
TS=400 MPa	0	200	0.89	5,000	21,200
		240	1.1	2,000	4,000
		285	1.3	1,000	1,100
		320	1.4	500	404
		400	1.8	200	170
		460	2.0	100	110
Cooper and Smith (8)					
	0.32	290	1.3	2,000	42,000
	0.12	430	1.9	800	1,930
	0.03	540	2.4	400	475

TABLE 20

Observed Distances Between Section Plane and Crack Initiation Site for Presectioned Specimens

Specimen No.	R Ratio	Load Range lbf	Life (in thousands or blocks-b)	Distances in.		Notes
201	-1	900	180	.02	.01	
202						damaged[1]
203	-1	600	1200	.015		
204	vlh	600max	180b	.01		<
205						not used
206						not used
207	vlh	600max	750b	.01		
208	vlh	800max	181	.005	.005	
209	-1	1000	150	.01	.005	
210	-1	450	>7000			runout
211					damaged in machining	
212						"
213						"
214						"
215	-1	1200	370	.01	.01	
216	0	1000	25			damaged
217	$-\infty$	1000	400	.01	.005	
218	-1	700	600	.01	<.005	
219	0	600	320	.01	<.005	
220	-1	500				runout
221	-1	500				runout
222	-1	500	1857	.01	<.005	
223						damaged
224	0	400	940			
225	-1	500	3500	.01	<.005	

[1] Indicates that information was not available from marred fracture surface.

TABLE 21

Distances between Maximum Crack Depth and Centerline of Nugget

Specimen ID	Percent Life	Maximum Crack Depth (in.) Primary	Maximum Crack Depth (in.) Secondary	Distance (in.) Primary	Distance (in.) Secondary
A Series: 800 lbf (3.6 kN) Load Range, R=0, Average Life: 54,000 Cycles					
AH	9	0.0011	None	0.009	
AC	19	0.0023	0.0006	0.013	0.024
AN	28	0.0077	0.0004	<.005	<.005
AT	28	0.0100	0.0030	NA	NA
AD	37	0.0043	0.0026	NA	NA
AU	46	0.0066	0.0050	NA	NA
AQ	56	0.0084	0.0031	0.009	0.017
A3	74	0.0602	0.0192	0.016	0.016
A4	93	0.0434	0.0049	<.005	<.005
A5	>100	0.0448	0.0079	<.005	<.005
B Series: 500 lbf (2.2 kN) Load Range, R=0, Average Life: 431,000 Cycles					
BH	12	0.0033	None	<.005	
BC	23	0.0045	0.0013	<.005	0.009
B3	42	0.0148	0.0039	<.005	<.005
BS	46	0.0254	0.0049	<.005	0.007
B4	59	0.0463	0.0164	<.005	<.005
BT	70	0.0128	0.0087	0.007	0.013
B5	75	0.0291	0.0042	<.005	<.005
BD	93	0.0551	0.0527	<.005	<.005
BU	>100	0.0529	0.0528	0.011	0.009
C Series: 400 lbf (1.8 kN) Load Range, R=0, Average Life: 1,200,000 Cycles					
C9	17	0.0060	None	0.008	
CA	32	0.0011	None	<.005	
C4	42	0.0255	None	<.005	
CB	54	0.0061	None	<.005	
C10	67	0.0240	None	0.010	
C11	94	0.0476	None	0.007	
CC	>100	0.0033	0.0010	0.011	<.005
D Series, 350 lbf (1.6 kN) Load Range, R=0, Average Life: 3,650,000 Cycles					
D8	27	0.0025	None	<.005	
D11	69	0.0115	None	<.005	
D6	96	0.0515	None	<.005	
D7	>100	0.0006	None	<.005	

(Continued)

TABLE 21 (Continued)

Distances between Maximum Crack Depth and Centerline of Nugget

Specimen ID	Percent Life	Maximum Crack Depth (in.) Primary	Maximum Crack Depth (in.) Secondary	Distance (in.) Primary	Distance (in.) Secondary
E Series: 1400 lbf (6.2 kN) Load Range, R=-1, Average Life: 20,000 Cycles					
26	10	0.0029	None	<.005	
8	20	0.0024	0.0014	<.005	<.005
9	20	0.0055	0.0045	<.005	0.025
27	30	0.0050	0.0037	0.018	0.005
14	40	0.0052	0.0030	<.005	0.010
15	40	0.0363	0.0214	0.010	0.020
28	50	0.0133	0.0084	0.014	0.014
16	60	0.0166	0.0121	0.021	0.021
17	60	0.0120	0.0085	0.009	0.020
32	70	0.0146	0.0084	NA	NA
18	80	0.0198	0.0079	0.010	0.010
25	80	0.0272	0.0076	<.005	<.005
F Series: 900 lbf (4.0 kN) Load Range, R=-1, Average Life: 151,000 Cycles					
50	12	0.0007	None	<.005	
35	24	0.0071	0.0019	0.009	<.005
36	24	0.0057	0.0019	0.016	<.005
37	36	0.0074	0.0029	0.016	0.009
41	48	0.0170	0.0032	<.005	<.005
42	48	0.0111	0.0043	<.005	0.029
43	60	0.0198	0.0087	0.010	0.010
44	72	0.0097	0.0075	0.012	<.005
45	72	0.0550	None	NA	NA
46	84	0.0095	0.0063	0.010	0.019
47	96	0.0550	0.0163	<.020	0.020
G Series: 500 lbf (2.2 kN) Load Range, R=-1, Average Life: 1,200,000 Cycles					
61	21	0.0019	0.0004	0.014	0.008
63	31	None	None		
13	42	0.0012	None	0.020	
21	50	0.0009	0.0006	0.006	0.006
29	60	0.0007	None	<.005	
30	60	0.0004	0.0002	<.005	0.005
40	70	0.0540	None	<.005	
38	80	0.0014	0.0006	0.010	0.010
49	80	0.0115	None	<.005	<.005
39	90	0.0035	None	<.005	

(Continued)

TABLE 21 (Continued)

Distances between Maximum Crack Depth and Centerline of Nugget

Specimen ID	Percent Life	Maximum Crack Depth (in). Primary	Secondary	Distance (in.) Primary	Secondary
II Series: 1400 lbf (6.2 kN) Load Range, R=-1, Average Life: 400,000 Cycles Specimens Treated by Coining Method, 10,000 lbf (45 kN)					
118	13	0.0173	0.0030	<.005	0.008
106	25	0.0149	0.0107	0.013	<.013
119	25	0.0252	0.0145	0.013	0.017
107	50	0.0163	0.0071	<.005	<.005
108	100	0.0328	0.0215	<.005	<.005
I Series: 800 lbf (3.6 kN) Maximum Load Average Life: 143 Blocks Edited Ford Variable Load History					
113	10	0.0066	None	<.005	
114	20	0.0057	0.0024	0.017	<.005
115	30	0.0410	0.0030	0.024	<.005
116	60	0.0271	0.0136	<.005	0.017
117	80	0.0379	0.0040	0.010	0.010

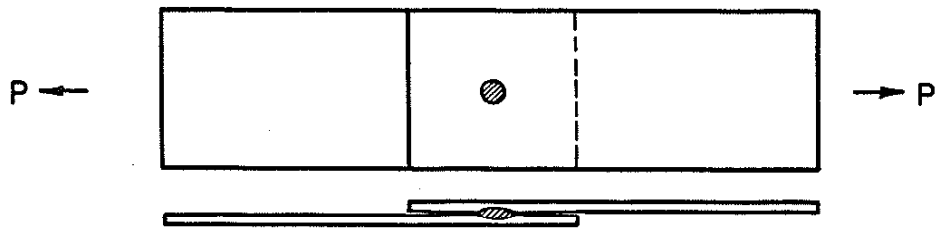

TS: TENSILE-SHEAR

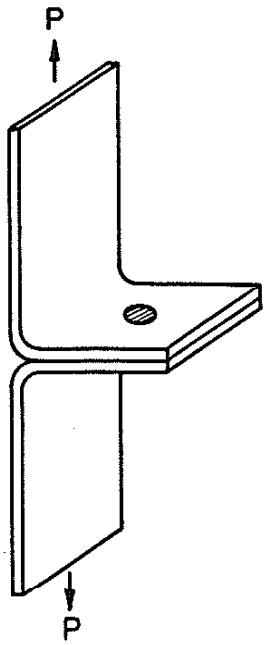

CP: COACH-PEEL

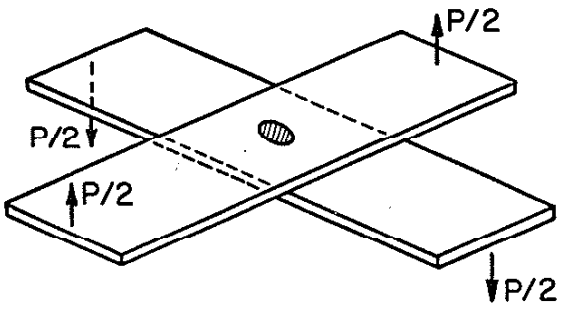

CT: CROSS-TENSION

Fig. 1 Common Test Configurations for Spot Weldments. TS: Tensile-Shear, CP: Coach-Peel, CT: Cross-Tension.

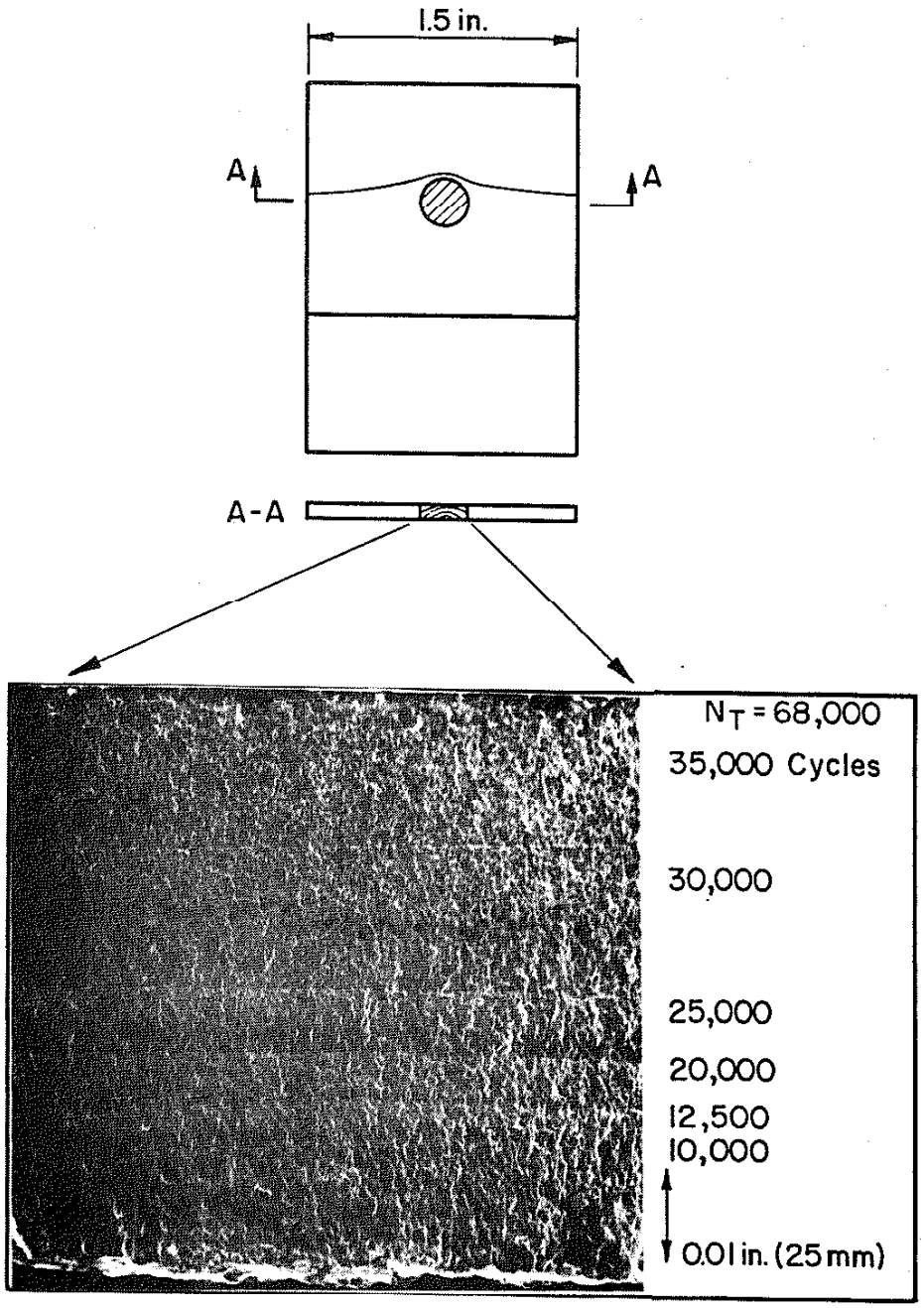

Fig. 2 Fatigue Crack Propagation in a TS Spot Weldment. Section A-A shows fatigue crack striations produced by overloads during fatigue. SEM magnification: 45 X.

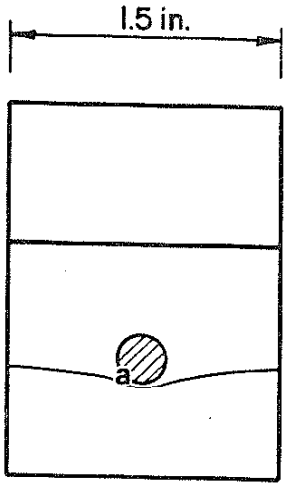

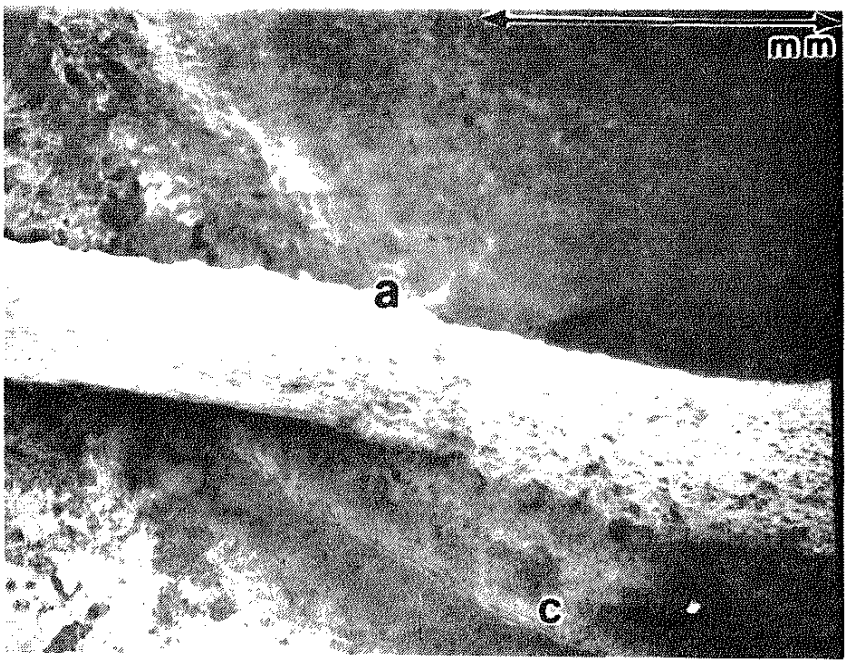

Fig. 3 Transition Between Stage II and Stage III. Through-thickness propagation (Stage II) is followed by across-width propagation (Stage III) which begins at point "a". Point "c" denotes the normal ring of zinc explusion.

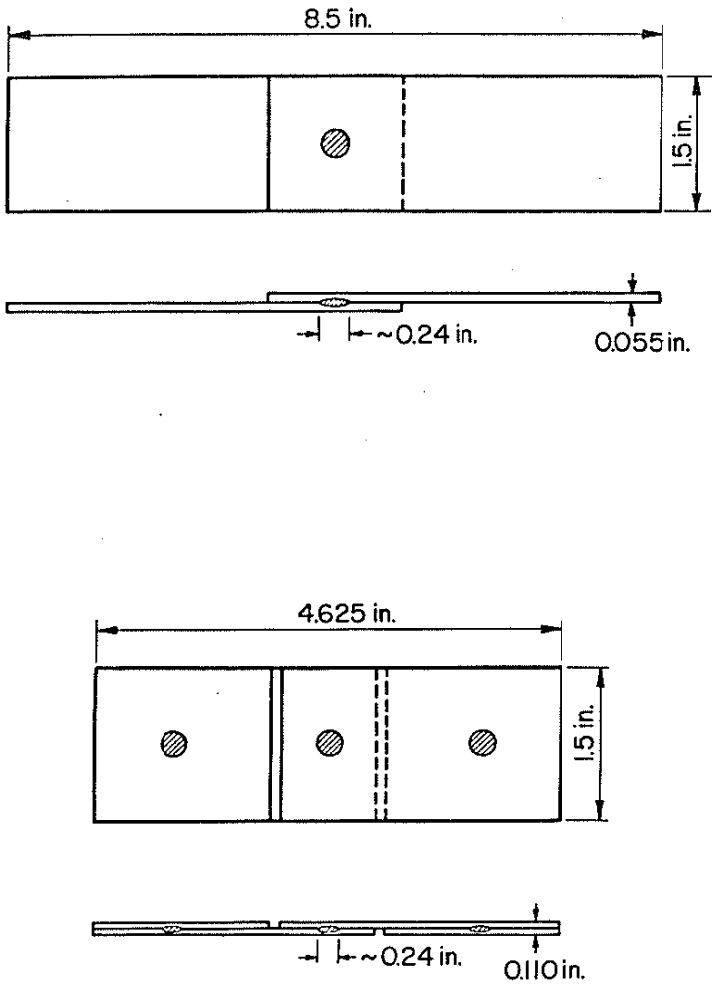

Fig. 4 Standard Tensile-Shear Spot Weldment Fatigue Test Specimens. Top: R = 0 specimen. Bottom: R = -1 specimen. Shorter specimens were used for R = -1 testing to minimize buckling problems.

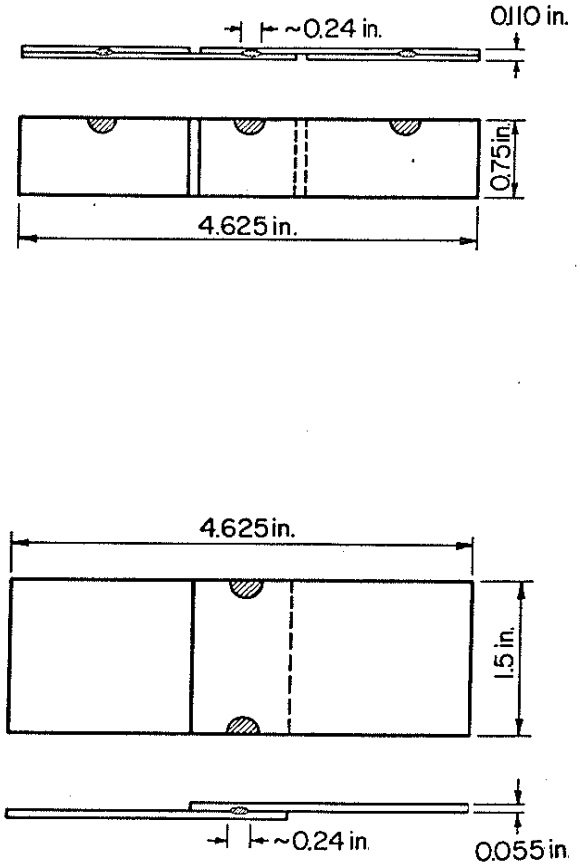

Fig. 5 Presectioned Specimens Used for Fatigue Crack Monitoring. Top: Initial design which was abandoned because of asymmetric loading. Bottom: Final design used for this study was symmetric. Cracks on the exposed sections of both "half-nuggets" were monitored during fatigue testing.

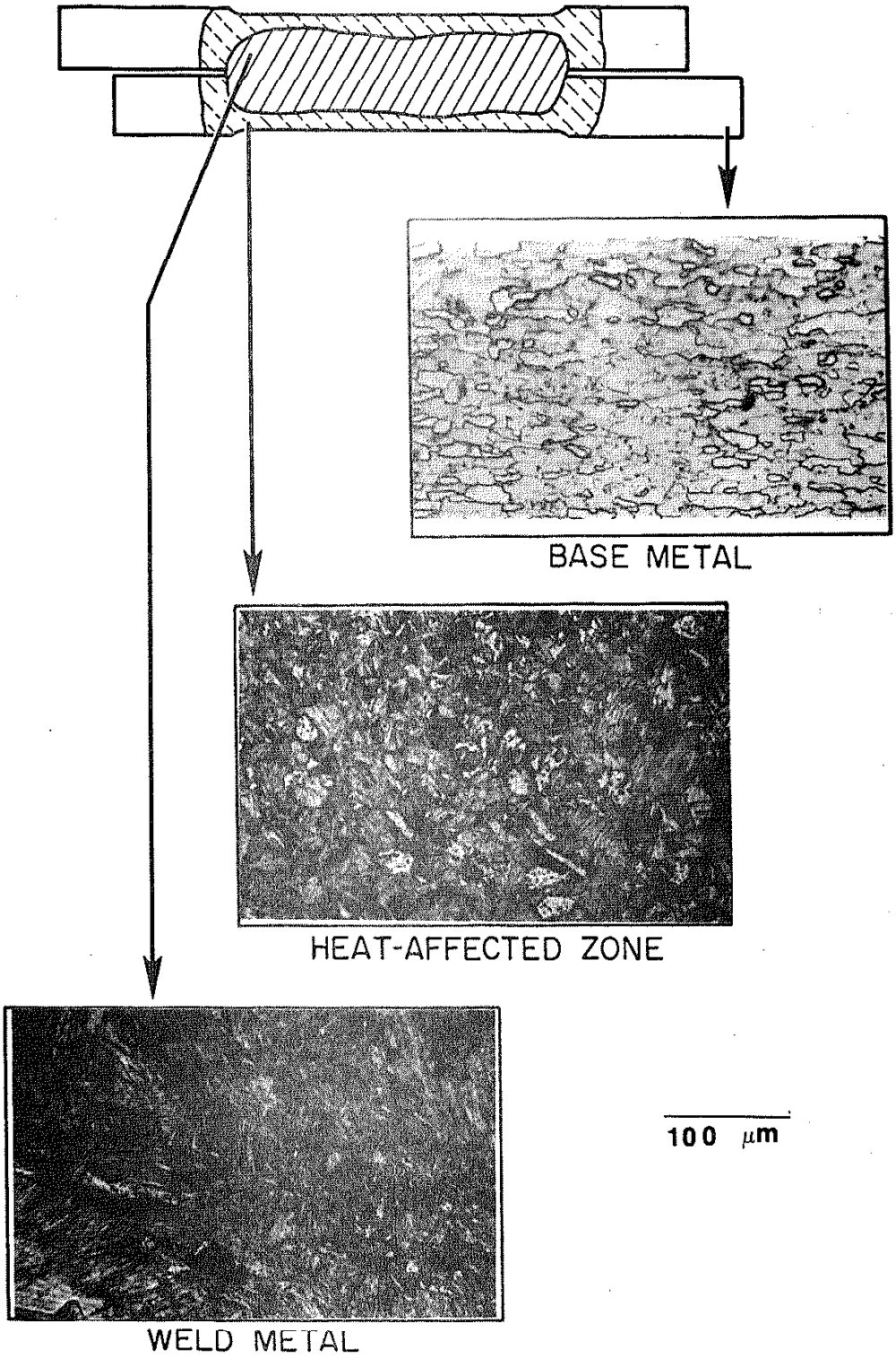

Fig. 6 Metallographic Sections of The Base Metal (Top), Heat-Affected Zone (Middle), and Weld Metal (Bottom). Etch: 2% Nital, Magnification: 200 X.

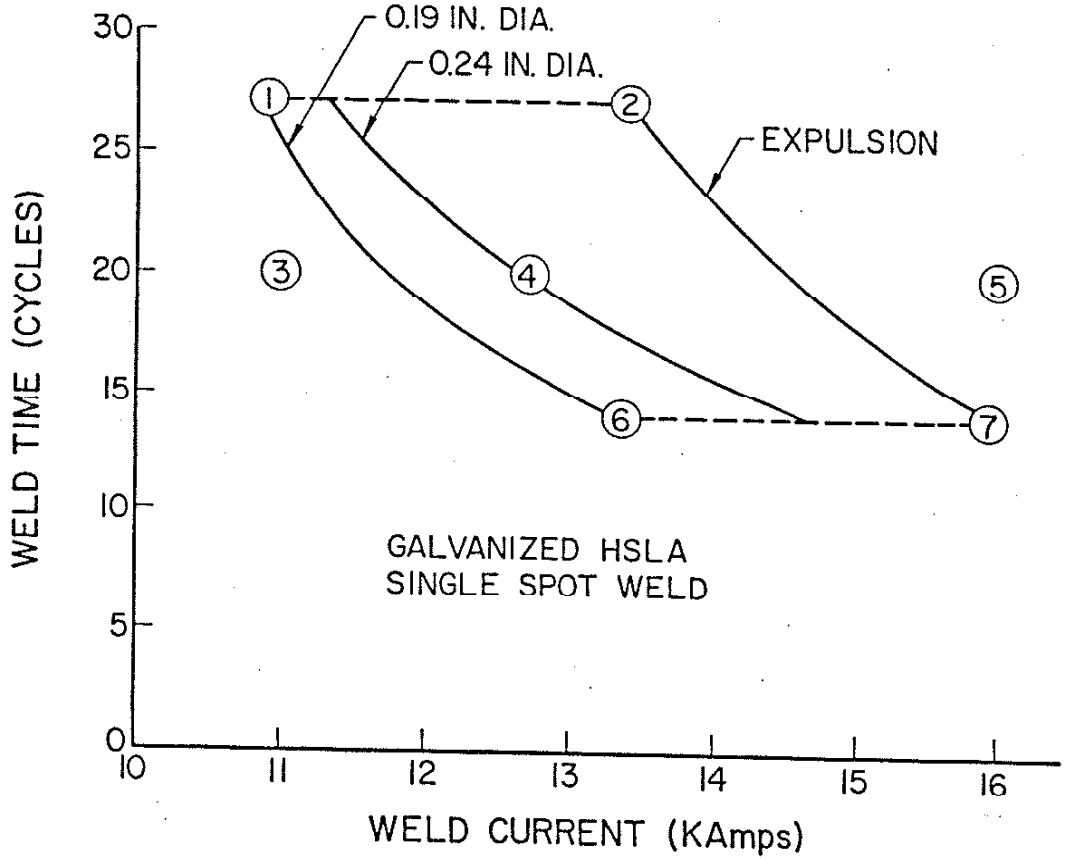

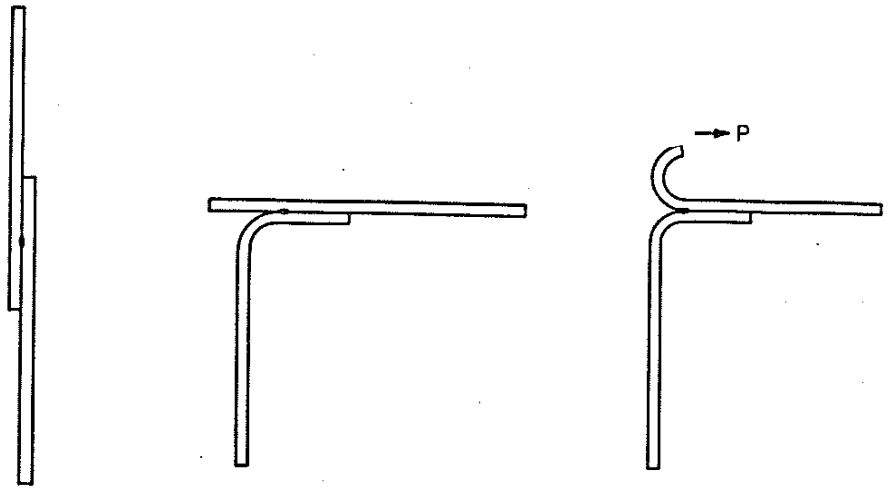

Fig. 7 Top: Welding Lobe Diagram for Galvanized HSLA (16-78 B) Spot Welds. Constant nugget diameter conditions are represented by the solid lines. Point 4 represents nominal welding conditions. Bottom: Schematic of Peel Test Used to Determine Nugged Diameter.

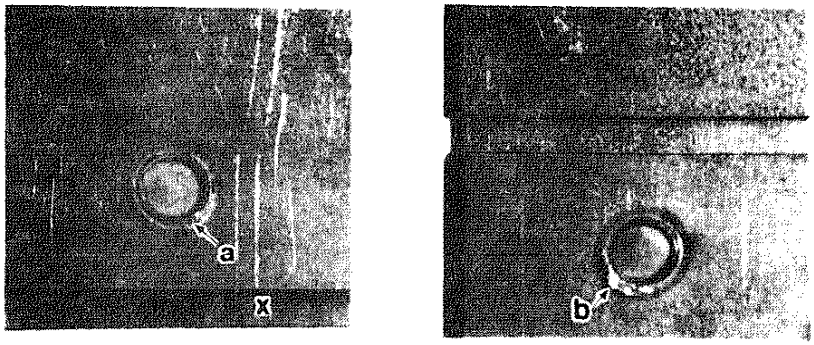

Front **Back**

A-B. Front and Back Surface Details

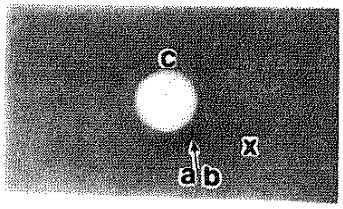

C. Unground Specimen Radiograph

D. Ground Specimen Radiograph

x Expulsion
a,b Various Surface Details, Zinc Build-Up
c Normal Ring of Expelled Zinc

Fig. 8 Radiographic Inspection of Spot Welds. A and B show the front and back surfaces of a weldment. Various surface details (a,b) appear on the radiograph of the unground specimen (Fig. 8-C) but are absent on that of the ground specimen (Fig. 8-D). Remaining details in Fig. 8-D are those in the interface between the two welded sheets. Magnification: 1.3 X.

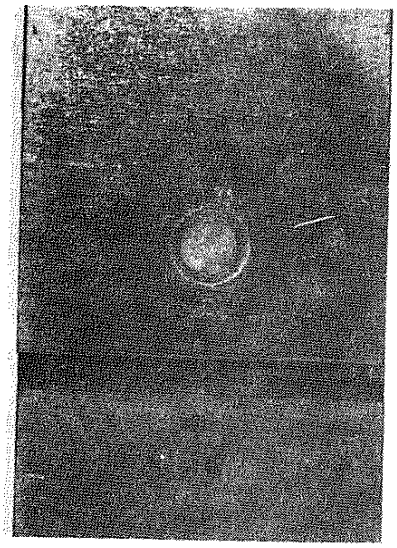

Untested Specimen, 1.3x

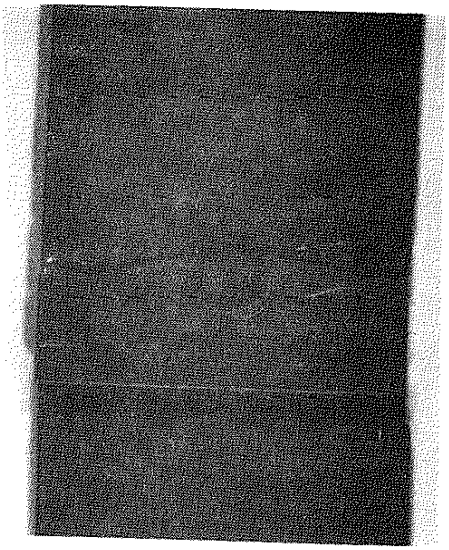

After Fatigue 1.3x

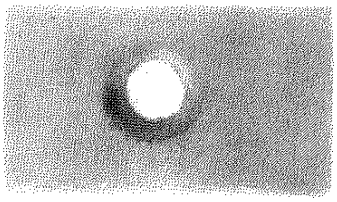

Radiograph of Nugget with Bulge, 1.3x

Fig. 9 Bulge (detail e) in Nugget. Specimens having noncircular nugget shapes were rejected.

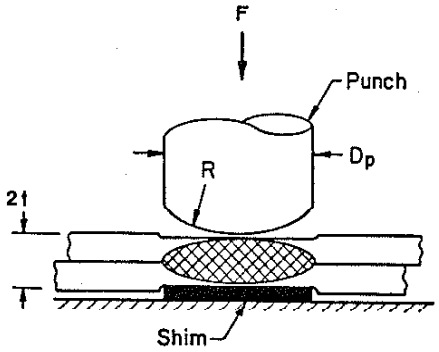

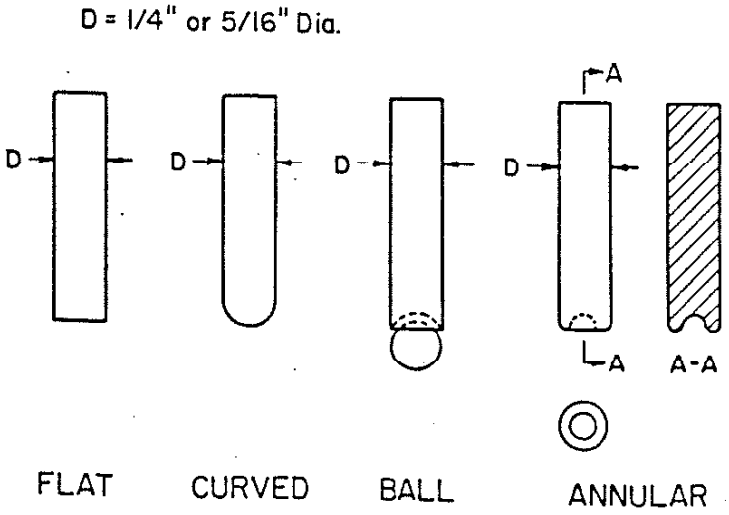

Fig. 10 Schematic of The Coining Fatigue-Strength Improvement Technique. The compressive force of coining leaves compressive residual stresses in the notch-root area. Different pins can be used for coining (lower diagram). The curved pin design was used for the current study.

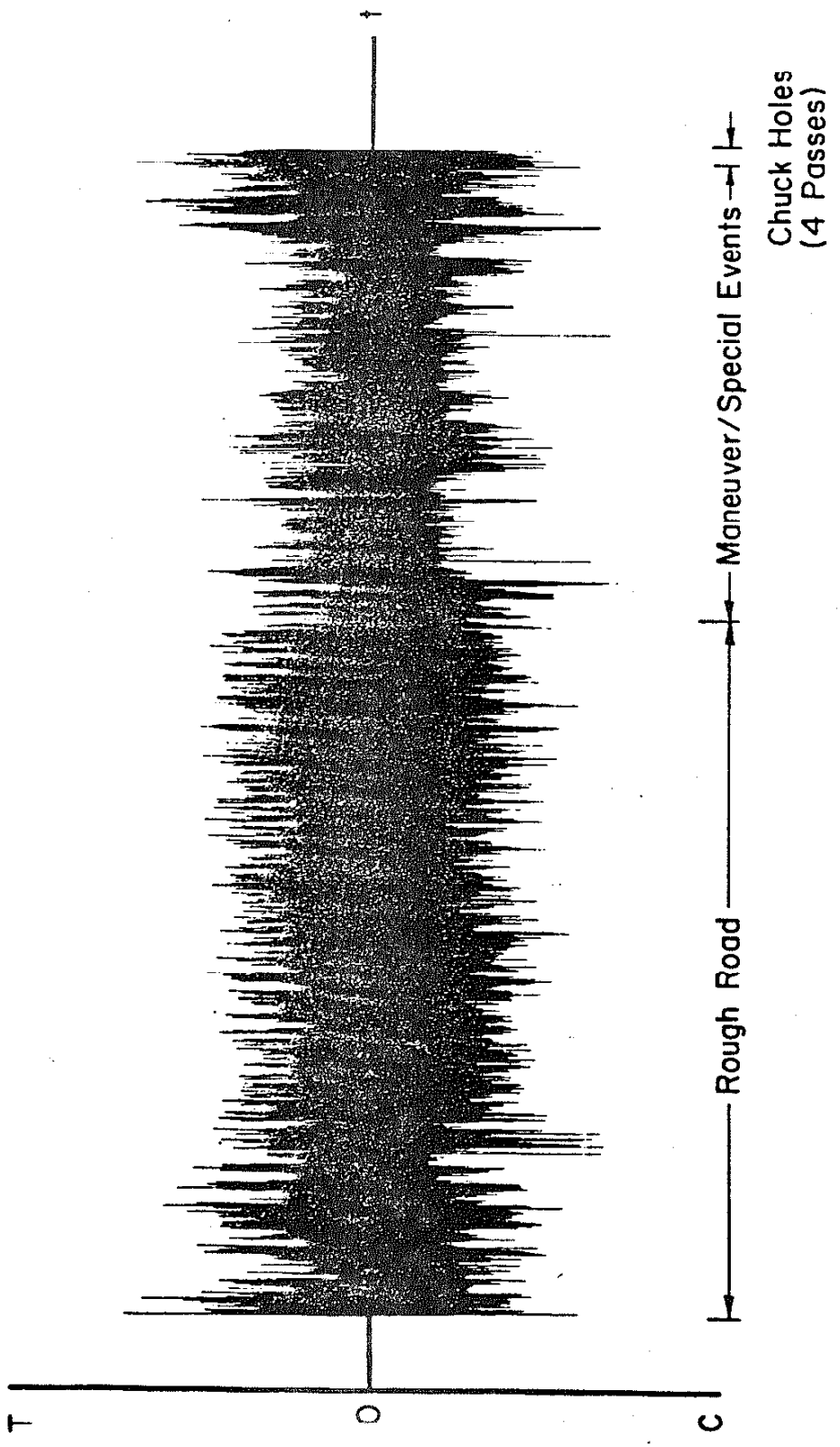

Fig. 11 Trace of The Edited Ford History. The history contains 5320 reversals and has a mean stress close to zero.

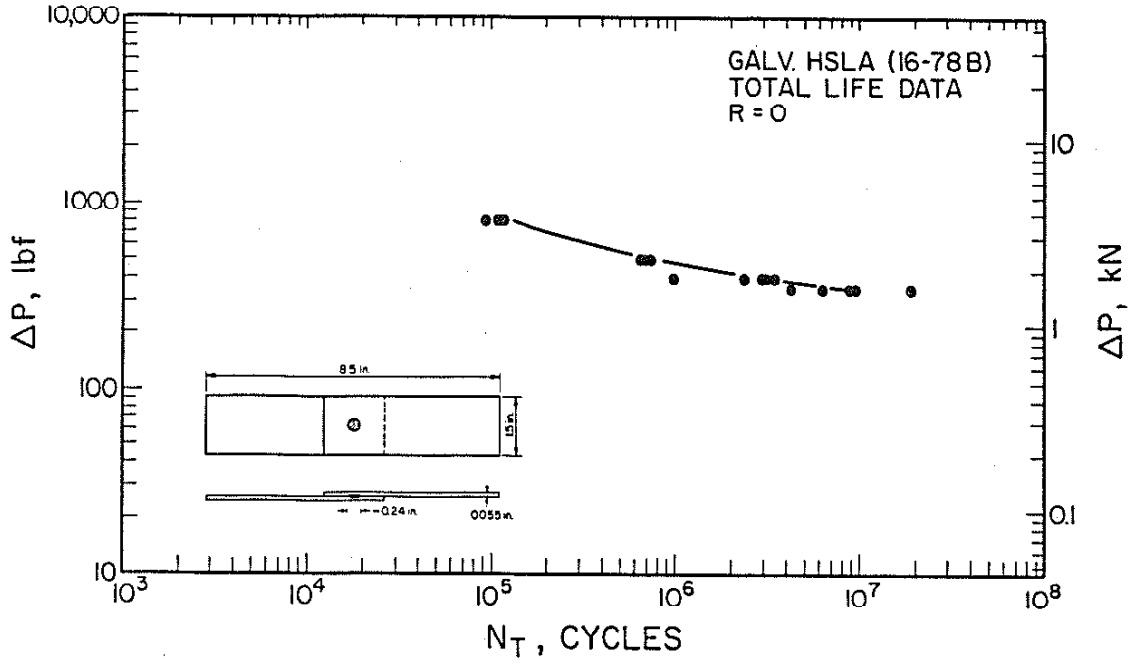

Fig. 12 Base-Line Fatigue Data for Galv. HSLA (16-78 B), R=0.

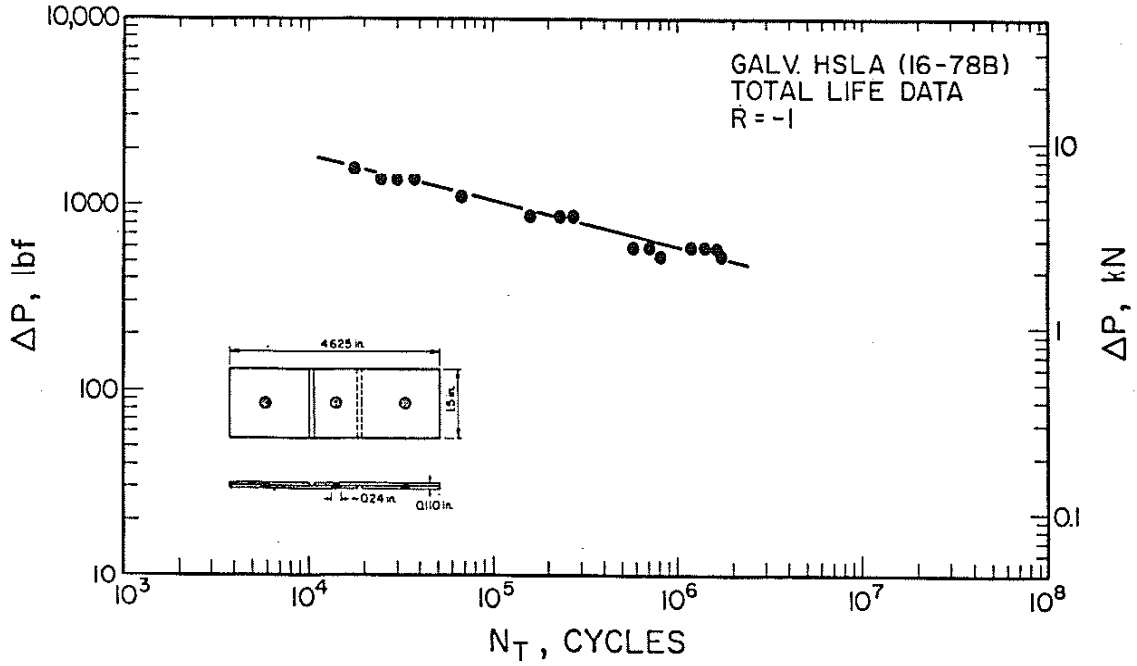

Fig. 13 Base-Line Fatigue Data for Galv. HSLA (16-78 B), R=-1.

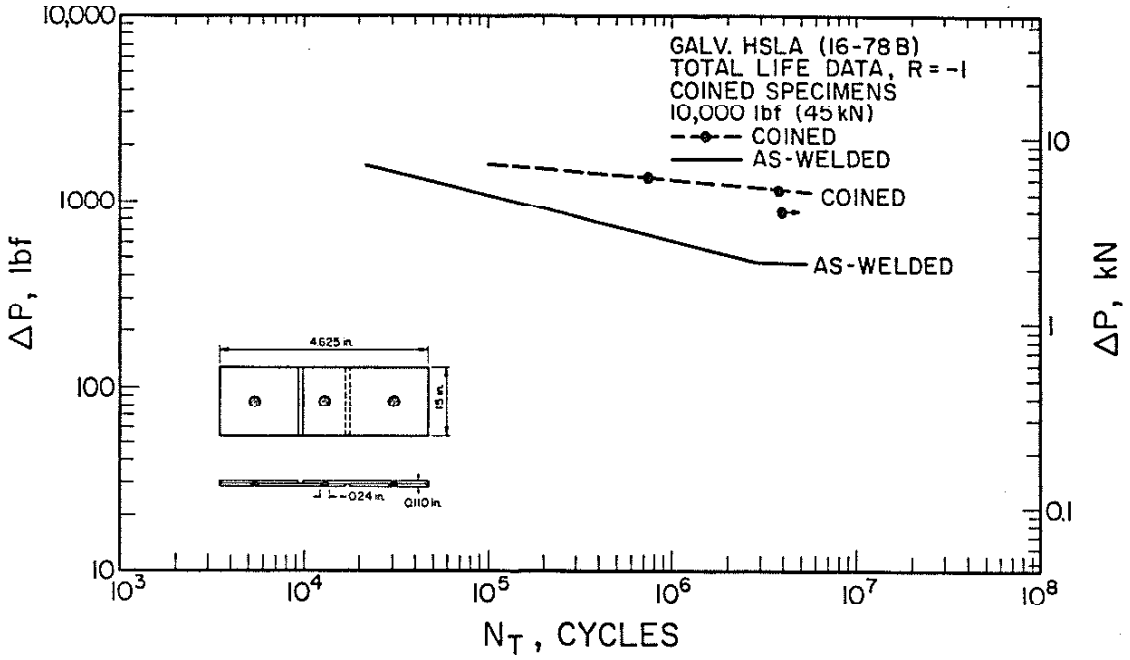

Fig. 14 Base-Line Fatigue Data for Coined Galv. HSLA (16-78 B), R=-1. Coining load: 10,000 lbf (45 kN).

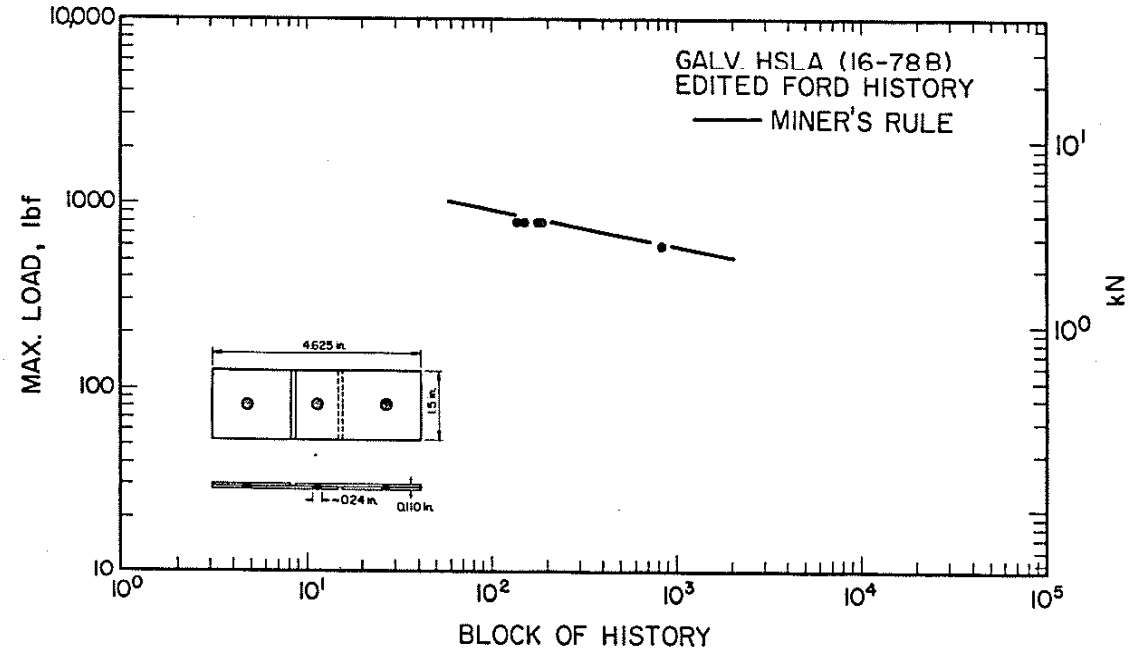

Fig. 15 Base-line Fatigue Data for Galv. HSLA (16-78 B), Edited Ford History. Life predicted by Miner's Rule (linear damage summation) shown by solid line.

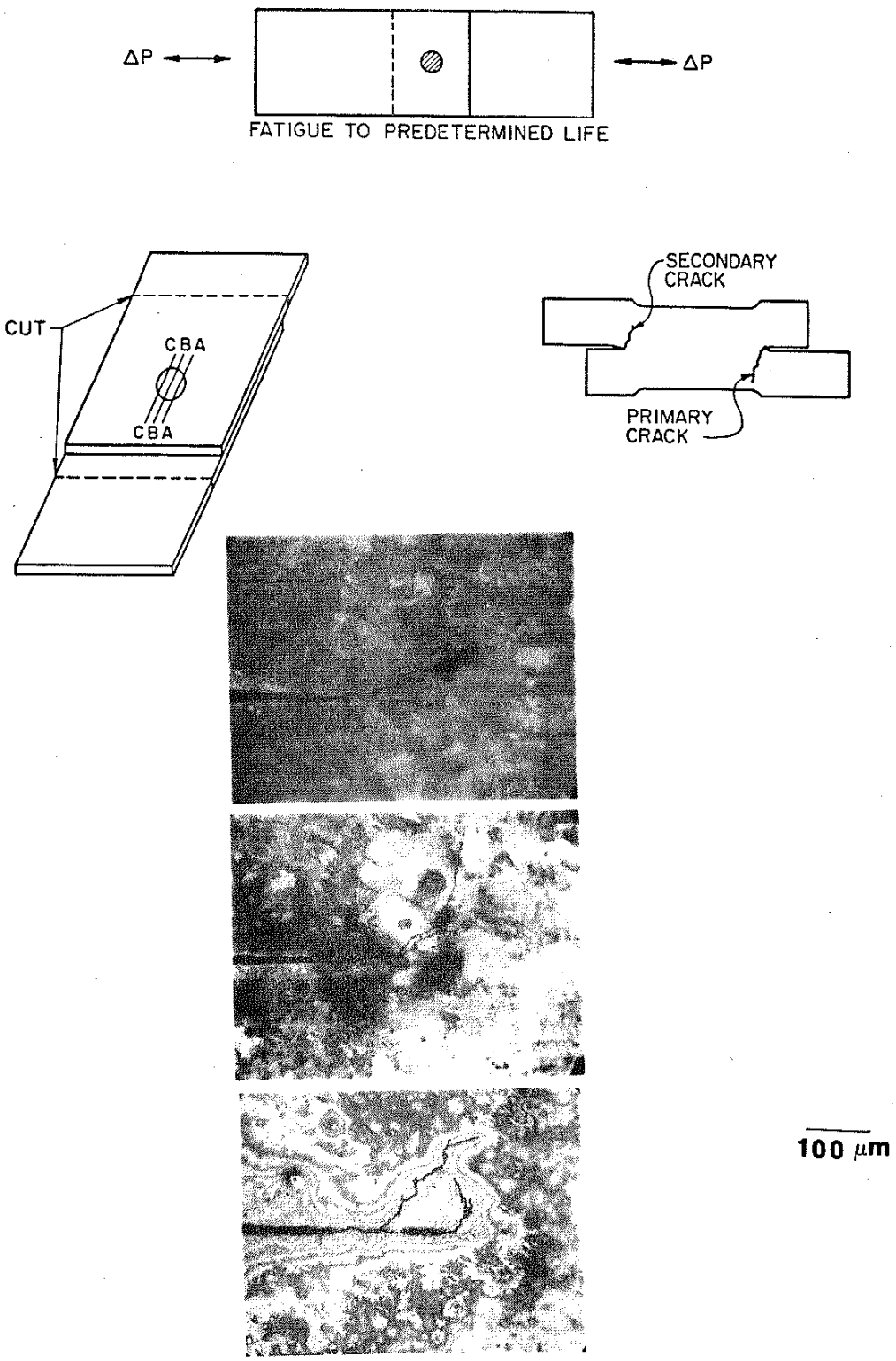

Fig. 16 Schematic of the Sectioning of Companion Specimens. Successive sections (AA,BB,CC...) are exposed by polishing through the nugget which reveal the shape and depth of the fatigue crack (see lower photographs).

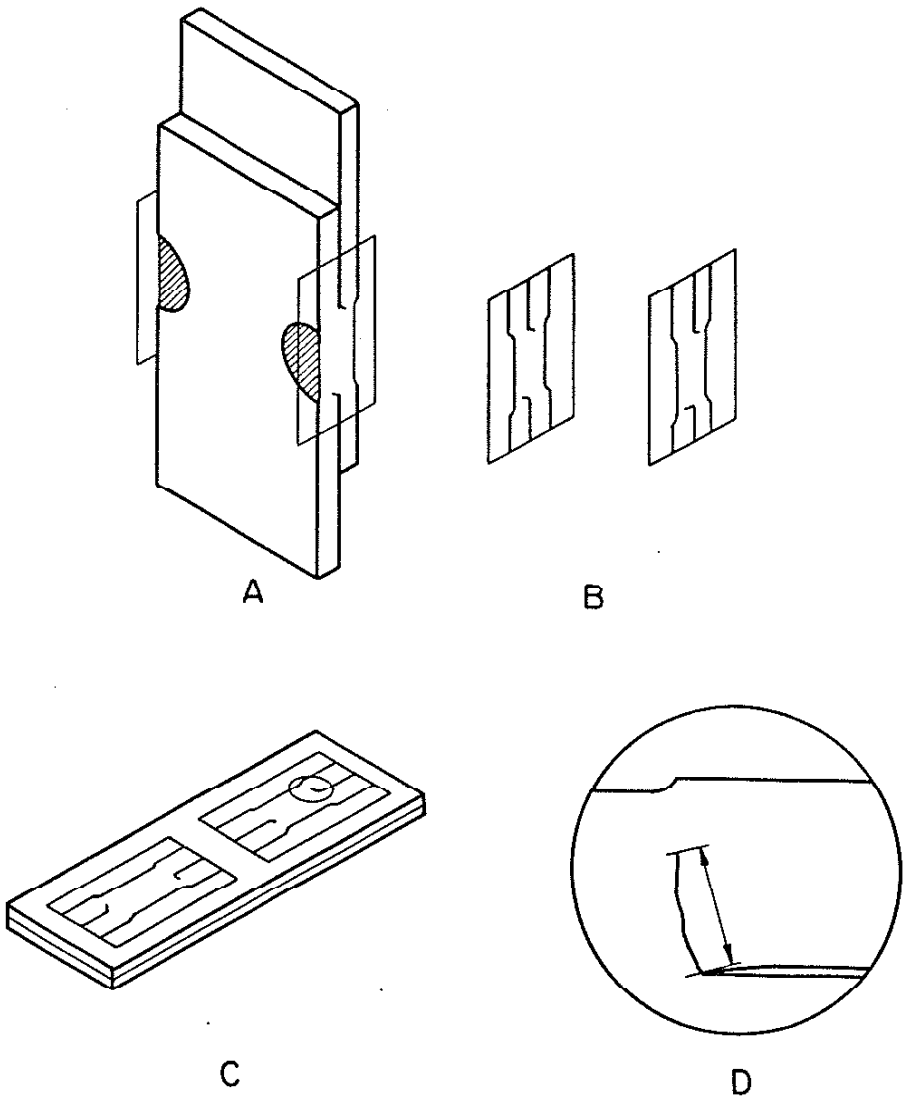

Fig. 17 Schematic of the Presectioned-Specimen Method of Monitoring Fatigue Cracks in Spot Weldments. A: Replicas are made of the exposed surfaces. B: Replicas can be removed while the specimen remains gripped in the fatigue testing machine. C: The replicas are placed between glass microscope slides. D: The replicas of the fatigue cracks are measured under a microscope using a calibrated eyepiece.

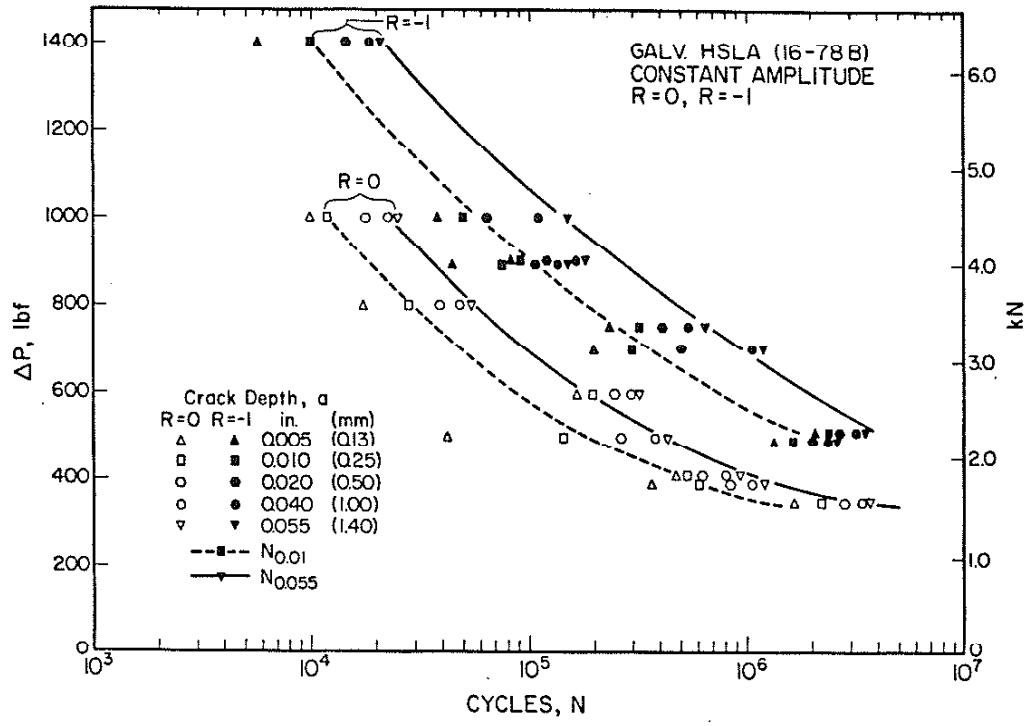

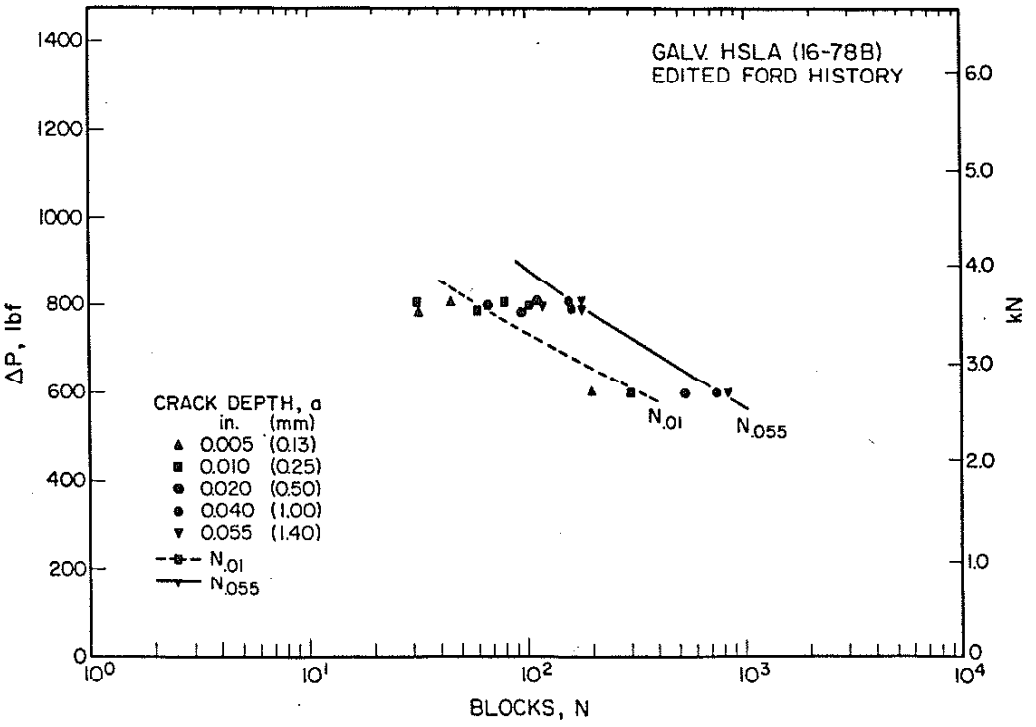

Fig. 18 (Top) Summary of R=0 and R=-1 Constant Amplitude Fatigue Test Results of Both Companion and Presectioned Specimens.

Fig. 19 (Bottom) Variable History Loading. For both figures the different shaped symbols represent the observed fatigue crack depths over the life of the specimens. Fatigue crack initiation (as defined as a 0.01 inch crack) and total life are represented by the dashed and solid lines, respectively.

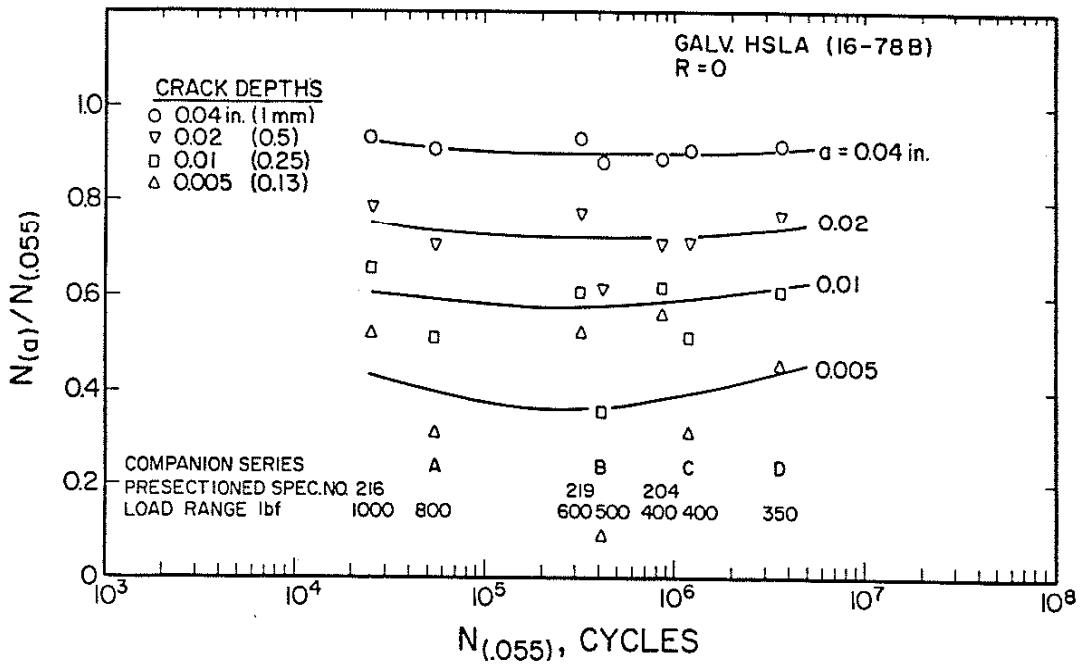

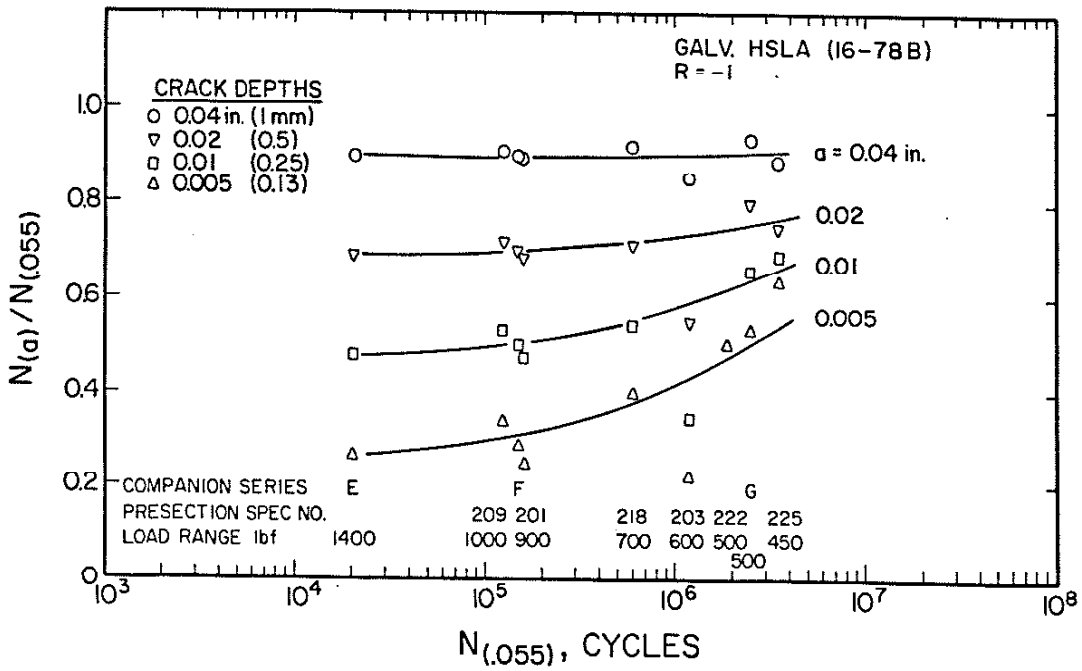

Fig. 20 (Top) Fraction of Life for Fatigue Cracks to Grow to Different Depths vs. Total Life, R=0 Tests.

Fig. 21 (Bottom) Fraction of Life for Fatigue Cracks to Grow to Different Depths vs. Total Life, R=-1 Tests. Results of both the companion and presectioned specimens are shown.

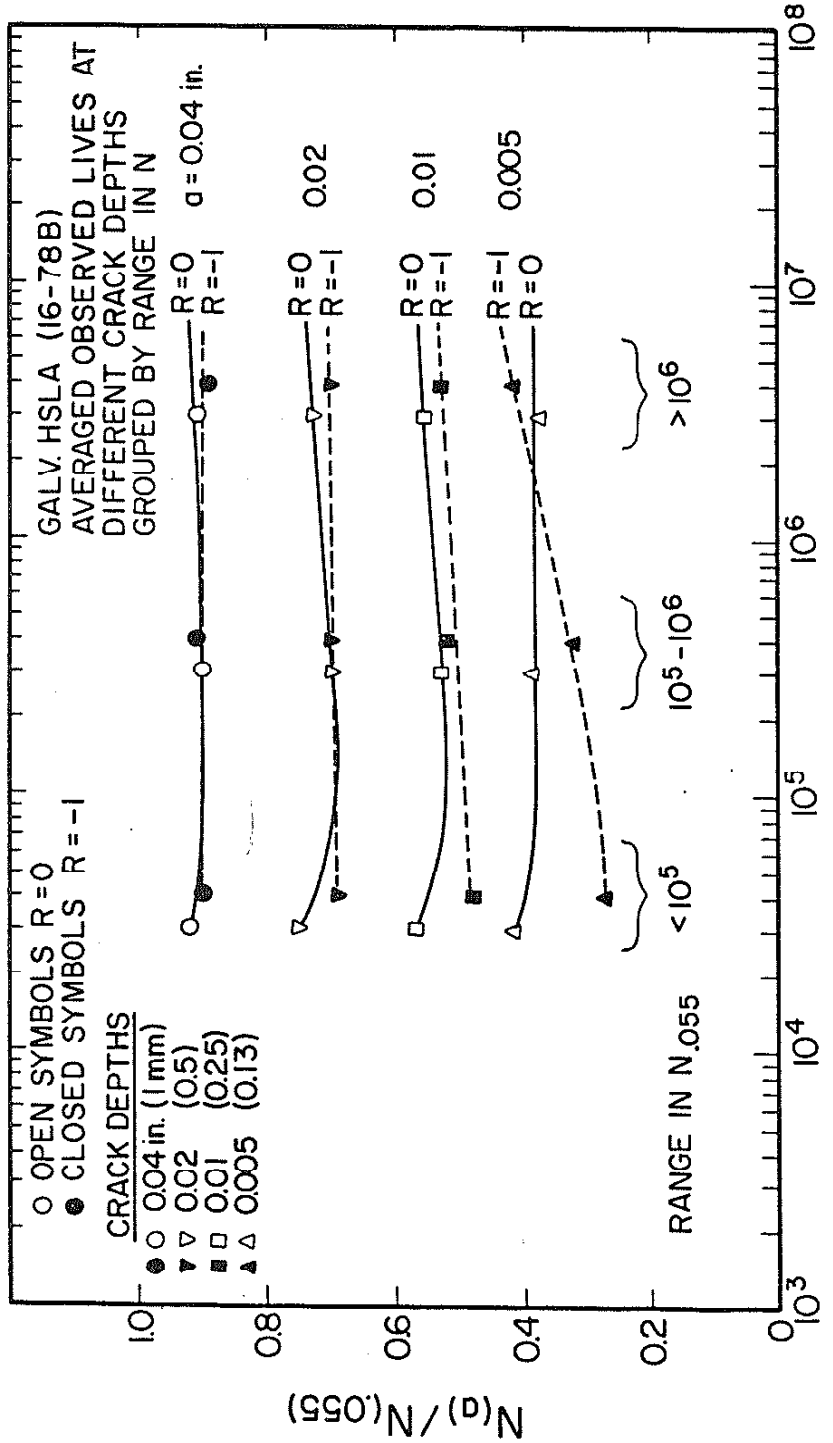

Fig. 22 Summary of Figures 21 and 22. Data was grouped by range in total life: less than 10^5 cycles; 10^5 to 10^6 cycles; and greater than 10^6 cycles.

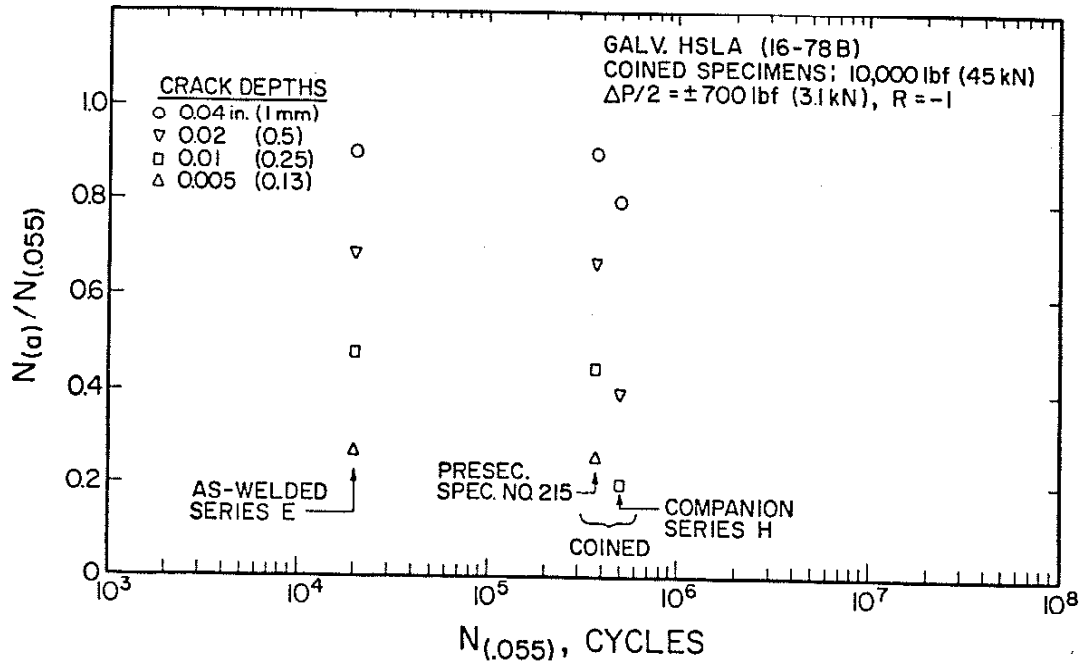

Fig. 23 Fraction of Life for Fatigue Cracks to Grow to Different Depths vs. Total Life for As-Welded and Coined Specimens.

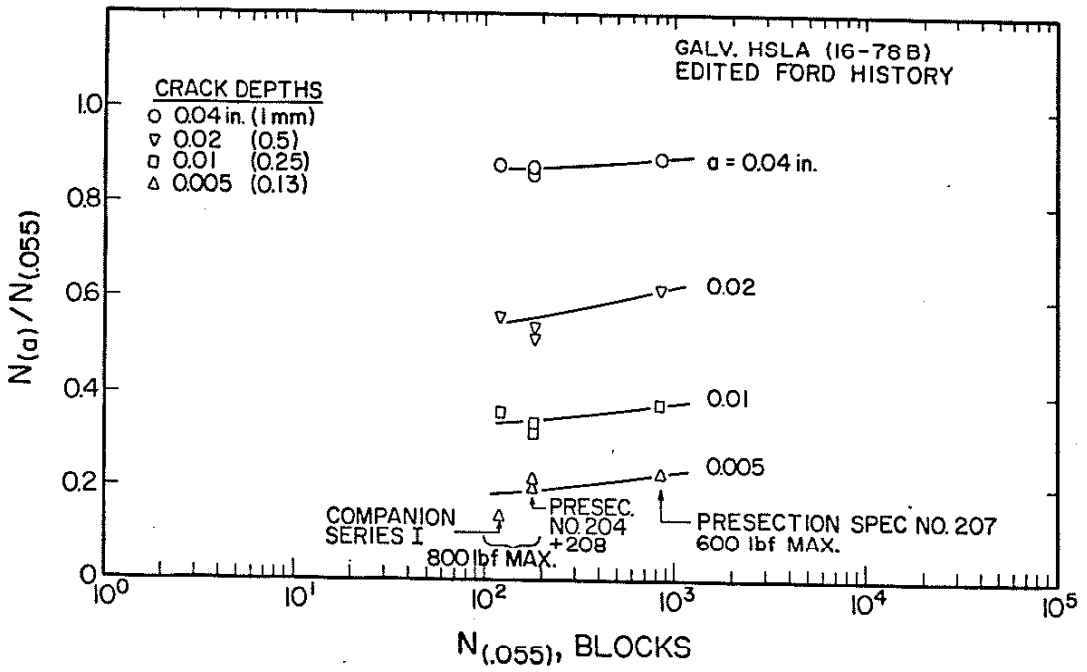

Fig. 24 Fraction of Life for Fatigue Cracks to Grow to Different Depths vs. Total Life for Specimens Tested under The Edited Ford History.

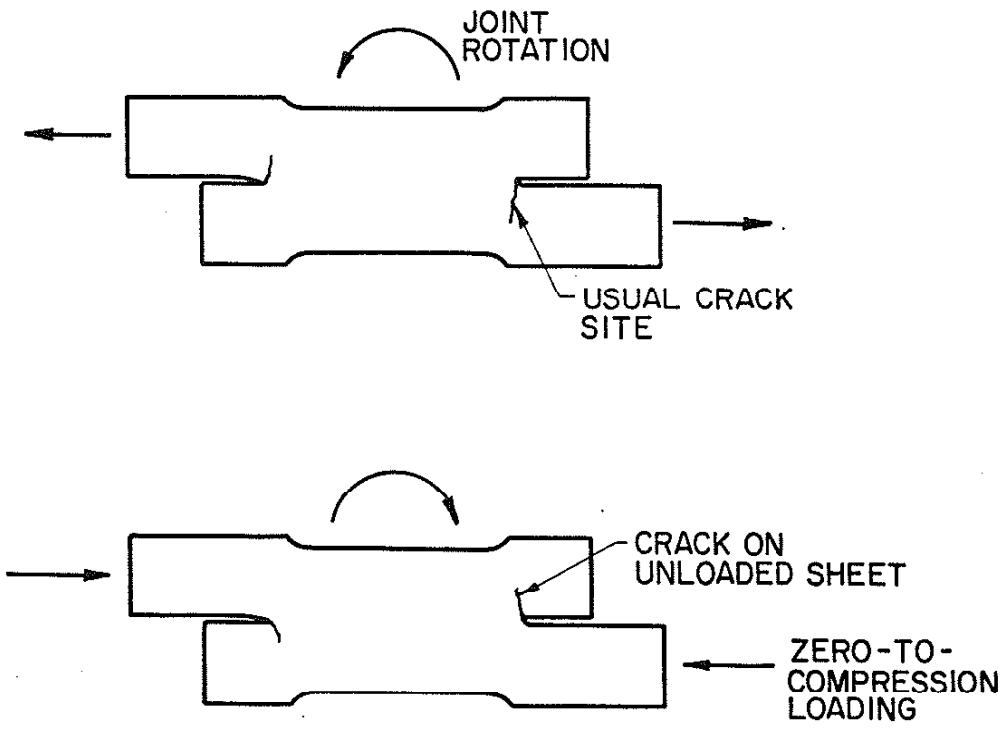

Fig. 25 Anomalous Fatigue Crack Site in a Specimen Subjected to Zero-to-Compression Loading. Top diagram shows usual crack site and direction of nugget rotation when loaded in tension. Lower diagram shows nugget rotation in the specimen subjected to reverse loading. This rotation caused the unloaded sheet to hit the gripped sheet and caused a bending moment to be placed on the "unloaded" sheet which shifted the crack site to the new location.

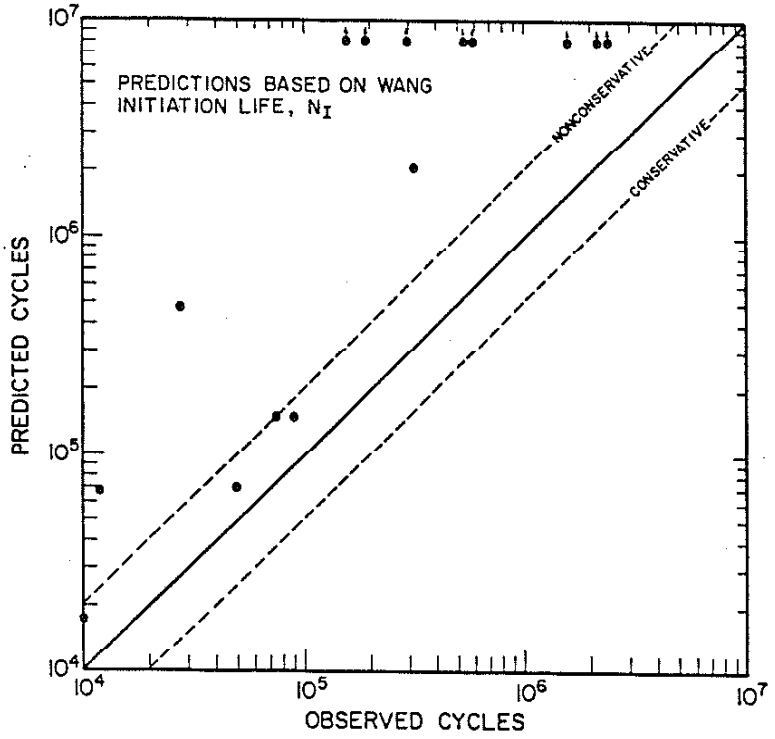

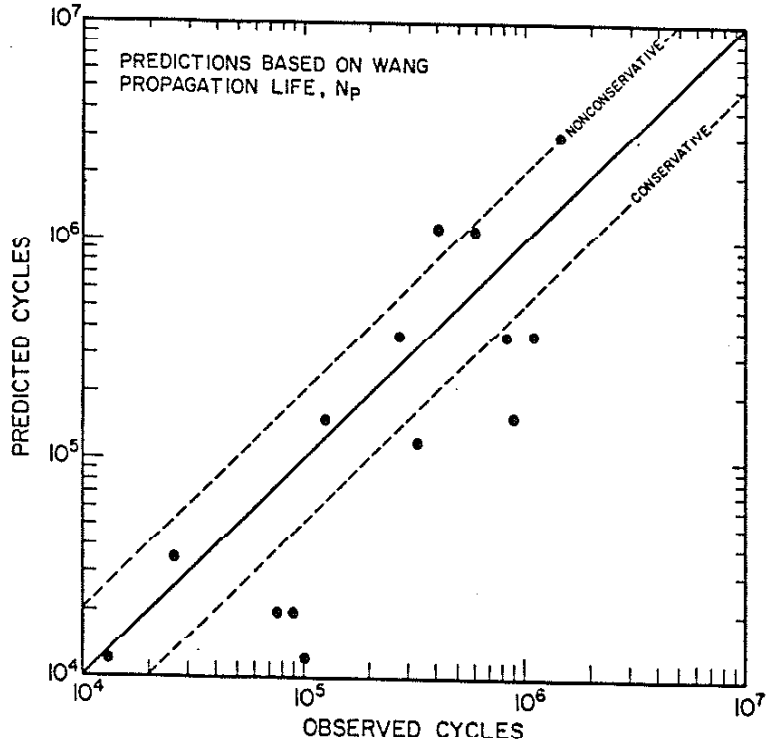

Fig. 26 (Top) Fatigue Crack Initiation Life Predictions Made for Galv. HSLA (16-78 B) Using Wang's Model.

Fig. 27 (Bottom) Fatigue Crack Propagation Life Predictions Made for Galv. HSLA (16-78 B) Using Wang's Model.

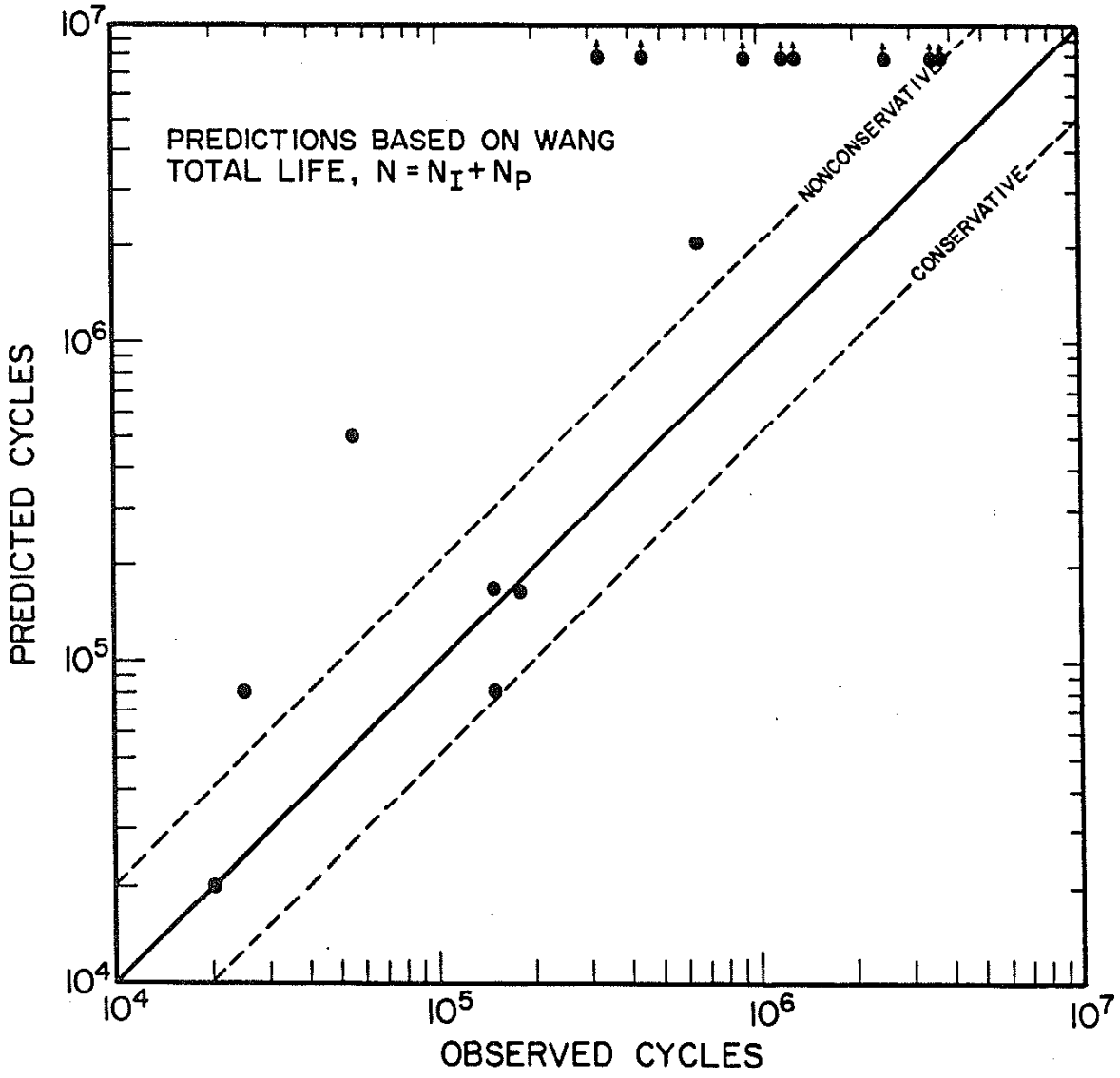

Fig. 28 Total Life Predictions for Galv. HSLA (16-78 B) Using Wang's Model.

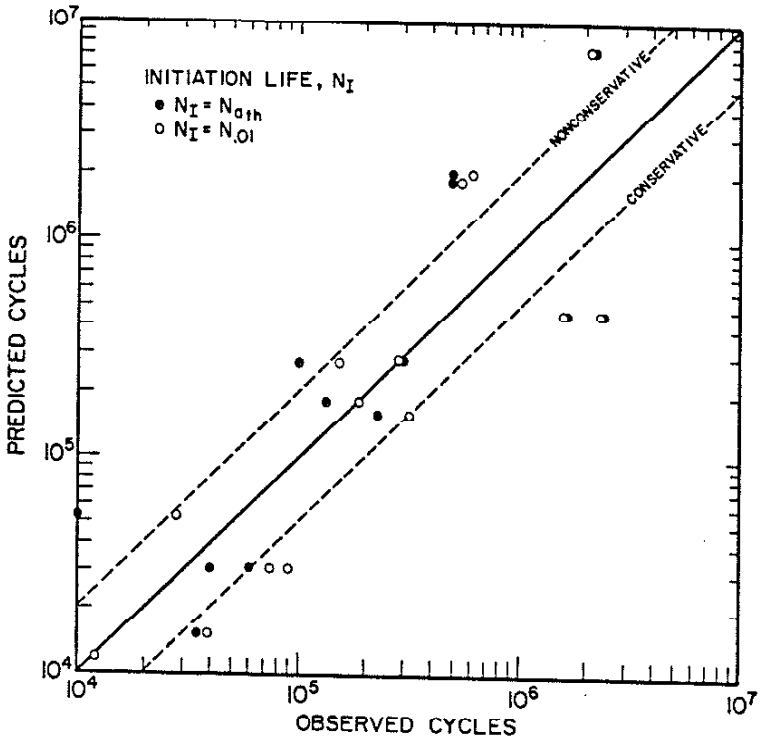

Fig. 29 Fatigue Crack Initiation Life Predictions Made for Galv. HSLA (16-78 B) Using the IP Model.

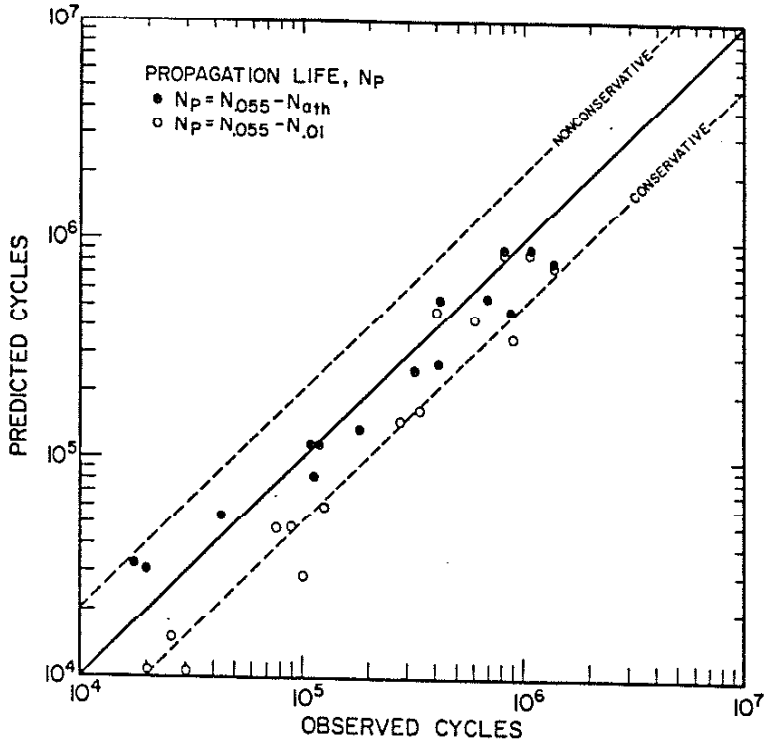

Fig. 30 Fatigue Crack Propagation Life Predictions Made for Galv. HSLA (16-78 B) Using the IP Model. Filled and open symbols represent lives predicted using 0.01 inch and a_{th} as the depth of an initiated crack, respectively.

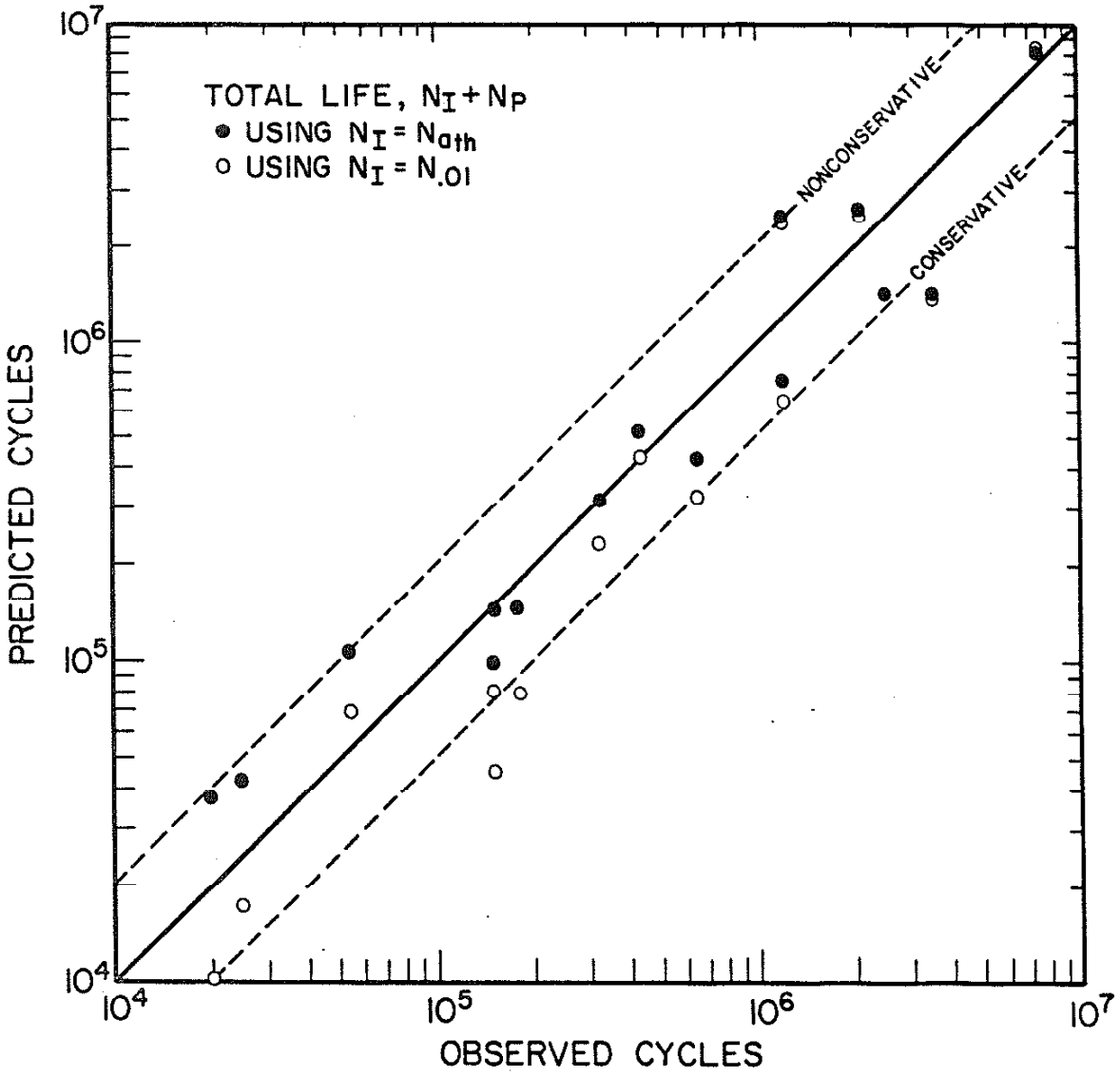

Fig. 31 Total Fatigue Life Predictions for Galv. HSLA (16-78B) Using the IP Model Described in the Current Study.

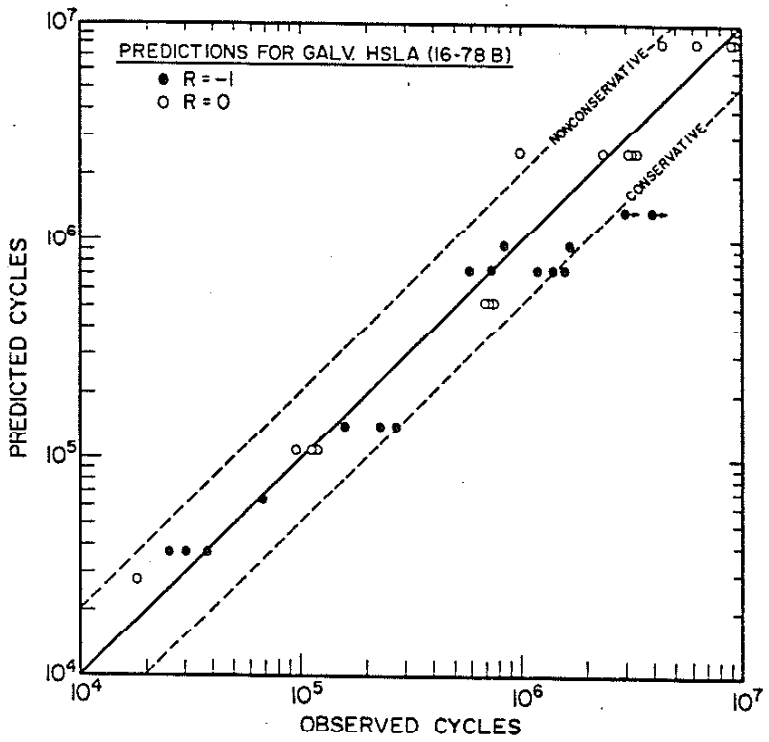

Fig. 32 Total Life Predictions Made for Galv. HSLA (16-78 B). The tests were performed to specimen separation (Stages I-III). The IP model predictions omitted State III but sufficiently predicted the total life.

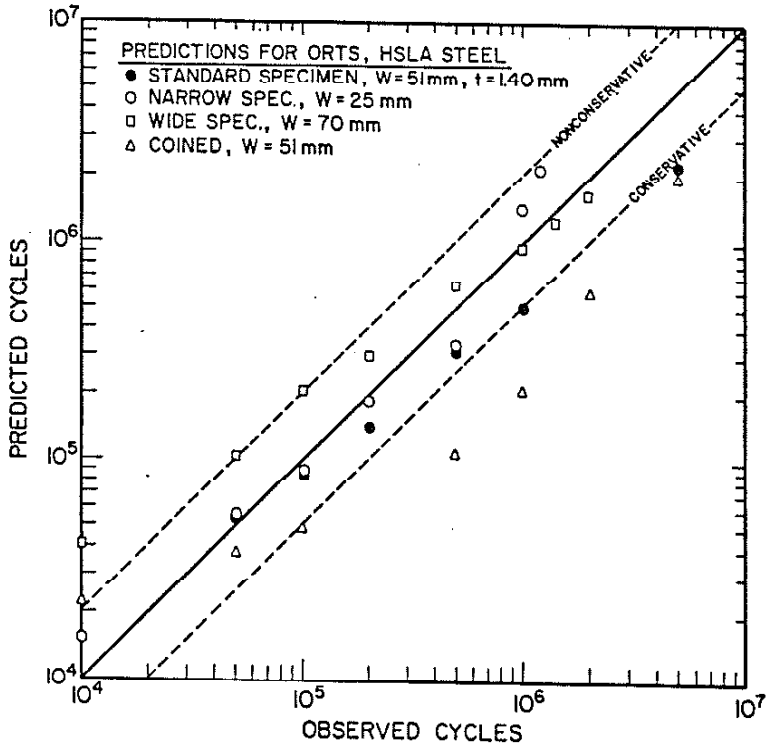

Fig. 33 Total Life IP Model Predictions for Specimens Tested by Orts (5).

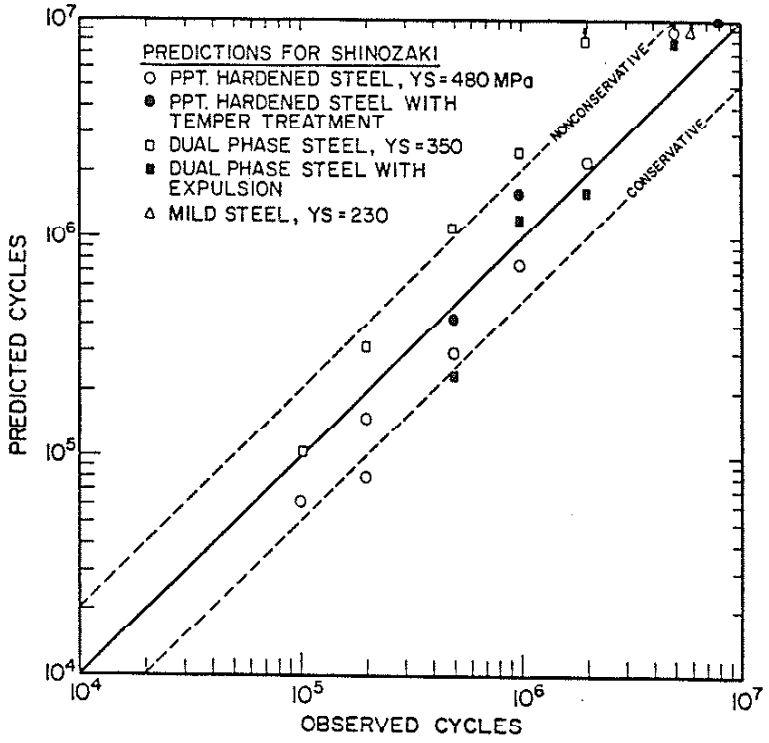

Fig. 34 Total Life IP Model Predictions for Specimens Tested by Shinozaki (14).

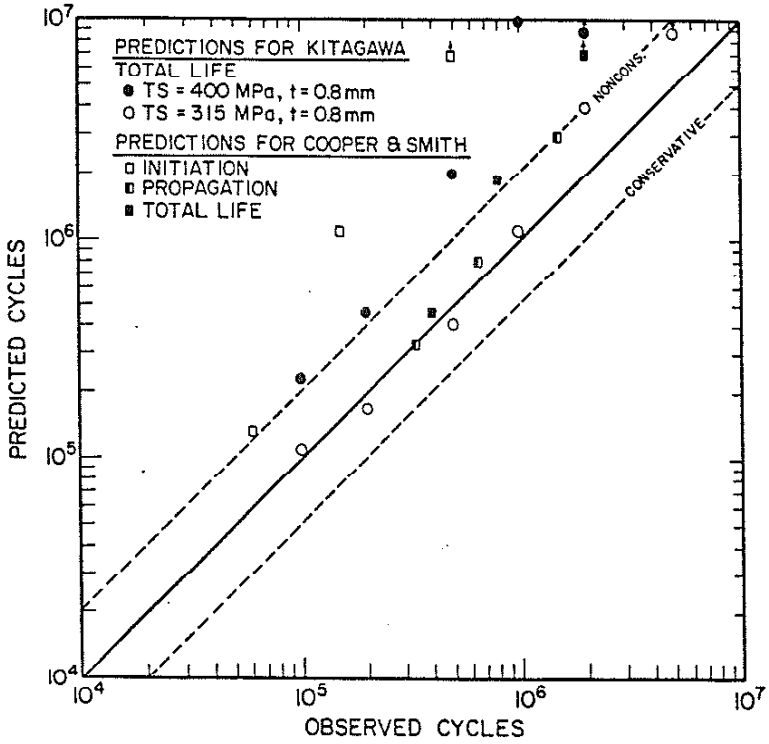

Fig. 35 Initiation, Propagation and Total Life Predictions Made for Specimens Tested by Kitagawa (15) and Cooper (8) Using the IP Model.

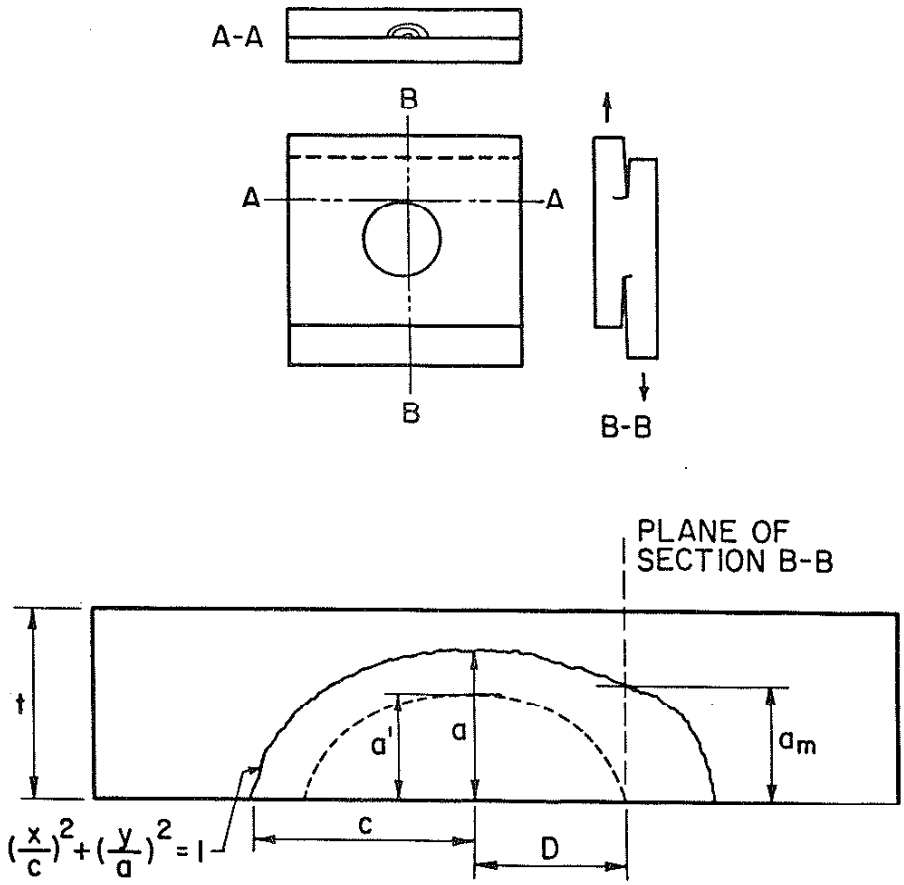

t: SHEET THICKNESS
c: MJR. ELLIPSE AXIS
a: MAX. CRACK DEPTH
a_m: MEASURED CRACK DEPTH AT B-B
a': MAX. UNDETECTED CRACK FOR D AND c/a
D: DISTANCE BTWN. MAX a AND PLANE B-B

Fig. 36 Error Analysis of Measurements of Fatigue Cracks. This diagram applies to both the companion and presectioned specimens. The crack shown has an actual depth of "a" but its measured depth at section BB is "a_m." The dashed line represents a crack of depth a' which is undetected at section BB.

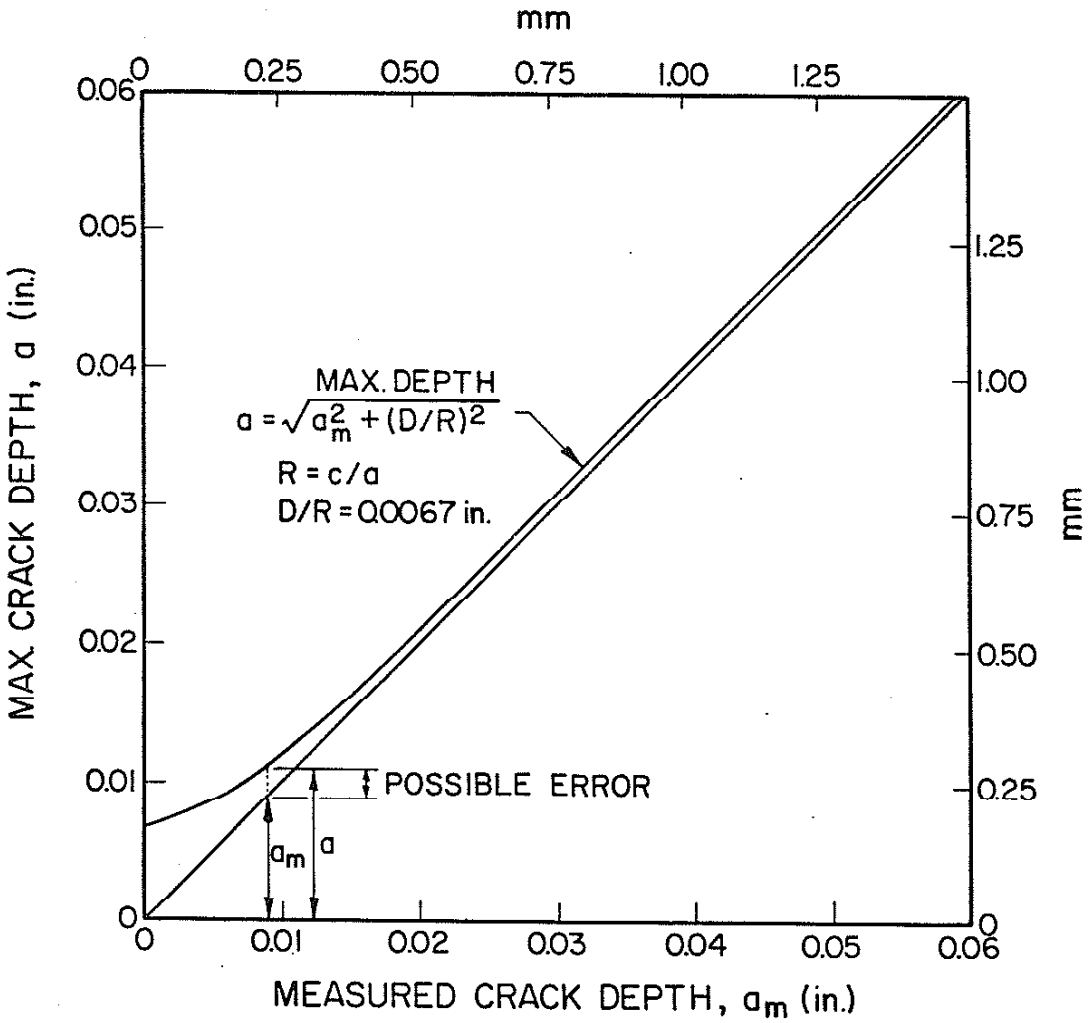

Fig. 37 Possible Error in Measurement of Fatigue Crack Depths. The error depends on the crack aspect ratio (R) and the distance between the location of maximum depth and the section plane (D). The largest errors occur at small crack depths.

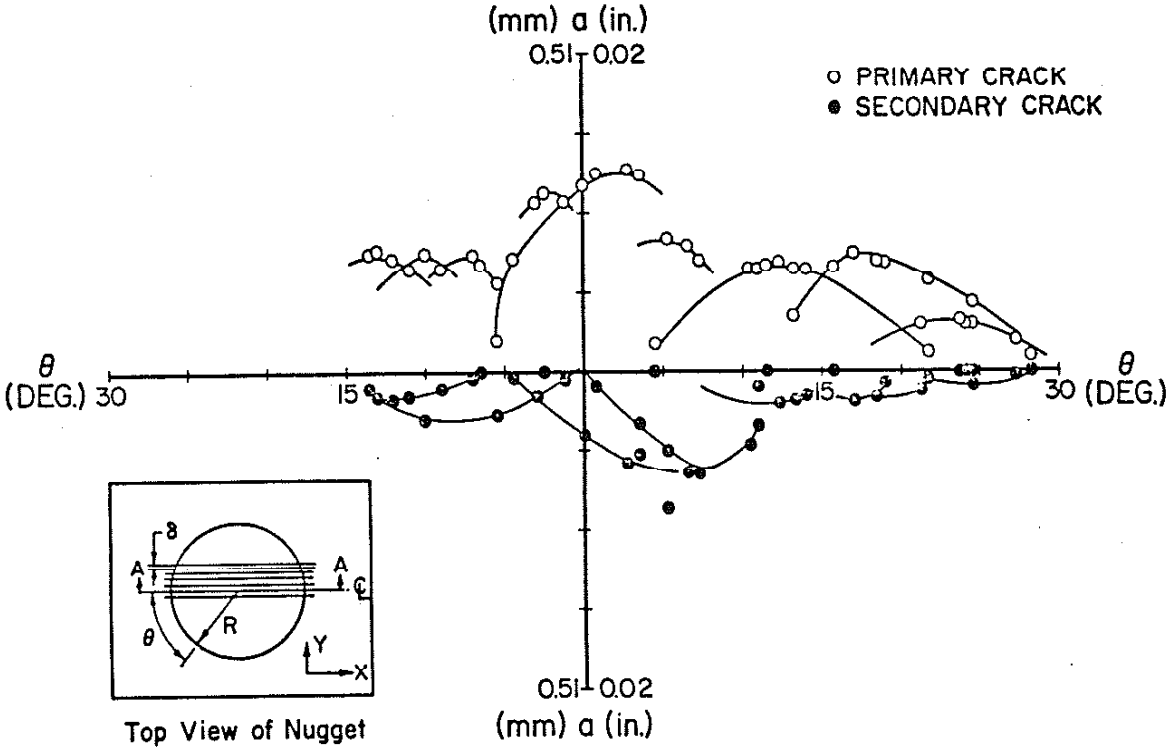

Fig. 38 Fatigue Crack Depth vs. Angle from Nugget Centerline. The specimen was subjected to 300,000 cycles at 2.2 kN load, R=0. From Smith (7).

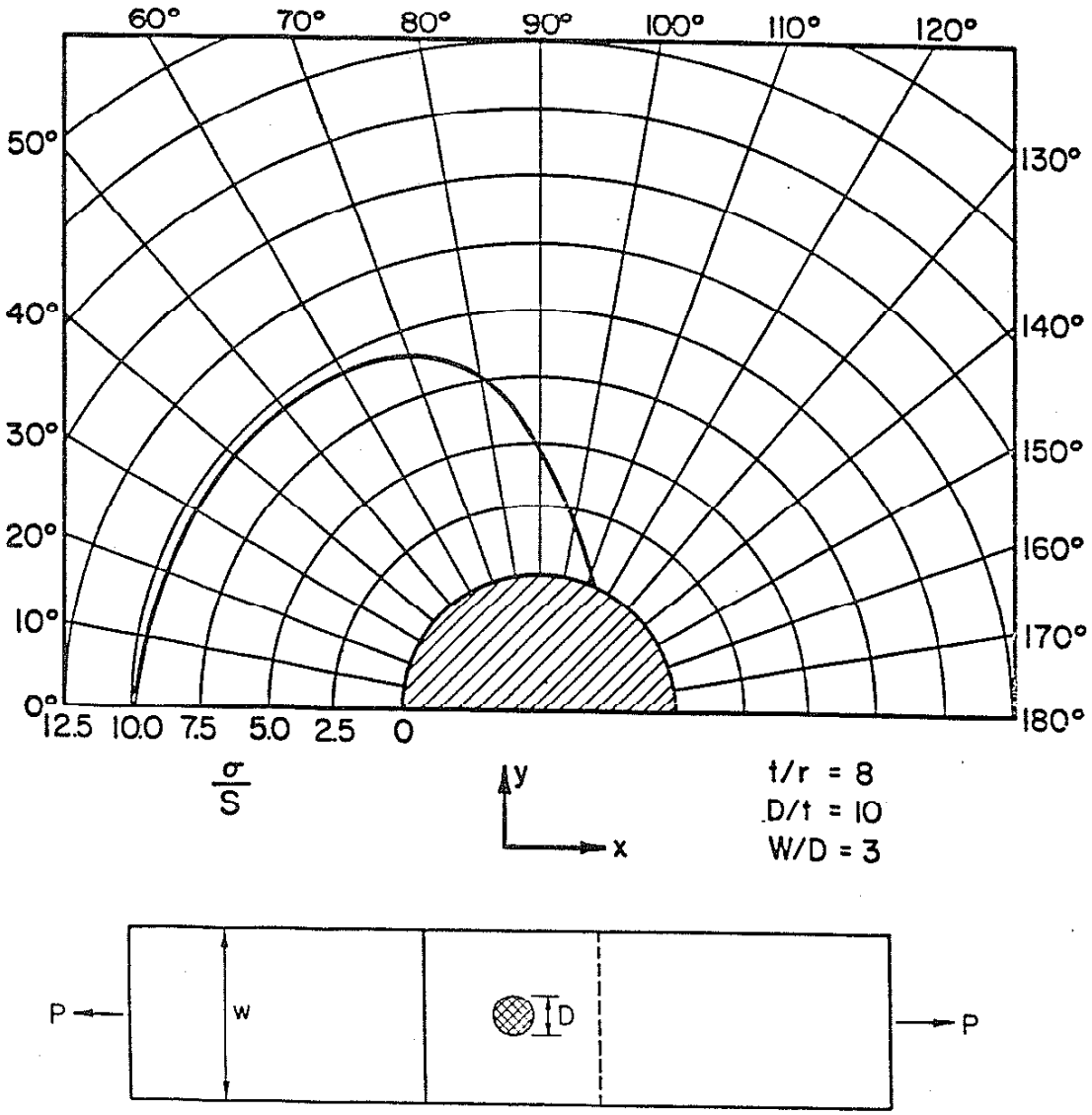

Fig. 39 Principal Stress Distribution Around the Nugget Circumference. The principal stresses remain as high as 90% of the maximum as far as sixty degrees from the centerline. From Smith (7).

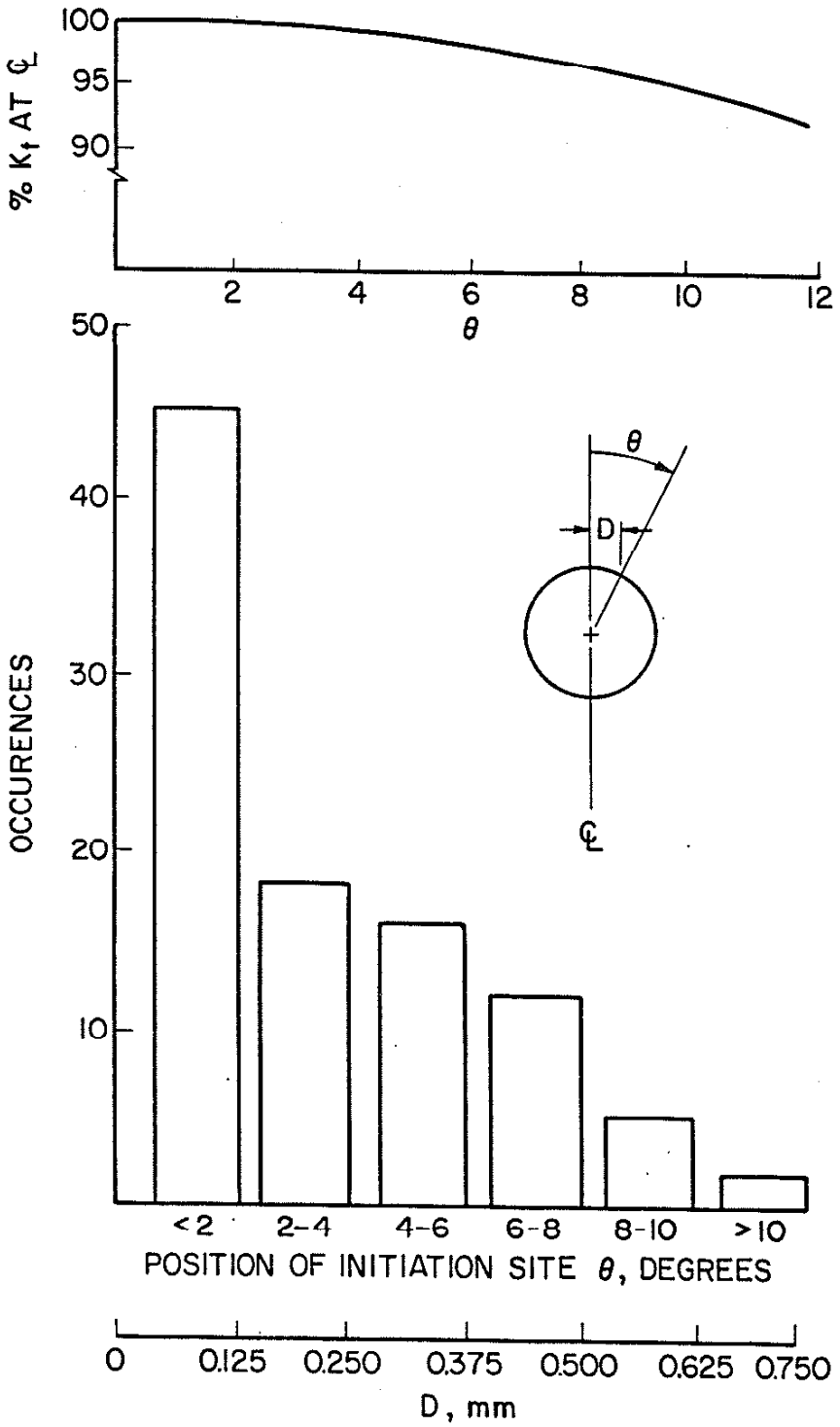

Fig. 40 (Top) Distribution of K_t (from previous figure) vs. Angle from the Weld Centerline.
(Bottom) Histogram of the Observed Positions of the Initiation Sites in Companion Specimens.

APPENDIX A

EXAMPLE FIGURES OF ORIGINAL DATA

This report has been condensed from the Ph.D. thesis of James McMahon. Only the figures of the appendix which are referenced in the text have been included in this report. Complete sets of the data in tabular and graphic form are available upon request from the authors.

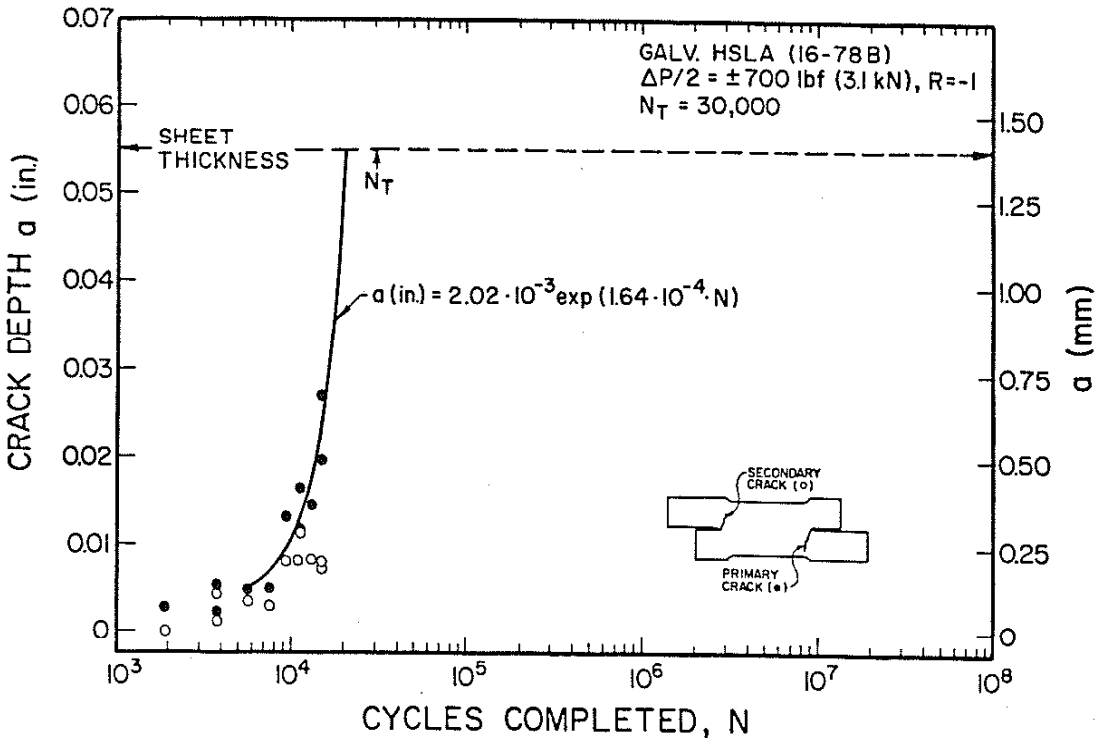

Fig. 41 Companion Specimen Data from Series E. Load Range: 6.2 kN, R=-1.

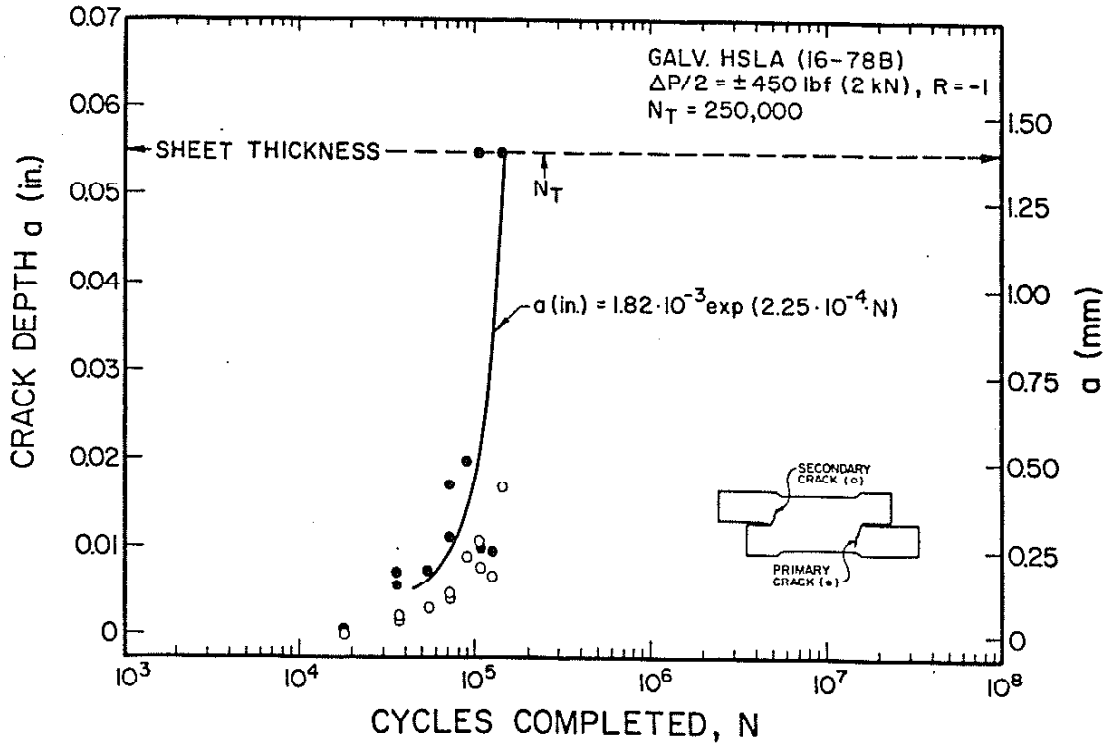

Fig. 42 Companion Specimen Data from Series F. Load Range: 4.0 kN, R=-1.

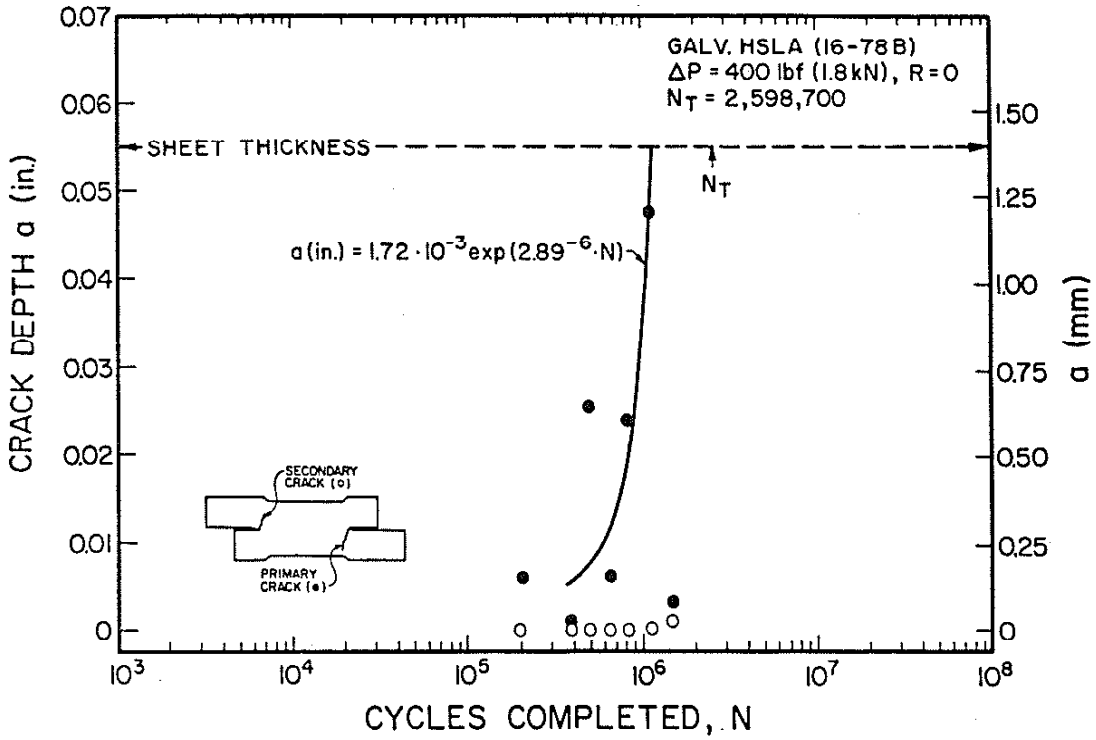

Fig. 43 Companion Specimen Data from Series C. Load Range: 1.8 kN, R=0.

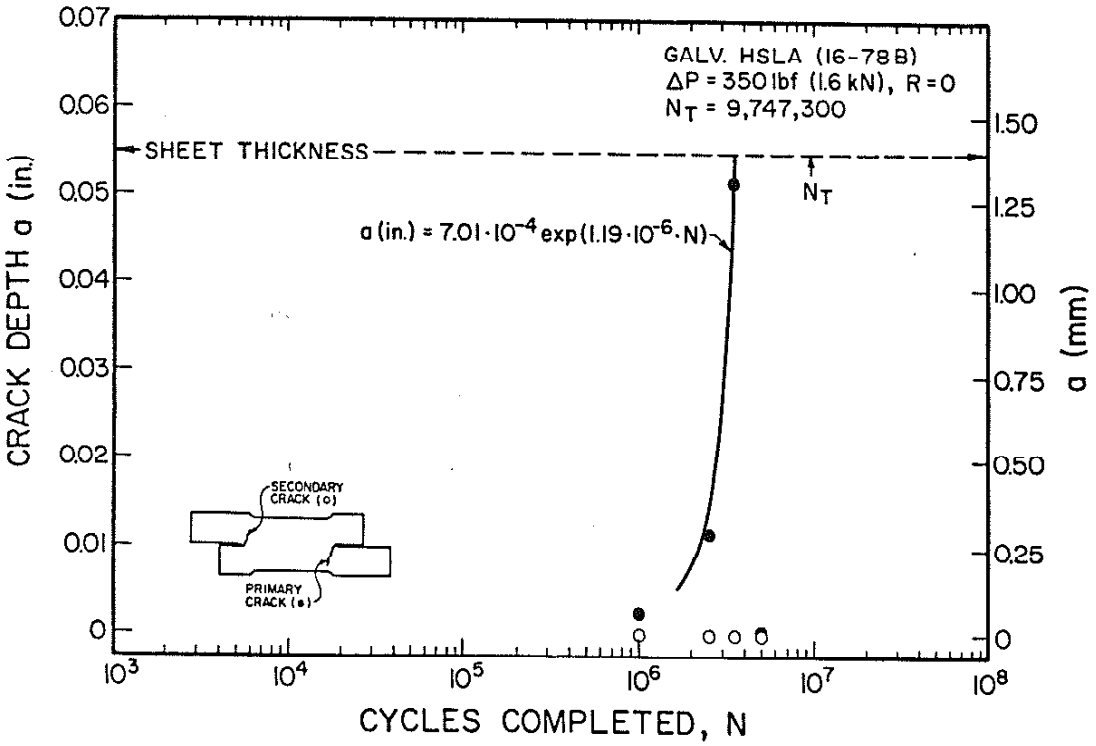

Fig. 44 Companion Specimen Data from Series D. Load Range: 1.6 kN, R=0.

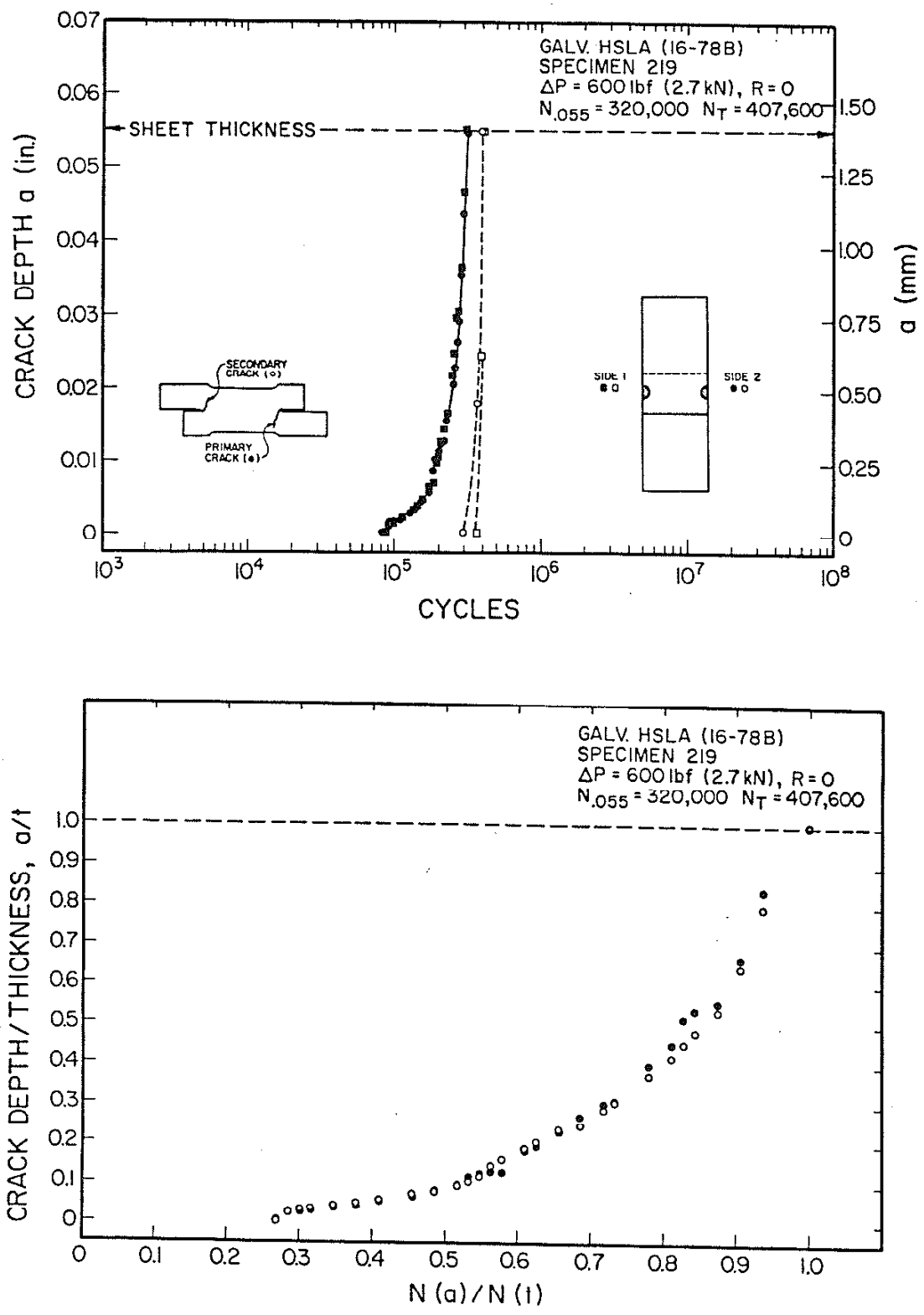

Fig. 45 Data Recorded from Presectioned Specimen 219.
Load Range: 2.7 kN, R=0.

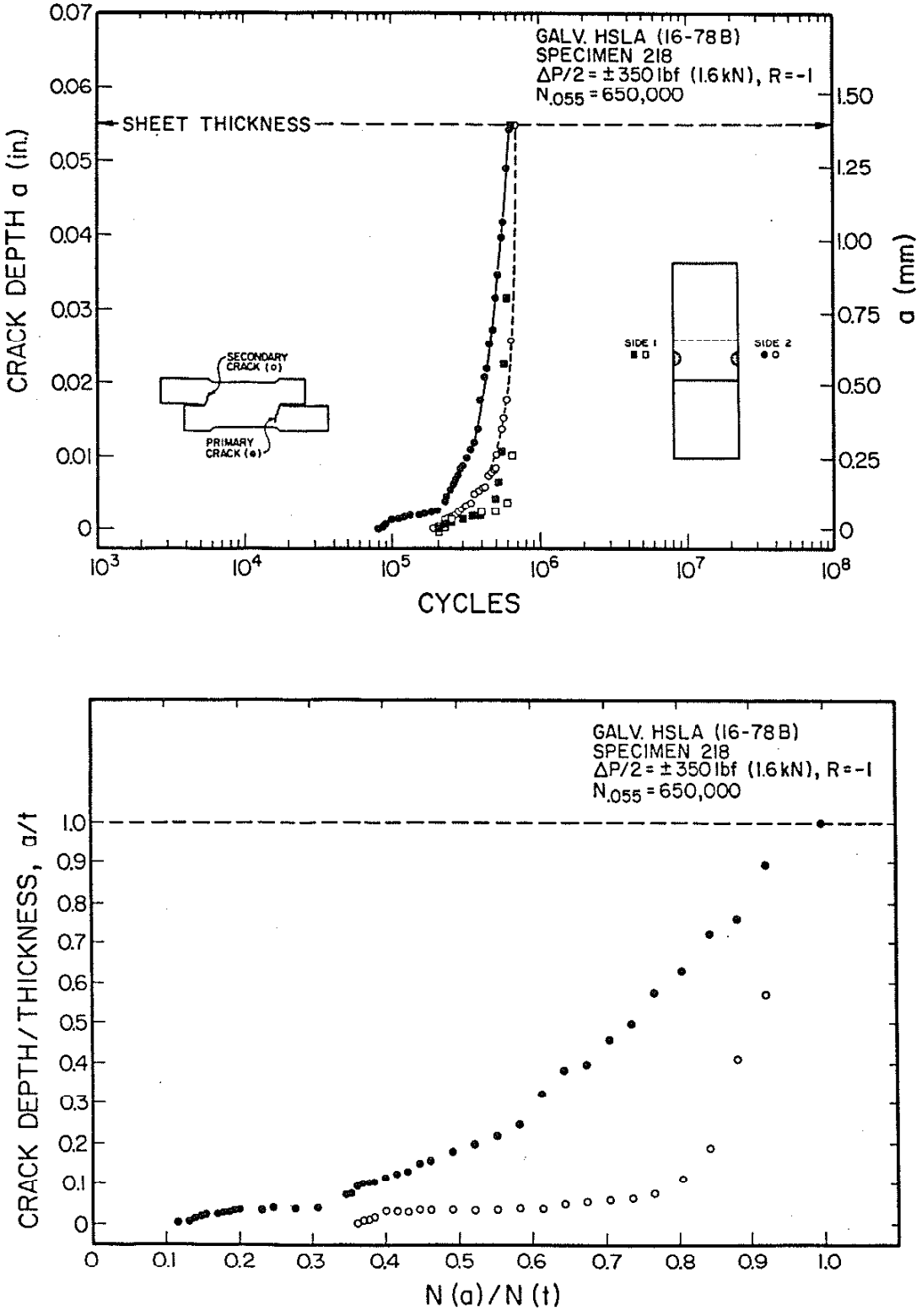

Fig. 46 Data Recorded from Presectioned Specimen 218. Load Range: 3.2 kN, R=-1.

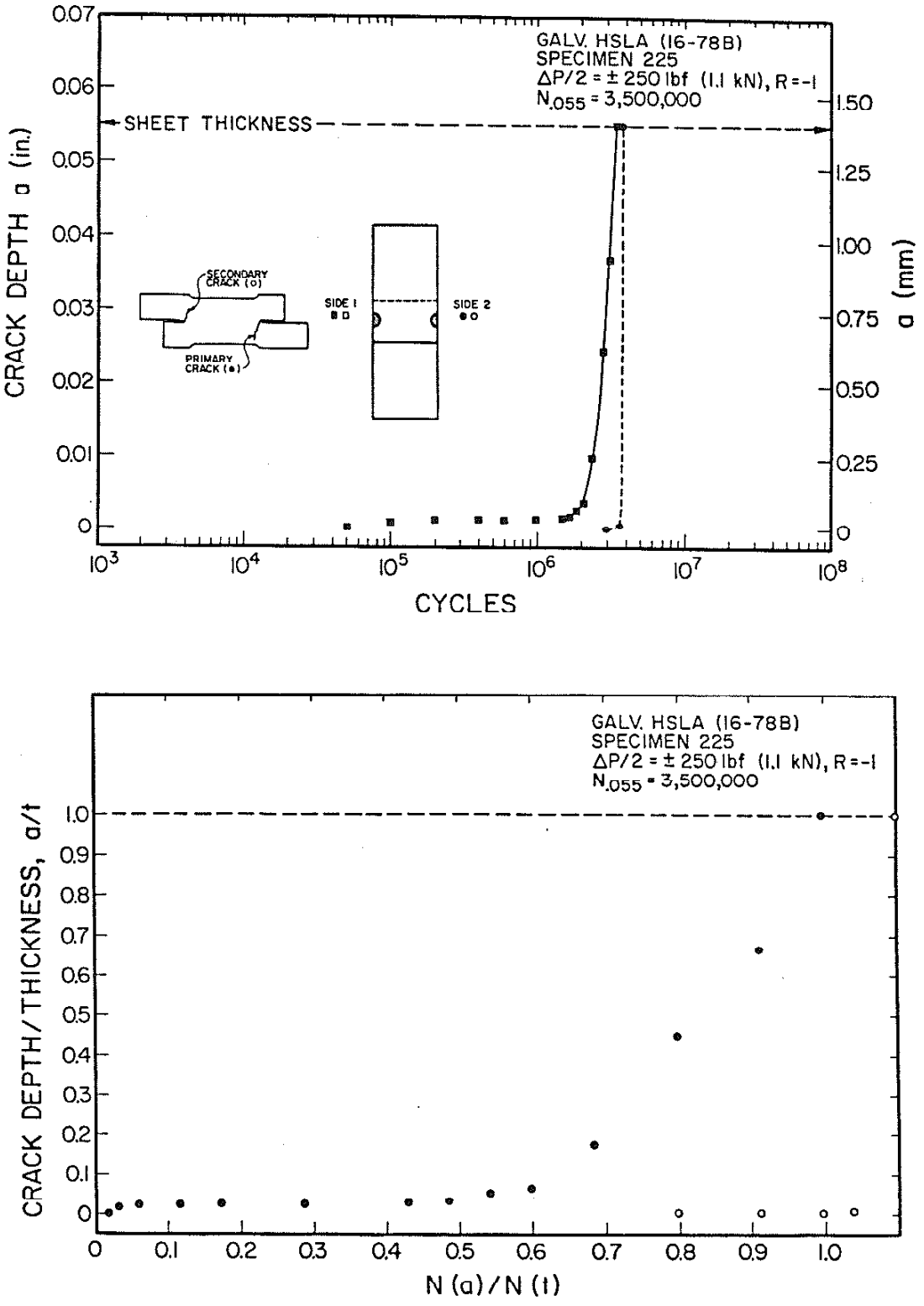

Fig. 47 Data Recorded from Presectioned Specimen 225. Load Range: 2.2 kN, R=-1.

APPENDIX B

REVIEW OF MODELS FOR PREDICTING THE FATIGUE LIFE OF SPOT WELDMENTS

This appendix summarizes the fatigue life prediction model developed by Wang (1) and the modifications made to his initiation-propagation model by the current study. Models based solely on either the fatigue crack initiation fatigue crack propagation life will also be discussed.

B.1 The Initiation-Propagation Model: Calculation of the Initiation Life

The fatigue crack initiation lives are estimated by summing the damage at the notch root. This damage is calculated using a local-strain analysis which relates remote loadings to cyclic stress-strain behavior at the root of the notch. Mean stresses and stress ranges are determined by a set-up cycle (see Fig. 48 and Ref. (12)) and are influenced by residual stresses and fatigue notch factor.

Wang (1) estimated the elastic stress concentration and fatigue notch factors for the TS spot weld. The elastic stress concentration factor was derived from Pook's expressions for the stress field of a TS spot weld (13).

$$K_t = \frac{Wt}{(\pi r)^{\frac{1}{2}} D^{\frac{3}{2}}} [1.61\ (D/t)^{.397} + .593 + .34\ (D/t)^{.710}] \qquad (4)$$

The fatigue notch factor was estimated using Peterson's equation:

$$K_f = 1 + \frac{K_t - 1}{1 + \frac{a}{r}} \qquad (5)$$

where r is the notch root radius and the material parameter, a, can be related to the strength of the steel. Microscopic examination of weldments reveals that nearly any radius of notch can be present so analyses of welded joints employ the concept of using the maximum value of K_f, which is given by the following equation for spot welds (16):

$$K_{fmax} = 1 + 0.00241\ W\ S_u\ D^{-1}\ t^{\frac{1}{2}}\ f(t/D) \quad \text{(MPa-mm units)} \tag{6}$$

For the steel considered in the present study and for the steel's nominal spot welding parameters, K_{fmax} has a value of approximately 7.7, and the function f(t/D) has a value of 0.73.

Set-Up Cycle

The set-up cycle procedure outline by Wang (1) was used for the current study with some modifications suggested by Reemsynder (19) and is shown in Fig. 48. The stress- and strain-concentration factors, K_σ and K_ε, are related by Topper's (20) adaptation of Neuber's rule:

$$K_f = \sqrt{K\sigma \cdot K\varepsilon} \tag{7}$$

where $K_\sigma = \sigma/S$ and $K_\varepsilon = \varepsilon/e$. K_{fmax} may be used in place of K_f in the following equations. Remote stress and strain are denoted by S and e, and local stress and strain by σ and ε. Combining the above:

$$\sigma \cdot \varepsilon = K_\sigma S \cdot K_\varepsilon e \tag{8}$$

When the remote stresses are in the elastic range then Eq. 8 can be stated as:

$$\sigma \cdot \varepsilon = K_f^2 \cdot S^2 / E \tag{9}$$

The right hand side can be considered as a constant for a given remote loading, and the equation "$\sigma \cdot \varepsilon$ = Constant" is solved by using the relationship between σ and ε. The stress-strain relationship can have different forms, but the most used version is the Ramberg-Osgood form:

$$\varepsilon = \frac{\sigma}{E} + \left(\frac{\sigma}{K}\right)^{\frac{1}{n}} \tag{10}$$

where the total strain is expressed as the sum of the elastic and plastic portions of strain.

The maximum stresses and strains are used to evaluate the first reversal of fatigue. Equation 9 was modified to include the residual stress, σ_r, present after welding:

$$\sigma_{max} \cdot \varepsilon_{max} = (K_f \, S_{max} + \sigma_r)^2 / E \tag{11a}$$

or

$$\sigma_{max} \cdot \varepsilon_{max} = K_f^2 (\, S_{max} + \sigma_r / K_f)^2 / E \tag{11b}$$

The residual stress is assumed to be equal to the value of the yield strength of the base metal. For sharp notches, K_f is greater than K_σ, and consequently the term σ_r / K_f tends to yield nonconservative results and should be replaced with σ_r / K_σ as suggested by Reemsynder (19):

$$\sigma_{max} \cdot \varepsilon_{max} = K_f^2 (S_{max} + \sigma_r / K_\sigma)^2 / E \tag{12}$$

When the remote loading is elastic:

$$(S_{max} + \sigma_r / K_\sigma) / (e_{max} + \varepsilon_r / K_\varepsilon) = E \tag{13}$$

Combining Eqs. 7, 10, 12 and 13 leads to an expression of K_f as a function of K_σ, S_{max}, σ_r, and the constants of the stress-strain equation. Generally, it is K_σ and not K_f which is unknown, and K_σ is solved for using a iterative procedure. After K_σ is determined, the σ_{max}-ε_{max} combination can be solved for using Eq. 10.

Mean stresses are determined by estimating the cyclic stress-strain response due to subsequent cyclic loading. The stress and strain follow the $\Delta\sigma$-$\Delta\varepsilon$ curve which is of the same form as Eq. 10, but stresses and strains are expressed in terms of ranges:

$$\frac{\Delta\varepsilon}{2} = \frac{\Delta\sigma}{2E} + \left(\frac{\Delta\sigma}{2K'}\right)^{\frac{1}{n'}} \tag{14}$$

Neuber's rule is applied again, and the following expression is solved for $\Delta\sigma$ and $\Delta\varepsilon$:

$$\Delta\sigma\ \Delta\varepsilon = (K_f\Delta S)^2/E \tag{15}$$

Substituting for $\Delta\varepsilon$,

$$\frac{(K_f\Delta S)^2}{E} = \frac{\Delta\sigma^2}{E} + \left(\frac{\Delta\sigma^A}{K'^B}\right)2^C \tag{16}$$

where $A=(n'+1)/n'$, $B=1/n'$, and $C=(n'-1)/n'$. The local stress range, $\Delta\sigma$, is found by solving Eq. 16. The results of the first and second reversals provide the maximum local stress and the stress range, respectively, The initial mean stress is given by:

$$\sigma_o = \sigma_{max} - \frac{1}{2}\Delta\sigma \tag{17}$$

Initiation Life Calculation

For high-cycle fatigue, the fatigue crack initiation life is calculated by using Basquin's equation modified to include the effects of mean stress.

$$2N_f = \left(\frac{\Delta\sigma}{2\sigma_f'} - \sigma_o\right)^{\frac{1}{b}} \tag{18}$$

However, the mean stress can relax during fatigue, especially when high local plastic strains are present. Under such circumstances one needs to use linear damage summation to calculate the fatigue crack initiation life N_I:

$$\int_1^{2N_I} \left[\left(\frac{\sigma_f'}{\Delta\sigma/2}\right)\left(1-\sigma_o(2N)^k/\sigma_f'\right)\right]^{\frac{1}{b}} dN = 1 \tag{19}$$

where k is the mean stress relaxation exponent. The current study used the relationship established by Burk (21) to determine k from the local strain. Using standard numerical methods, the equation above can be integrated and solved for the initiation life. See Appendix C for the computer program used in this study.

B.2 Calculation of the Propagation Life

Fatigue crack propagation can be represented by the Paris power law:

$$\frac{da}{dN} = C\ \Delta K^m \tag{20}$$

and the propagation life can be calculated by integrating the above:

$$N_p = \frac{1}{C} \int_{a_i}^{a_f} \Delta K^{-m} da \qquad (21)$$

The fatigue crack propagation life calculated by the above equation is influenced by the material properties C and m, the limits of integration (initial and final flaw size), the range in the stress-intensity factor K, and the relationship between K and the crack length.

The values of C and m given by Wang (1) were used for the current study: $C = 1.0 \times 10^{-13}$ $MPa^{-5}m^{-3/2}$, $m = 5.0$.

Different values can be used for the initial flaw size such as the dimension of a known defect or some arbitrary length. The different initial sizes used for the current study will be discussed later. The sheet thickness was used as the final crack size.

Mean Stress Effect

From the summary graph presented in Fig. 18, one can see that the load ratio (R) has a pronounced effect on all portions of the fatigue life of spot weldments, including propagation. Compare the fatigue crack growth curves for the two groups of specimens fatigued with a 2.2 kN (500 lbf) load range but under different load ratios (R=0 and R=-1). The group fatigued under completely reversed conditions had lives much greater than the group fatigued under zero-to-tension loading. This trend was observed at all load levels.

This shift in fatigue lives observed between the different loading ratios can be explained by a crack closure phenomenon. During reversed loading the crack may close before the minimum load. This closure would effectively reduce the stress-intensity factor range at the crack tip. Such a reduction

would explain the shift to longer lives by specimens having completely reversed loading.

An another commonly proposed effective stress-intensity factor range is defined as:

$$\Delta K_{eff} = K_{max} - K_{th} \tag{22}$$

where K_{th} is the threshold stress-intensity factor. Barsom (22) proposed that the changes in crack growth rates observed for different R ratios be explained by defining K_{th} as a function of the R ratio and using Eq. 22 to define the effective stress-intensity factor. The threshold range proposed by Barsom was:

$$\Delta K_{th} = 6.4\ (1-0.85R) \quad \text{for } R > 0.1 \quad \text{(MPa units)} \tag{23}$$

However, defining ΔK_{th} as a function of R and using Eq. 22 simply reduces the effective range in K as does defining an effective stress-intensity factor based on proposed closure events. The adjustment based on closure was chosen as the modification of the current study's method of calculating the through-thickness propagation life of tensile-shear spot weldments.

Opening levels corresponding to using nine-tenths of the load range for zero-to-tension loading and seven-tenths for the completely reversed loading were chosen for the calculations made in the current study and were based empirically on the observed difference of fatigue strengths exhibited by the R=0 and R=-1 data.

Stress-Intensity Factor of the Presectioned Specimen

The difference between the stress-intensity factors of the presectioned specimen having two half-nuggets on its edges and the standard single spot weld specimen having one nugget positioned in its center was assumed to be similar to the difference between a double-edge crack specimen and a center crack specimen. The crack of a tensile-shear spot weldment is a surface crack and an analysis of its stress-intensity factor accounts for the free back surface. The cracks of the presectioned specimens were considered to be quarter-elliptical cracks having two free surfaces.

An analysis of the stress-intensity factor of a semi-elliptical crack in a plate of finite width and thickness includes the following correction factors:

$$K_s = \sigma \sqrt{\pi a}\ f(a/w)\ C_1\ M_k \tag{24}$$

where: f(a/w) is a correction for the finite width of the specimen and its value approaches 1.0 as a/w becomes approaches 0; C_1 is the back free-surface correction and accounts for the difference between a center crack and an edge crack or between an embedded crack and a surface crack and has a value of 1.12; M_k is the front free-surface correction factor which accounts for finite specimen thickness and it approaches 1.0 as a/t becomes very small.

An analysis of the stress-intensity factor of a quarter-elliptical crack in a plate of finite width and thickness includes the following correction factors:

$$K_q = \sigma \sqrt{\pi a}\ f(a/w)\ C_1\ C_2\ M_k \tag{25}$$

where the same definitions apply as described above with the addition of C_2, which is the back free-surface correction for the second free surface present in the quarter-elliptical crack.

It has been assumed that for small a/w and a/t the correction factors C_1, M_k, f(a/w) are identical for K_s (semi-elliptical) and K_q (quarter-elliptical). Thus, K_q and K_s differ by a factor of C_2:

$$K_q/K_s = C_2 \tag{26}$$

The second back free-surface correction has been found experimentally to be less than C_1, and generally a factor of 1.2 is used for the product of C_1 and C_2 instead of C_1C_1, 1.25 (23). A finite element analysis (24) of these crack configurations found K_q and K_s to differ by a factor of 1.074 or a total factor of 1.20 for the product C_1C_2. As a result of this difference, the load amplitudes for the presectioned specimens were reduced by a factor of 1.07 so that the stress-intensity factors of the presectioned specimens would be equivalent to those of the unsectioned spot welds in the companion specimens.

Use of Experimental Data to Find K

The propagation life was found using the following:

$$K = Y\ S\ \sqrt{\pi\ a}, \qquad Y = f(a) \tag{27}$$

$$\Delta K_{eff} = K_{max} - K_{open} \tag{28}$$

$$\frac{da}{dN} = C(\Delta K_{eff})^{m} \tag{29}$$

$$N = \frac{1}{C}\int_{a_i}^{a_f} \Delta K_{eff}^{-m} da \tag{30}$$

The geometry factor, Y, was found by fitting a cubic equation to the observed da/dN data of the companion and presectioned specimens:

$$Y = 14.39 - 19.54(a/t) + 20.24(a/t)^2 - 8.2(a/t)^3 \quad (31)$$

Crack growth rate data was found from spline fits of the "a versus N" data. Early crack growth data having rates faster than predicted were excluded from this fitting process (generally for $a < 0.05$ mm). This factor included the corrections for the front and back face surfaces and the eccentricity of the loading. The factor Y did not include corrections for high values of nugget rotation which may occur at high loads. It was assumed that this rotation effect is secondary in the intermediate-life and long-life regimes.

Different values of the material properties, C and m, have been proposed (3) for HSLA sheet steel. The use of different values of C and m would alter the expression derived for the geometry factor, Y (Eq. 31), but would not significantly change the fatigue crack propagation life predictions because of the circular definition of Y; that is, Y was derived from assumed values of C and m and from known values of load, crack growth rate, and crack length. In turn, the fatigue crack growth rates (Eq. 29), and consequently the fatigue crack propagation lives (Eq. 30), were calculated using the derived geometry factor, Y.

B.3 Other Models for Predicting Spot Weld Fatigue Life

One alternative to using the IP model is using models based solely on fatigue crack propagation, of which there are a few variations. Table 14 summarizes the models used and compares their predictions. The assumed functional relationship between the stress-intensity factor (K) and the crack depth (a) for the different models are compared in Fig. 49.

Model 1, the simplest, integrated the Paris power law (Eq. 30) from a very small initial crack size (close to zero) using the same method described

for calculating the propagation life in Section 4.2. Crack growth rates for small cracks were underestimated; and consequently, the predicted lives were nonconservative (Fig. 50).

Models 2 and 3, two other fatigue crack propagation models, integrated Eq. 30 from a finite crack depth: 0.25 mm (0.01 in.) or a_{th}. These models ignored the initiation life and early crack growth, and their predictions were conservative (Figs. 51-52).

Model 4 used a constant, finite initial value of K from Pook (13) until a depth where the K calculated from Eq. 24 exceeded this initial value. This method of using an initial value of K gave good predictions and worked best at short lives (Fig. 53).

Crack growth rates can be higher than predicted by LEFM when the crack is under the influence of the notch plasticity. As shown by the first method, if this fact is not accounted for in a propagation model, the predicted lives can be nonconservative. Model 5 is an all-propagation model which calculated these higher crack growth rates by reducing the predicted crack closure load when the crack was smaller than the notch plastic zone size, a_{pz} (25). Model 5 also used the initial value of K given by Pook. This method was nonconservative at long lives where a_{pz} was small (Fig. 54), and therefore the early crack growth rates may have been underestimated.

Model 6 made predictions of total life based solely on the calculated initiation life (see Sec. B.1). As shown in Fig. 55, using initiation alone gave conservative estimates of life. Better predictions were obtained by using the IP model (#7) which combines the initiation life with propagation life (see Figs. 31 and 32).

B.4 Definition of the Length of an Initiated Fatigue Crack

The possible range of crack size at initiation has been given by Socie and Artwohl (26) who stated that fatigue cracks "begin with dislocation movement on the first cycle and end with fracture; crack initiation occurs between these two events." A more restrictive definition is that the cracked area equals that of the specimens from which the low-cycle fatigue properties were obtained. This definition would not be appropriate for the current study because a crack of this size would be larger than the thickness of the spot weld specimen and would be in the last stage of crack propagation across the width of the base metal sheet.

Another definition of initiation length is the threshold crack length a_{th} for the spot weld specimen and for the given load range that is being applied. As described in earlier in this appendix, low-cycle fatigue concepts can be used to predict the initiation life of a crack and fracture mechanics can be applied to calculate the life of the crack as it grows from the length a_{th} to a depth equal to the thickness of the sheet. However, this definition is not acceptable to those researchers who consider the gap between the sheets of the specimen to be a long crack and not a notch.

The question remains whether a_{th} should be used in the definition of the fatigue crack initiation length. For consistency, if one uses a_{th} as the lower bound of the propagation life, then a_{th} should be used as the initiation crack depth. One may argue that the use of a_{th} is as arbitrary as the use of 0.25 mm (0.01 in.), but a_{th} has the advantage of being capable of accounting for changes in loading and geometry while the use of a fixed length does not reflect such changes. Furthermore, the use of a_{th} is also supported by the fact that no "nonpropagating crack" was observed in the current study which was longer than the calculated a_{th} (see Fig. 56).

For sharp notches, it is possible that the local stress is higher than the minimum required to initiate a crack, but that this crack will not continue to grow unless some (higher) threshold stress level is exceeded.

This phenomenon was observed for a few of the presectioned specimens which had fatigue cracks that would initiate and only grow a little (0.025 to 0.125 mm) and then would stop growing. A "nonpropagating" crack was defined to be a crack in a presectioned specimen which initiated and grew to any length (generally this was less than 0.25 mm) and stopped growing for 40 percent or more of its fatigue life. Often one of these cracks would begin to grow again when a longer crack on the opposite half-nugget grew sufficiently large that load was shed to the side of the presectioned specimen having the "nonpropagating" crack. This behavior was displayed by presectioned specimens 218 and 225 (see Figs. 46 and 47).

To test the idea of these "nonpropagating" cracks, the load range is plotted versus the crack depths of the cracks in Fig. 56. These depths ranged from approximately 0.025 mm (0.001 in.) for the highest load ranges to 0.25 mm (0.01 in.) for the lowest load ranges. A line representing the calculated threshold crack length is plotted on Fig. 56. A threshold stress intensity of 6 MPa $m^{1.5}$ and the shape function, Y, described in earlier in this appendix were used to calculate values for the line. Although these observed "nonpropagating" cracks can not be confirmed to be truly nonpropagating cracks, all their observed crack depths are at or below this line.

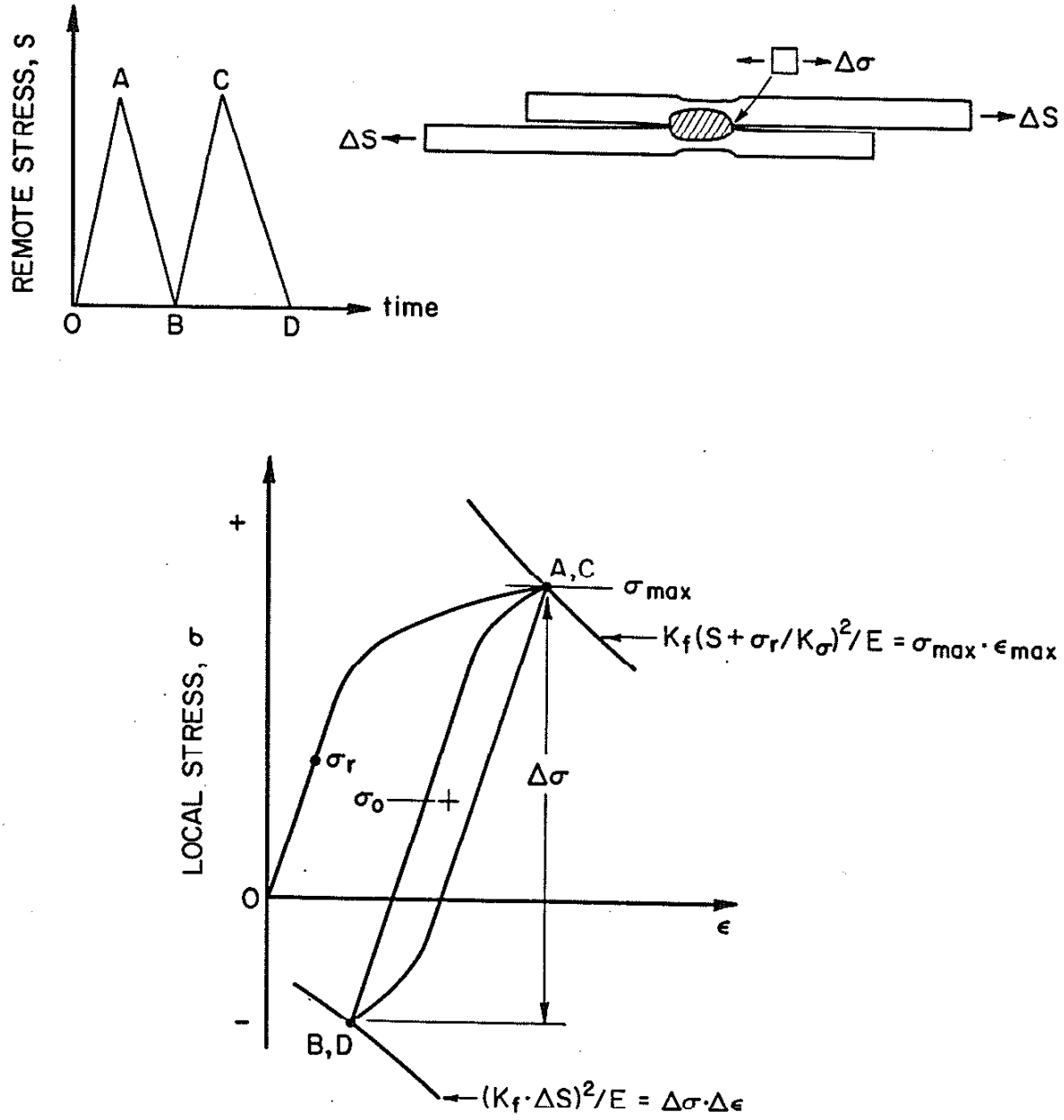

Fig. 48 Schematic of the Set-Up Cycle. The set-up cycle was used to determine the local stress range and mean stress from the remote stress conditions.

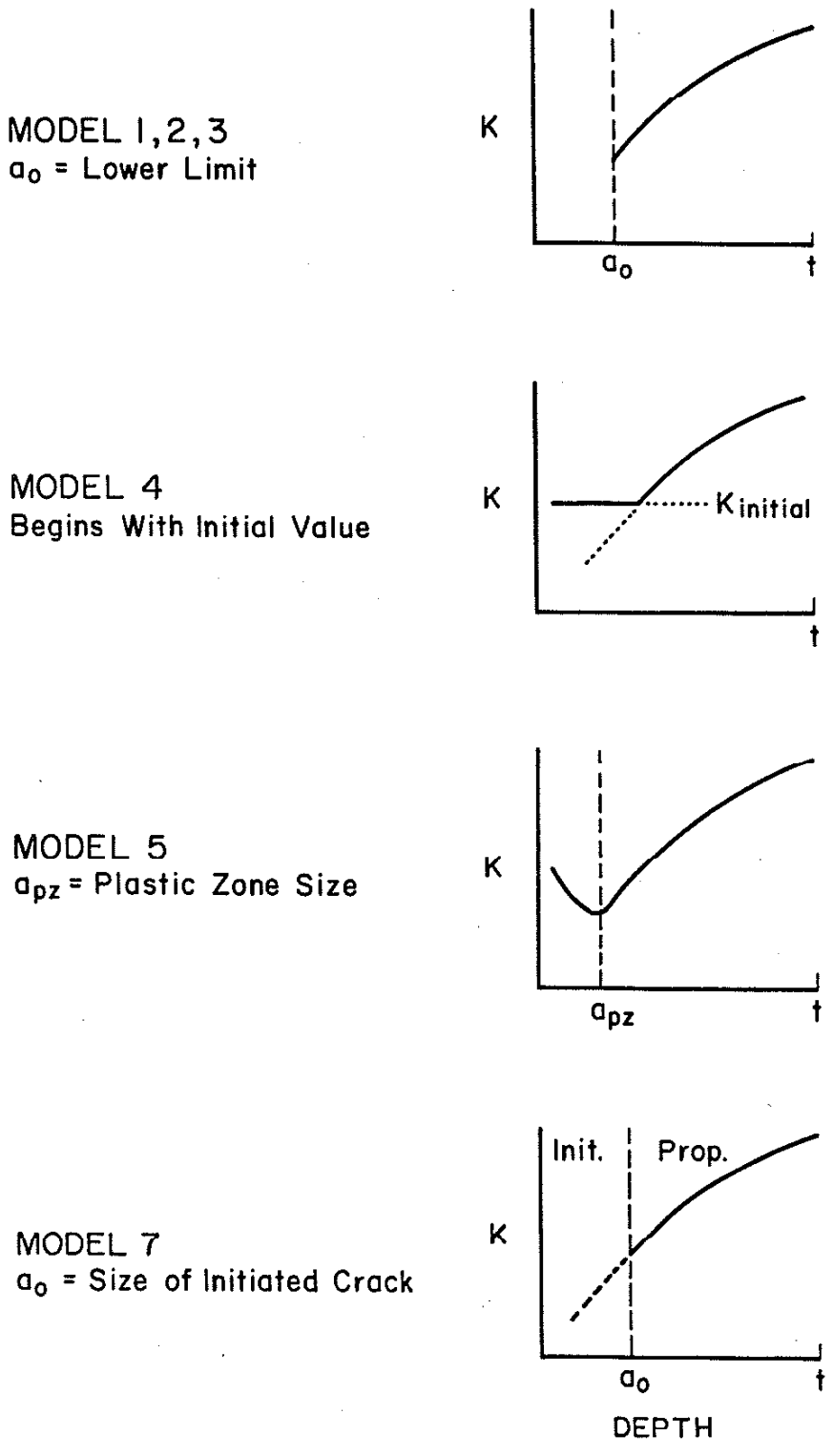

Fig. 49 The Functional Relationship of the Stress-Intensity Factor (K) and Crack Depth (a) Used by the Different Fatigue Life Prediction Models. Model 6, initiation only, is not included above because it does not use K in the estimation of fatigue life.

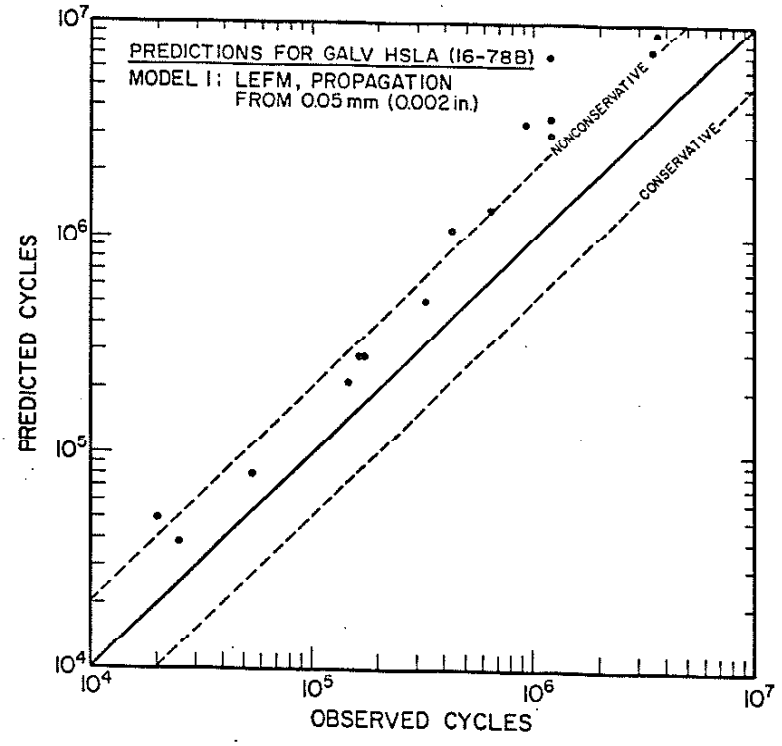

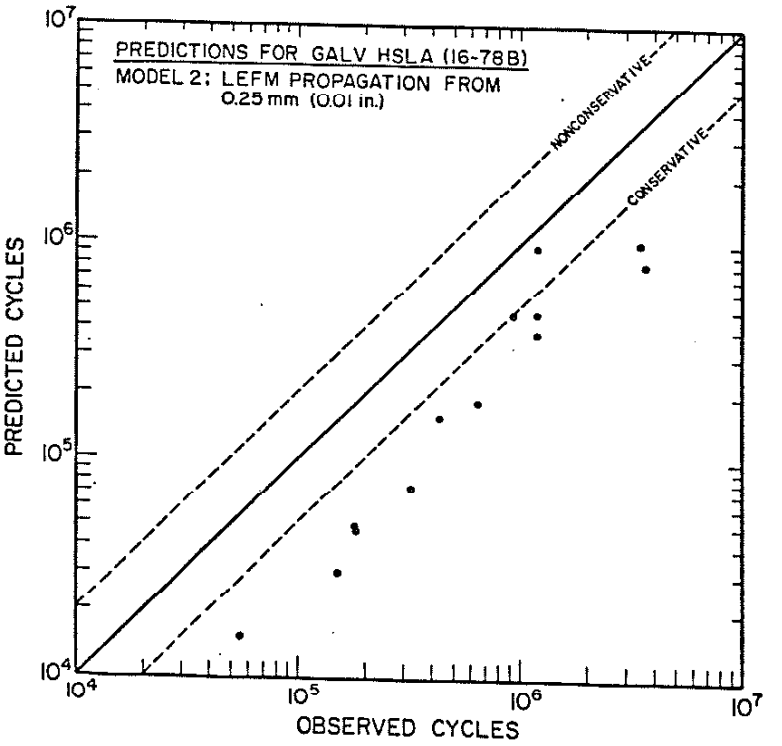

Fig. 50 (Top) Total Life Predictions Made Using Model 1, Propagation from 0.05 mm (0.002 in.)

Fig. 51 (Bottom) Total Life Predictions Made Using Model 2, Propagation from 0.25 mm (0.01 in.).

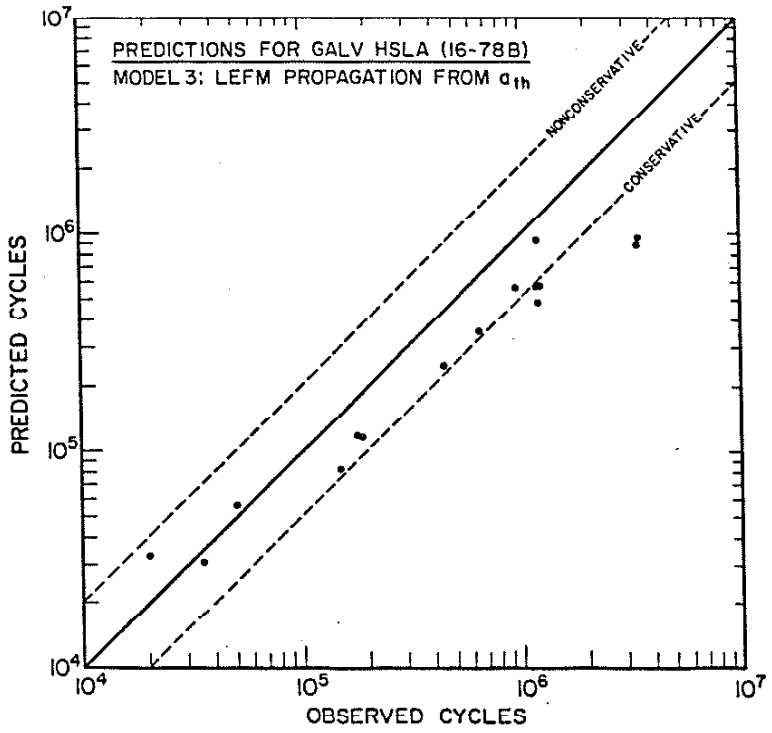

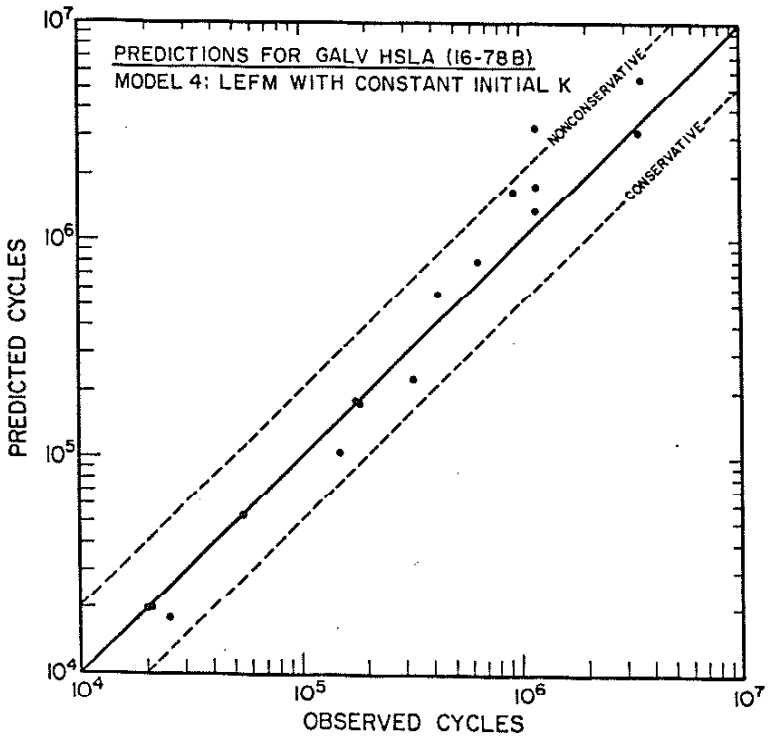

Fig. 52 (Top) Total Life Predictions Made Using Model 3, Propagation from a_{th}.

Fig. 53 (Bottom) Total Life Predictions Made Using Model 4, Propagation with Constant Initial K.

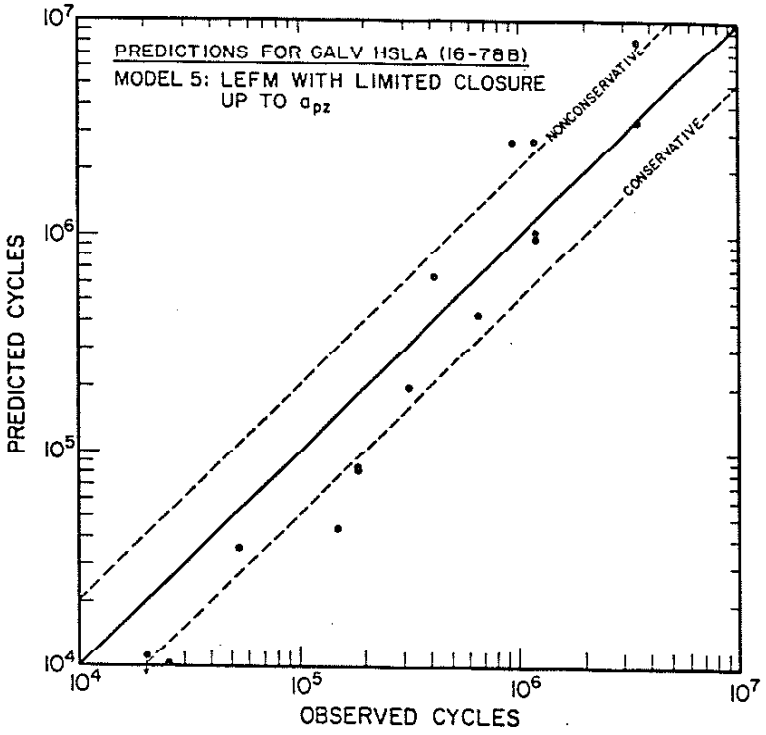

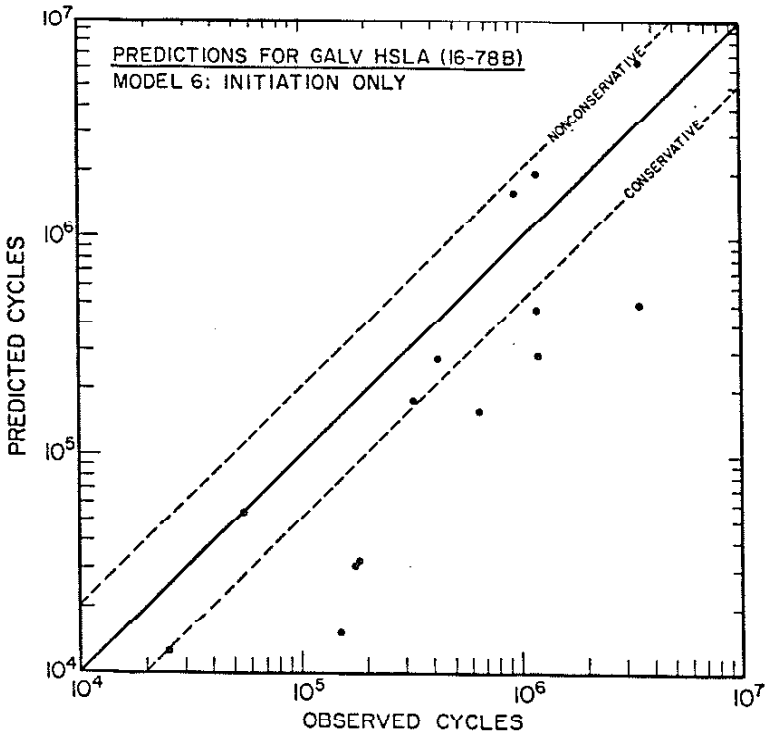

Fig. 54 (Top) Total Life Predictions Made Using Model 5, Propagation with Limited Closure to a_{pz}.

Fig. 55 (Bottom) Total Life Predictions Made Using Model 6, Initiation Only.

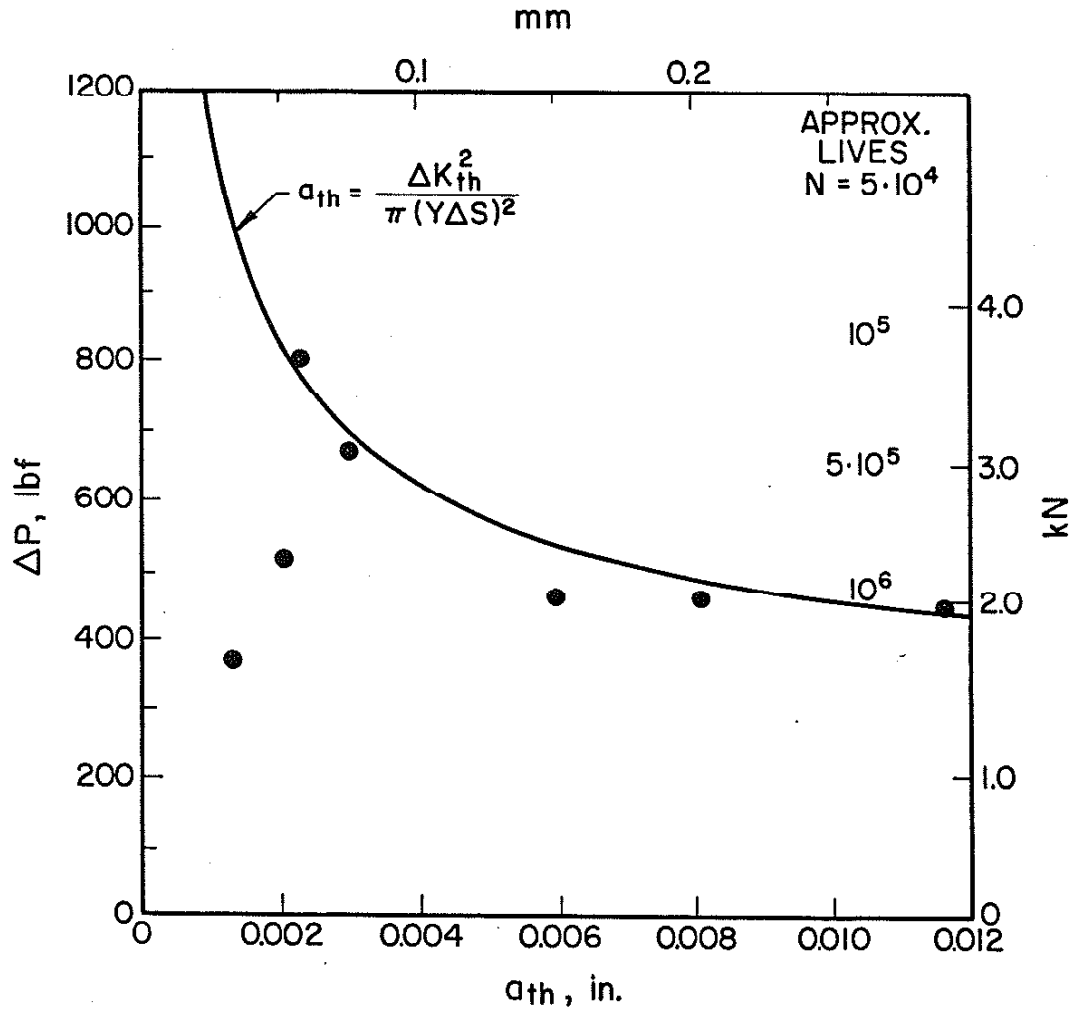

Fig. 56 The Calculated Threshold Crack Size. Depths of observed "nonpropagating" cracks (data points) are shown to be equal to or smaller than the calculated threshold crack size (line).

APPENDIX C: COMPUTER PROGRAM AND SAMPLE EXECUTION

Fatigue Life Computer Program

```
10 CLS:REM MAIN PROGRAM: CALCULATES FATIGUE-CRACK INITIATION AND PROPAGATION
11 REM:                  LIVES OF TENSILE-SHEAR SPOT WELDMENTS
12 REM:                  WRITTEN BY: JAMES C. McMAHON, 1 DEC 1985
20 FIRST=1
30 GOSUB 1000
40 GOSUB 1500
50 GOSUB 1750
60 WHILE FIRST <>1
70      PRINT"DO YOU WANT TO CHANGE THE RELAXATION PATTERN?";
80      GOSUB 7160
90      IF ANS=1 THEN GOSUB 1500
100     PRINT"DO YOU WANT TO CHANGE THE TYPE OF PROBLEM(OR END-Y5)?";
110     GOSUB 7160
120     IF ANS=1 THEN GOSUB 1750
130 WEND
140 FIRST=2:GOTO 60
150 END
160 REM ************************************************************************

1000 REM SUB READ AND ECHO
1020 REM READS AND ECHOS DATA FROM MATERIAL DATA FILE
1030 REM USERS MAY USE DEFAULT FILE OR NAME THEIR OWN FILE
1040 REM DEFAULT FILE NAME IS "DATAF.DAT"
1050 PRINT "USE THE DEFAULT FILE?";:GOSUB 7160
1060 IF ANS=1 THEN FILEN$="DATAF.DAT"
1070 IF ANS=0 THEN INPUT "GIVE NAME OF YOUR FILE"; FILEN$
1080 REM
1090 CLOSE #1
1100 OPEN FILEN$ FOR INPUT AS #1
1110 INPUT #1, MATNAM$
1120 INPUT #1, SFP,B,K,N
1130 INPUT #1, RS,E,KK2
1140 INPUT #1, W,T,KF
1150 CLOSE #1
1160 REM
1170 DEV$="SCRN:"
1180 GOSUB 1270
1190 PRINT "IS THIS THE CORRECT FILE?": GOSUB 7160
1200 IF ANS=1 THEN GOTO 1230
1210 PRINT "DO YOU WANT TO END THE PROGRAM?": GOSUB 7160
1220 IF ANS=1 THEN END ELSE GOTO 1050
1230 PRINT "DO YOU WANT A HARDCOPY OF THIS MATERIAL FILE?": GOSUB 7160
1240 IF ANS=1 THEN DEV$="LPT1:": GOSUB 1270
1250 RETURN
1270 REM************************************************************************

1280 REM SUB ECHO DATA
1290 REM DEV$ IS THE OUTPUT DEVICE, USUALLY SCRN: OR LPT1:
1300 REM
1310 OPEN DEV$ FOR OUTPUT AS #2
```

```
1320 PRINT #2, "MATERIAL:";MATNAM$
1330 PRINT #2, "SFP, B, K, N:";SFP;B;K;N
1340 PRINT #2, "RS, E, K2:";RS;E;KK2
1350 PRINT #2, "W, T, KF:";W;T;KF
1360 CLOSE #2:RETURN
1370 REM************************************************************************

1500 REM RELAXATION OPTION SUB
1505 RESTORE 9200:GOSUB 9000:REM MENU READER
1510 IF CHOICE =1 THEN DEF FNK2(KK2)=0   :KOPT$=" NO RELAX"
1520 IF CHOICE=2 THEN DEF FNK2(KK2)=KK2 :KOPT$=" PARTIAL RELAX"
1530 IF CHOICE=3 THEN DEF FNK2(KK2)=20*KK2 :KOPT$=" FULL RELAX"
1540 IF CHOICE=4 THEN DEF FNK2(KK2)=.1-60*DEPS:KOPT$=" FUN. OF EPS"
1550 IF CHOICE=5 THEN END
1560 RETURN
1570 REM************************************************************************

1745 REM PROBLEM OPTION SUB
1750 RESTORE 9280 :GOSUB 9000 :PROB=CHOICE:REM MENU READER
1760 ON PROB GOSUB 2000,2300,2500,1000,150
1770 RETURN
1780 REM ************************************************************************

2000 REM SUB FOR SINGLE LOAD AND R
2020 GOSUB 7250 : REM CHOOSES OUTPUT DEVICE
2030 INPUT "ENTER THE LOAD RATIO, R:",R
2040 PRINT #1,,"LOADING RATIO:";R,"RELAXATION OPTION:";KOPT$
2050 INPUT "ENTER THE LOAD RANGE (KIPS):";P
2060 GOSUB 7000 : REM PRINTS HEADING
2070 GOSUB 2800 : REM COMBINED SUB FOR 1ST AND 2ND REVERSAL AND Ni INTEGR.
2080 GOSUB 7070 : REM PRINT OUTPUT
2090 RETURN
2100 REM************************************************************************

2300 REM SUB FOR LOOP OF R AND P
2320 GOSUB 7250 : REM    CHOOSES OUTPUT DEVICE
2330 PRINT "ENTER RANGE OF R RATIO AND INCREMENT. USE FORM Rlo,Rhi,Rincr:";
2340 INPUT RLO,RHI,RINC:RHI=RHI+RINC/10
2350 PRINT "ENTER RANGE OF LOADS AND INCREMENT(KIPS). USE FORM
     Plo,Phi,Pincr:";
2360 INPUT PLO,PHI,PINC:PHI=PHI+PINC/10
2370 FOR R=RLO TO RHI STEP RINC
2380     PRINT#1,"":PRINT#1,,"LOADING RATIO:";R,"RELAXATION OPTION:";KOPT$
2390     GOSUB 7000:REM PRINTS HEADING
2400     FOR P=PLO TO PHI STEP PINC
2410     GOSUB 2800: REM COMBINED SUB FOR 1ST & 2ND REV, Ni INTEGR.
2420     GOSUB 7070:  REM PRINT RESULTS
2430     NEXT P
2440 NEXT R
2450 RETURN
2460 REM************************************************************************

2500 REM ROUTINE TO FIND P TO GIVE A GIVEN INITIATION LIFE
2520 GOSUB 7250:REM CHOOSES OUTPUT DEVICE
2530 INPUT "ENTER THE DESIRED LIFE:";LIFE
```

```
2540 INPUT "ENTER THE LOAD RATIO:";R
2550 P1=.4 : P2=1! : REM INITIAL LOAD GUESSES
2560 P=P1 : GOSUB 2800 :REM**PRINT P,NI
2570 L1=NI : IF ABS(LIFE-NI)/LIFE <.001 THEN GOTO 2670
2580 P=P2 : GOSUB 2800 :REM**PRINT P,NI
2590 L2=NI : IF ABS(LIFE-NI)/LIFE <.001 THEN GOTO 2670
2600 LPP=LOG(P2/P1):LLL=LOG(L2/L1):LLA=LOG(LIFE/L1)
2610 LOGP=LPP*LLA/LLL
2620 P=P1*EXP(LOGP) :PRINT ".";
2630 GOSUB 2800 : L=NI:REM**PRINT P,NI
2640 IF ABS(LIFE-L)/LIFE <.001 THEN GOTO 2670
2650 L1=L2 : L2=L : P1=P2 : P2=P
2660 GOTO 2600
2670 PRINT #1,,"LOADING RATIO:";R,"RELAXATION OPTION:";KOPT$
2680 PRINT #1,,"Ni         ";"LOAD RANGE (KIPS)":PRINT #1,"",
2690 PRINT #1,USING "##.###^^^^  ";NI;:PRINT #1,USING "##.###";P
2700 RETURN
2710 REM*************************************************************************

2800 REM SUB WHICH GROUPS SEVERAL OTHER SUBS. NEEDED FOR ITERATION OPTION
2820     GOSUB 3000: REM          1ST REVERSAL
2830     GOSUB 3500: REM          KE AND STRAINS
2840     GOSUB 4000: REM          2ND REVERSAL
2850     GOSUB 4500: REM          INTEGRATE TO Ni
2860     GOSUB 5000: REM          PROP LIFE
2870 RETURN
2880 REM*************************************************************************

3000 REM SUB FOR FIRST REVERSAL
3020 S=P/(W*T): C1=E/(K^(1/N)) : C2=(1-N)/N
3030 SMAX=S/(1-R) : EMAX=S/E/(1-R)
3040 KS1=KF : KS2=KF/2 : REM FIRST GUESSES BEFORE ITERATIONS
3050 DEF FNKS(X)=X*(1+C1*ABS(X*SMAX+RS)^C2)^.5
3060 A1=FNKS(KS1) : A2=FNKS(KS2)
3070 IF ABS(A2-KF)/KF < .005 THEN KS=KS2 : RETURN
3080 ITR=1
3090 KS=KS1+(KS2-KS1)*(KF-A1)/(A2-A1)
3100 A=FNKS(KS)
3110 IF ABS(A-KF)/KF < .005 THEN RETURN
3120 ITR=ITR+1 : IF ITR > 10 THEN PRINT "ITR > 10" : RETURN
3130 KS1=KS2 : KS2=KS : A1=A2 : A2=A
3140 GOTO 3090
3150 REM*************************************************************************

3500 REM SUB FOR KE AND STRAINS
3520 KE=KF*KF/KS
3530 SIGMAX=KS*SMAX + RS
3540 EPMAX=KE*EMAX + ER
3545 RETURN
3550 REM
3560 REM*************************************************************************

4000 REM SUB FOR 2ND REVERSAL ITERATIVE SOLUTION
4020 H2=(KF*S)^2/E : REM 2ND NUEBER HYPERBOLA CONSTANT
4030 C3=2^((N-1)/N) : C4=(N+1)/N : C5=K^(1/N)
```

```
4040 DEF FNH(X)=(X^2)/E + C3*((X^C4)/C5)
4050 REM
4060 DSIG1=20 : DSIG2=120 :REM 1ST GUESSES BEFORE ITERATION
4070 A1=FNH(DSIG1) : A2=FNH(DSIG2)
4080 IF ABS(H2-A2)/H2 < .005 THEN DSIG=DSIG2 : GOTO 4200
4090 ITR =1
4095 REM NEW GUESS, .75 FACTOR TO DAMP OSCILLATIONS IN ITERATIONS
4100 DSIG=DSIG1+(DSIG2-DSIG1)*(H2-A1)/(A2-A1)
4102 IF DSIG < DSIG1 AND DSIG >DSIG2 THEN 4110
4104 IF DSIG > DISG1 AND DSIG <DSIG2 THEN 4110
4106 DSIG=DSIG1+(DSIG2-DSIG1)*(H2-A1)/(A2-A1)*.75
4110 A=FNH(DSIG)
4120 IF ABS(A-H2)/H2 < .005 THEN 4200
4130 ITR=ITR +1 : IF ITR > 10 THEN PRINT "ITR > 10" :GOTO 4200
4140 A1=A2 : A2=A : DSIG1=DSIG2 : DSIG2 = DSIG
4150 GOTO 4100
4200 REM
4210 DEPS=2*( DSIG/2/E+(DSIG/2/K)^(1/N) )
4220 SO=SIGMAX-DSIG/2 : EO=EPMAX-DEPS/2
4230 RETURN
4240 REM*************************************************************************

4500 REM SUB TO INTEGRATE TO GET Ni
4515 K2=FNK2(KK2): IF K2>0 THEN K2=0
4520 DEF FNF(X)=((2*SFP/DSIG)*(1-SO/SFP*(2*X)^K2))^(1/B)
4530 LOWLIM=.5 : UPLIM=5000 : G1=UPLIM
4540 GOSUB 8000 : REM SOLVES INTEGRAL FROM LOWLIM TO UPLIM
4550 F1=INTEGRAL : REM 1ST GUESS
4560 UPLIM=100000! : G2=UPLIM
4570 GOSUB 8000 : F2= INTEGRAL : REM 2ND GUESS
4580 G=G1+(G2-G1)*(1-F1)/(F2-F1)
4590 IF G<100 THEN UPLIM=100 ELSE UPLIM=G
4600 GOSUB 8000
4610 IF ABS(INTEGRAL-1)<.005 THEN GOTO 4800
4620 G1=G2 : G2=G : F1=F2 :F2=INTEGRAL
4630 GOTO 4580
4800 NI=G/2 : REM G OR UPLIM WAS IN REVERSALS, NI IN CYCLES
4810 SWT=(2*SIGMAX*DEPS*E)^.5
4820 EP=2*(DSIG/2/K)^(1/N)
4825 RETURN
4850 REM*************************************************************************

5000 REM SUB FOR LIFE CALCULATIONS
5005 ORDER=3:C1(1)=14.39:C1(2)=-19.54:C1(3)=20.24:C1(4)=-8.2
5007 C=6.2E-12:M=5
5010 FCL0=.9:FCL1=.7
5030 IF R<0 THEN FCL=FCL1 ELSE FCL=FCL0
5042 AI=.01:AF=T:DA=.0005:REM OR AI=FN(LOAD,GEOM.)
5055 SUMN=0
5060 S=FCL*P/T/W
5080 FOR A=AI TO AF+DA/2 STEP DA
5090     L3=(P*FCL*A^.5)/T/W
5100     Z=A/T
5110     Y=C1(1)
5120     FOR J=2 TO ORDER+1
```

```
5130         Y=Y+C1(J)*Z^(J-1)
5140      NEXT J
5150      DELK=Y*L3
5160      DN=DA/C/DELK^M
5170      SUMN=SUMN+DN
5180 NEXT A
5190 NP=SUMN
5200 RETURN
5299 REM*************************************************************************

7000 REM SUB FOR HEADING
7020 PRINT #1,"          ";
7030 PRINT #1,"LOAD RNG    Ni          Np         NTOTAL"
7040 RETURN
7060 REM*************************************************************************

7070 REM SUB OUTPUT
7100 PRINT #1,"          ";
7110 PRINT #1,USING "##.##      ";P;
7120 PRINT #1,USING "##.##^^^^";NI;NP;NI+NP
7130 RETURN
7150 REM*************************************************************************

7160 REM SUB YES
7170 REM RETURNS VALUE OF ANS=1 IF Y OR y IS GIVEN AS ANSWER
7180 REM RETURNS VALUE OF ANS=0 FOR ALL OTHER ANSWERS
7190 PRINT "Y=YES, N=NO":
7200 A$=INKEY$ : IF A$="" THEN 7200
7210 IF A$="y" OR A$="Y" THEN ANS=1 ELSE ANS=0
7220 RETURN
7240 REM*************************************************************************

7250 REM SUB FOR CHOOSES OUTPUT DEVICE
7260 CLOSE
7270 RESTORE 9360 : GOSUB 9000
7280 IF CHOICE =1 THEN DEV$="SCRN:"
7290 IF CHOICE=2 THEN DEV$="LPT1:"
7300 OPEN DEV$ FOR OUTPUT AS #1
7310 RETURN
7320 REM*************************************************************************

8000 REM THIS SUBROUTINE IS USED TO EVALUTATE INTEGRALS
8020 REM BEFORE IT CAN BE USED:
8030 REM  1. DEFINE THE FUNCTION OF THE INTEGRAND IN THE CALLING PROGRAM.
8040 REM     EXAMPLE: 10 DEF FNF(X) = X^2 + 2*X + 5.  BE SURE TO NAME
8045 REM                                              THE FUNCTION FNF
8050 REM  2. DEFINE THE LOWER AND UPPER LIMITS OF INTEGRATION.
8060 REM     EXAMPLE: 20 LOWLIM = 0 : UPLIM = 2.0
8070 REM              USE THE VARIABLE NAMES LOWLIM AND UPLIM
8080 REM  3. ERROR TOLERENCE WILL BE 0.1% UNLESS YOU CHANGE LINE 8180
8120 REM  4. VALUE OF THE INTEGRAL WITLL BE RETURNED UNDER THE
8130 REM     VARIABLE NAME "INTEGRAL"
8140 REM  5. CALL THIS SUBROUTINE BY USING THE STATEMENT GOSUB 8000
8150 REM  6. TEST SUBROUTINE WITH INTEGRALS OF KNOWN SOLUTIONS.
8160 REM SUBROUTINE WRITTEN BY J.C. MCMAHON, 1 DEC 1985
```

```
8170 REM
8180 TOL=.1  : REM TOLERENCE ERROR IS .1%
8230 REM ************************************************************************

8240 MP=(UPLIM+LLIM)/2  : REM MP IS MIDPOINT OF INTEGRATION
8250 WID=UPLIM-LOWLIM     : REM WID IS WIDTH OF RANGE OF INTEGRATION
8260 RESTORE 8340 : REM TO READ DATA STARTING FROM CORRECT DATA LINE
8270 FOR J=1 TO 6
8280     FOR I=1 TO 6
8290             READ R(J,I),A(J,I)  : REM GAUSS POINTS AND VALUES
8300     NEXT I
8310 NEXT J
8320 REM ************************************************************************

8330 REM TABLE OF GAUSS POINTS AND GAUSS VALUES
8340 DATA 0,2,0,0,0,0,0,0,0,0,0,0
8350 DATA .57735,1,-.57735,1,0,0,0,0,0,0,0,0
8360 DATA .7746,.555556,-.7746,.555556,0,.888889,0,0,0,0,0,0
8370 DATA .86114,.34785,-.86114,.34785,.33998,.65215,-.33998,.65215,0,0,0,0
8380 DATA .90618,.23692,-.90618,.23692,.53847,.47863,-.53847,.47863
8390 DATA 0,.56889,0,0
8400 DATA .93246,.17132,-.93246,.17132,.66121,.36076,-.66121,.36076
8410 DATA .23862,.46791,-.23862,.46791
8420 RESTORE
8430 REM ************************************************************************

8440 J=1
8450 SUM=0
8460 FOR I=1 TO J
8470     SUM=SUM+A(J,I)*FNF(MP+R(J,I)*WID/2)
8480 NEXT I
8490 REM
8500 NEWINTGRL=SUM*WID/2:REM ACCOUNTS FOR GAUSS INT IS DONE OVER RANGE
     -1 TO 1
8510 IF J=1 THEN INTEGRAL=NEWINTGRL: J=J+1: GOTO 8450
8520 REM TEST OF ERROR TOLERENCE
8530 IF ABS((INTEGRAL-NEWINTGRL)/INTEGRAL)*100 < TOL THEN GOTO 8590
8540 IF J=6 THEN GOTO 8590:REM PRINT ST OPTIONAL FOR LAST QUADRATURE
8560 INTEGRAL=NEWINTGRL
8570 J=J+1 : REM IF DIFFERENCE IS GREATER THAN TOL THEN ITERATE AGAIN
8580 GOTO 8450
8590 INTEGRAL=NEWINTGRL
8600 RETURN
8610 REM ************************************************************************

9000 REM SUB MENU READER
9020 REM
9030 READ DLINES
9040 READ TITLE$
9050 PRINT TITLE$
9060 REM
9070 FOR I=1 TO DLINES
9080     READ L$:PRINT,L$
9090 NEXT I
9100 REM
```

```
9110 PRINT "^CHOOSE ONE OF THE ABOVE OPTIONS^"
9120 K$=INKEY$:IF K$="" THEN 9120
9130 IF K$<"1" OR K$>CHR$(DLINES+48) THEN 9140 ELSE 9150
9140 PRINT "INVALID CHOICE, CHOOSE 1-";DLINES:GOTO 9120
9150 CHOICE=ASC(K$)-48
9160 RETURN
9180 REM ************************************************************************
9190 REM BEGINNING OF DATA SECTION WHICH IS READ BY SUB9000
9200 DATA 5
9210 DATA "CHOICE OF RELAXATION PATTERNS"
9220 DATA "1. NO RELAXATION, FULL MEAN STRESS THROUGHOUT LIFE"
9230 DATA "2. PARTIAL RELAXATION"
9240 DATA "3. FULL RELAXATION, NO MEAN STRESS"
9250 DATA "4. RELAXATION AS A FUNCTION OF STRAIN"
9260 DATA "5. END THE PROGRAM"
9270 REM
9280 DATA 5
9290 DATA "CHOICE OF PROBLEMS"
9300 DATA "1. FIND Ni FOR A GIVEN LOAD AND R RATIO"
9310 DATA "2. FIND NT FOR A RANGE OF LOAD VALUES AND DIFFERENT R's"
9320 DATA "3. FIND THE LOAD TO YIELD A GIVEN Ni"
9330 DATA "4. CHOICE ANOTHER MATERIAL FILE"
9340 DATA "5. END THE PROGRAM"
9350 REM
9360 DATA 2
9370 DATA "CHOICE OF DEVICES FOR OUTPUT"
9380 DATA "1. OUTPUT TO MONITOR OR SCREEN (SCRN:)
9390 DATA "2. OUTPUT TO PRINTER (LPT1:)
9400 REM
9410 REM ************************************************************************
```

Example Execution

```
RUN "TOTLIFE"
USE THE DEFAULT FILE? Y=YES, N=NO
N
GIVE NAME OF YOUR FILE? C:\USERSDIR\JIM\BASIC\DADN\DATAF.DAT

MATERIAL: GALV. HSLA (16-78B), WITH ESTIMATED PROPERTIES
SFP, B, K, N: 120 - .085  90  .0681
RS, E, K2: 60.2  29000 -.2
W, T, KF: 1.5  .055  7.69
IS THIS THE CORRECT FILE?
Y=YES, N=NO
Y

CHOICE OF RELAXATION PATTERNS
          1.  NO RELAXATION, FULL MEAN STRESS THROUGHOUT LIFE
          2.  PARTIAL RELAXATION
          3.  FULL RELAXATION, NO MEAN STRESS
          4.  RELAXATION AS A FUNCTION OF STRAIN
          5.  END THE PROGRAM
^CHOOSE ONE OF THE ABOVE OPTIONS^
4

CHOICE OF PROBLEMS
          1.  FIND Ni FOR A GIVEN LOAD AND R RATIO
          2.  FIND NT FOR A RANGE OF LOAD VALUES AND DIFFERENT R's
          3.  FIND THE LOAD TO YIELD A GIVEN Ni
          4.  CHOICE ANOTHER MATERIAL FILE
          5.  END THE PROGRAM
^CHOOSE ONE OF THE ABOVE OPTIONS^
2

CHOICE OF DEVICES FOR OUTPUT
          1.  OUTPUT TO MONITOR OR SCREEN (SCRN:)
          2.  OUTPUT TO PRINTER (LPT1:)
^CHOOSE ONE OF THE ABOVE OPTIONS^
2

ENTER RANGE OF R RATIO AND INCREMENT.  USE FORM Rlo, Rhi, Rincr:? -1,-1,1
ENTER RANGE OF LOADS AND INCREMENT(KIPS). USE FORM Plo, Phi, Pincr:? .5, .7, .2

          LOADING RATIO:-1                    RELAXATION OPTION: FUN. OF EPS
     LOAD RNG        Ni          Np           NTOTAL
     0.50         4.74E+05    9.30E+05       1.40E+06
     0.70         1.59E+05    2.73E+05       4.32E+05

DO YOU WANT TO CHANGE THE RELAXATION PATTERN? Y=YES, N=NO
N
DO YOU WANT TO CHANGE THE TYPE OF PROBLEM (OR END -Y5)? Y=YES, N=NO
Y5

OK
```

REFERENCES

1. Wang, P.C. and Lawrence, F.V., Jr., "A Fatigue Life Prediction Method for Tensile-Shear Spot Welds," Materials Engineering -- Mechanical Behavior Report 113, University of Illinois, 1984.

2. Lawrence, F.V., Jr., Wang, P.C., Ho, N.J., and Corten, H.T., "The Fatigue Resistance of Thin Gauge Automotive Weldments, Phases I-IV," Technical Reports to the General Motors Corporation, College of Engineering, University of Illinois, 1984-85.

3. Lawrence, F.V., Jr., Corten, H.T., and McMahon, J.C., "Improvement of Steel Spot Weld Fatigue Resistance," Report to the Amer. Iron and Steel Inst., College of Engineering, University of Illinois, 1985.

4. Davidson, J. A., "A Review of the Fatigue Properties of Welded Sheet Steel," SAE Paper 830033, 1983.

5. Orts, D.H., "Fatigue Strength of Spot Welded Joints in HSLA Steel," SAE Paper 810355, 1981.

6. Wilson, R.B. and Fine, T.E., "Fatigue Behavior of Spot Welded High Strength Steel Joints," SAE Paper 810354, 1981.

7. Smith, G.A. and Lawrence, F.V., Jr., "Fatigue Crack Development in Tensile-Shear Spot Weldments," Materials Engineering -- Mechanical Behavior Report 108, University of Illinois, 1984.

8. Cooper, J.F. and Smith, R.A., "The Measurement of Fatigue Cracks at Spot-Welds," Int. J. Fatigue (7), No. 3, 1985.

9. Wojnowski, D.A., "Fatigue Fracture in Tensile-Shear Spot Weldments," M.S. Thesis, University of Illinois, 1983.

10. Lee, F. "Improving the Fatigue Resistance of Tensile-Shear Spot Weldments Through Residual Stress Techniques," M.S. Thesis, College of Engineering, University of Illinois at Urbana-Champaign, 1985.

11. Landgraf, R.W., Ford Motor Company, Private Communication, 1983.

12. Ho, N.J. and Lawrence, F.V., Jr., "The Fatigue of Weldments Subjected to Complex Loadings," FCP Report 45, College of Engineering, University of Illinois, 1983.

13. Pook, L.P., "Approximate Stress Intensity Factor for Spot Welds and Similar Welds," National Engineering Laboratory Report No. 588, April 1975.

14. Shinozaki, M., Kato, T.Irie, and Takahashi, I., "Fatigue of Automotive High Strength Steel Sheets and their Welded Joints," SAE Paper 830032, 1983.

15. Kitagawa, H., Satoh, T., and Fujimoto, M., "Fatigue Strength of Single Spot-Welded Joints of Rephosphorized High-Strength and Low-Carbon Steel Sheets, SAE Paper 850371, 1985.

16. Lawrence, F.V., Jr., Wang, P.C., Ho, N.J., Corten, H.T., "Estimating the Fatigue Resistance of Tensile-Shear Spot Welds," FCP Report No. 48, College of Engineering, University of Illinois at Urbana-Champaign, 1983.

17. Davidson, J.A. and Imhof, E.J., "The Effect of Tensile Strength on the Fatigue Life of Spot-Welded Sheet Steels," SAE Paper 840110 1984.

18. Sehitoglu, H., "Crack Opening and Closure in Fatigue," Engineering Fracture Mechanics, Vol. 21, No. 2, 1985.

19. Reemsnyder, H.S., "Evaluating the Effect of Residual Stresses on Notched Fatigue Resistance," Materials, Experimentation, and Design in Fatigue-Proceedings of Fatigue '81, Westbury Press, Guilford, England, 1981.

20. Topper, T.H., Wetzel, R.M., and Morrow, J., "Neuber's Rule Applied to Fatigue of Notched Specimens," Journal of Materials, Vol. 4, pp. 200-209, 1969.

21. Burk, J.D., Lawrence, F.V., Jr., "The Effect of Residual Stress on Weld Fatigue Life," Fracture Control Report No. 29, College of Engineering, University of Illinois at Urbana-Champaign, 1978.

22. Barsom, J.M., "Fatigue Behavior of Pressure-Vessel Steels," WRC Bulletin No. 194, May 1974, pp. 1-22.

23. Broek, D., Elementary Engineering Fracture Mechanics, Third Edition, Martinus Nij-hoff Pub., 1982.

24. Hibbitt, Karlsson, and Sorensen, ABAQUS, Version 4. Program provided courtesy of the authors, 1982.

25. Broek, D. and Leis, B.N.," "Similitude and Anomalies in Crack Growth Rates," Materials, Experimentation and Design in Fatigue, Westbury House, IPC Science Press, UK, 1981.

26. Socie, D.F. and Artwohl, P.J., "Effect of Spectrum Editing on Fatigue Crack Initiation and Propagation in a Notched Member," ASTM STP 714, Amer. Society for Testing Materials, 1980.